GLIOGENESIS IN THE ADULT SPINAL CORD:

SPATIOTEMPORAL HETEROGENEITY OF THE SPINAL CORD CENTRAL CANAL EPENDYMAL CELLS AND REMYELINATION PROGRAMMES IN HUMAN MULTIPLE SCLEROSIS

by

KATHRYN MICHELLE DOUGLAS

BSc, The University of British Columbia, 2013

A THESIS SUBMITTED IN PARTIAL FULFILLMENT OF
THE REQUIREMENTS FOR THE DEGREE OF

MASTER OF SCIENCE
in
THE FACULTY OF GRADUATE AND POSTDOCTORAL STUDIES
(Neuroscience)

THE UNIVERSITY OF BRITISH COLUMBIA
(Vancouver)

April 2016

ABSTRACT

The developing mammalian spinal cord can generate all required cell types; in the adult, there exists a subpopulation of progenitors able to generate multiple cell types. The ependymal cell (EC) layer of the central canal (CC) of the adult spinal cord is a neural stem cell niche possessing the potential to self-renew and differentiate into astrocytes and oligodendrocytes *in vivo* and *in vitro*, and neurons *in vitro*. However, the differences between a developmental EC and an adult EC are not well established. Further, it is unknown whether ECs have equivalent stem/progenitor abilities, and whether certain subpopulations may be better targets for regeneration. Multiple Sclerosis (MS) is a debilitating disease characterized by areas of chronically demyelinated CNS, and an attractive target for regenerative therapy. Little is known about why endogenous regenerative programmes in MS are unsuccessful. Using *in-situ* hybridization (*ISH*) data from the Allen Spinal Cord Atlas and immunofluorescent detection of antigen in mice, we revealed temporal and spatial segmentation of ECs expressing distinct groups of genes. The ages analyzed (postnatal day 4 and 56) are relevant to the mechanisms of neurogenesis and gliogenesis, as the spinal cord is capable of regaining greater functionality following injury at P4 than at P56. Gene ontology analysis suggests different regions of the CC may contribute in different ways to spinal cord repair. Furthermore, we found the EC niche experiences altered levels of proliferation after two different types of insult, SCI and demyelinating injury in mice. We then used MS spinal cord to test what extent such repair from demyelination takes place. We found that remyelination occurred, but was inadequate and highly variable both between and within patients. Abnormal myelinating cells of a unique phenotype were found in the CNS and PNS; the extent and prevalence of peripheral involvement has not been previously reported. Further work is needed to determine whether the human EC layer could be targeted to enhance remyelination. Overall, these results

reveal novel cell phenotypes engaged in repair in mouse and human spinal cord that may serve a basis for future therapeutic intervention.

PREFACE

All work presented here was performed by the candidate, Kathryn Michelle Douglas, unless otherwise stated here, in the text, or in footnotes.

Mr Dongho Lee performed the ASCA data mining and spatial/temporal categorization, and GeneMANIA analysis (data summarized in Fig. 3.1). The lysolecithin-lesioned Fabp7 mice used in the proliferation quantification (Fig. 3.7) were generated and the tissue was processed for immunofluorescence by Mr Raymundo Aguas, and the surgery and injection was performed by Dr Jie Liu, assisted by Mr Raymundo Aguas and Mr Greg Duncan. The crush-injured C57Bl/6 mice used in the proliferation quantification (Fig. 3.7) were obtained from Charles River; baseline and post-injury behavioural testing was performed by Dr Tao Meng and Mr Greg Duncan. Surgery was performed by Drs Tao Meng and Audrey Petit, assisted by Mr Brett Hilton. Tissue was processed by Drs Tao Meng and Audrey Petit. Ms Ashley Sanders and Ms Kathryn Westendorf processed the uninjured P5 Fabp7 spinal cord tissue used in Fig 3.5A,C and the uninjured adult spinal cord tissue used in Fig. 3.5D. I generated and processed all of the remaining uninjured adult mouse spinal cord tissue used. All animal work was performed in accordance with the Canadian Animal Care Committee standards, approved by the UBC Animal Care Committee under protocol A09-0741. Human tissue was gathered postmortem from patients who had given formal consent, and processed for tissue staining by members of the Dr Wayne Moore lab in accordance with the Clinical Research Ethics Board of the University of British Columbia, under approval number H11-03411.

The *ISH* images (Fig. 3.2, 3.3 and 3.6) were all taken from the ASCA.

The overall project was designed by Dr Jane Roskams. I designed and carried out the proliferation quantification experiments (Fig. 5.6 and 5.7), with guidance from Dr Catherine Cowan. I preformed the gene ontology analysis, with assistance from Ms Athena Chou. Mr Raymundo Aguas performed the immunohistochemistry for Fig. 5.9C-F, and I took the micrograph images and performed all of the other immunostaining, imaging, data analysis and statistics. I wrote the entirety of the text.

Two manuscripts are currently in progress based on the data presented here.

TABLE OF CONTENTS

LIST OF TABLES

LIST OF FIGURES

LIST OF ABBREVIATIONS

ADAMTS20 – A Disintegrase And Metallopeptidase with Thrombospondin motifs-20

ASCA – Allen Spinal Cord Atlas

BLBP – Brain Lipid Binding Protein

BMS – Basso Mouse Scale

CC – Central Canal

CNS – Central Nervous System

CSF – Cerebrospinal Fluid

DREZ – Dorsal Root Entry Zone

EC – Ependymal Cell

ECM – Extracellular Matrix

GO – Gene Ontology

ISH – *in-situ* Hybridization

LPC – Lysophosphatidylcholine

MS – Multiple Sclerosis

OPC – Oligodendrocyte Precursor Cell

P5 – Postnatal day 5

P56 – Postnatal day 56

P90 – Postnatal day 90

PCNA – Proliferating Cell Nuclear Antigen

PMI – Postmortem Interval

PNS – Peripheral Nervous System

PPMS – Primary Progressive Multiple Sclerosis

Rb1 – Retinoblastoma protein-1

SCI – Spinal Cord Injury

TrkB – Neurotrophic Tyrosine Kinase Receptor-2

WPL – Weeks Post Lesion

SVZ – Subventricular Zone

ACKNOWLEDGEMENTS

I am incredibly grateful for all who have assisted me in completing the work presented here. I owe particular thanks to Dr Jane Roskams, my supervisor, for taking a chance on me and inspiring me to continually strive for excellence. I also thank Dr Wolfram Tetzlaff, my committee chair, for going above and beyond in his support, and for always treating me as a colleague instead of just a student. I am grateful to the other members of my committee, Dr Fabio Rossi and Dr Wayne Moore, for balancing out my weaker areas and always making time for my questions or concerns.

Thank you to the members of the Roskams, Tetzlaff, and Moore labs, particularly Dr Catherine Cowan, Athena Chou, Nicole Janzen, Greg Duncan, Peggy Assinck, Brett Hilton, and Vlady Pavlova for providing invaluable insight and expertise, sharing reagents and tissue as well as wisdom and patience. Thanks also to my colleagues in the Neuroscience program and the Life Sciences Centre for their perpetual support.

I would like to thank the Rick Hansen Foundation for providing the lion's share of my funding during the first year of my research, and continuing to increase accessibility of graduate studies for students with disabilities.

Special thanks as well to my family and friends for their endless support in all of my endeavors.

1. INTRODUCTION

1.1. Neurogenesis, astrogenesis, and oligodendrogenesis in the developing mammalian spinal cord

During development, the ectodermal germ layer is induced to form the neural tube via signaling from the notochord in a process called neurulation. The neural tube is comprised of neuroepithelial cells, which transition into radial glia cells once neurulation is complete. Radial glia cells undergo neurogenesis and gliogenesis - the production of neurons and glia, respectively (Paridaen & Huttner, 2014). Gradients of morphogens such as FGFs, Wnts, BMPs, and SHH are established, and the relative concentration of morphogen at a given point dictates the fate of the radial glia daughter cells (Paridaen & Huttner, 2014). The formation of the different cell types – neurons, astrocytes and oligodendrocytes – is orchestrated temporally, with neurons being produced first, then astrocytes and oligodendrocytes (reviewed by F. D. Miller & Gauthier, 2007).

Once neurogenesis is complete, gliogenesis is induced by the expression of transcription factors Sox9 and NFIA (Deneen et al., 2006; Kang et al., 2012; Stolt et al., 2003). Factors released by newborn neurons, such as CT-1 and Jagged/delta, help induce astrocyte differentiation (Barnabé-Heider et al., 2005; Namihira et al., 2009). A comprehensive list of factors that influence astrocyte production is given in table 1.1. Astrocytes are likely produced by proliferative radial glia-derived astrocyte precursors (Tien et al., 2012). There are at least 9 subgroups of astrocytes (Emsley & Macklis, 2006), and molecularly-distinct astrocyte subpopulations are derived from different areas of the spinal cord (Hochstim, Deneen, Lukaszewicz, Zhou, & Anderson, 2008; Tsai et al., 2012). The developmental proteins BMP and Wnt regulate the production of astrocytes versus oligodendrocytes (Mekki-Dauriac, Agius, Kan, & Cochard, 2002; Vallstedt, Klos, & Ericson, 2005).

***Table 1.1* - Factors that influence astrocyte lineage production**

Factors	Process	Discovery
Sox9 NFIA SHH Notch	Astrocyte migration	(Kang et al., 2012) (Scott et al., 2010) (Namihira et al., 2009)
BMP Notch	Astrocyte fate restriction	(Grinspan et al., 2000; Namihira et al., 2009; Taylor, Yeager, & Morrison, 2007)
CT-1 Jagged/delta	Astrocyte differentiation	(Barnabé-Heider et al., 2010; Namihira et al., 2009)
CNTF JAK/STAT Gp130 BMP LIF	GFAP regulation/astrocyte differentiation	(Bonni, 1997) (Bonaguidi et al., 2005; F. D. Miller & Gauthier, 2007)

Developmental oligodendrocyte production is initiated by SHH, which activates Olig2, a transcription factor involved in differentiation along the oligodendrocyte lineage (Q R Lu et al., 2000). A list of factors that influence oligodendrocyte production is given in table 1.2. Oligodendrocytes and oligodendrocyte precursor cells (OPCs) are mainly derived from the area immediately surrounding the spinal cord central canal and the ventricular zones in the brain (reviewed by Aguirre & Gallo, 2007; Menn et al., 2006; Rowitch, 2004), although there may be other sources in the CNS (Kessaris et al., 2006). A pool of OPCs persists in the spinal cord and brain through adulthood, which is capable of proliferating and producing remyelinating cells as needed (Gensert & Goldman, 1997). OPCs can be produced from the ependymal cells of the adult spinal cord, but adult ependymal cells have a much higher propensity to produce astrocytes (Barnabé-Heider et al., 2010).

Table 1.2 **- Factors that influence oligodendrocyte lineage production**

Factors	Process	Reference
PDGF FGF Olig2 Olig1 Nkx2.2 LNTF	Oligodendrocyte maturation	(Calver et al., 1998; Fortin, 2005; McKinnon, Matsui, Dubois-Dalcq, & Aaronsont, 1990; R. H. Miller, 2002; Murtie, Zhou, Le, Vana, & Armstrong, 2005; Stankoff et al., 2002)
EGF NT-3 HGF	OPC proliferation/migration	(Aguirre & Gallo, 2007; Cohen, Marmur, Norton, Mehler, & Kessler, 1996; Mela & Goldman, 2013; Ohya, Funakoshi, Kurosawa, & Nakamura, 2007)
BDNF Cdk2 $P27^{Kip1}$ TNFα	Regulating the number of OPCs	(Caillava et al., 2011; Crockett, Burshteyn, Garcia, Muggironi, & Casaccia-Bonnefil, 2005; Vondran, Clinton-Luke, Honeywell, & Dreyfus, 2010; VonDran, Singh, Honeywell, & Dreyfus, 2011)
IGF-1 T3 IL-1β Sox17 TNFα RXRγ	OPC differentiation	(Mozell & McMorris, 1991) (Barres, Lazar, & Raff, 1994) (Chew et al., 2011; Huang et al., 2011; Mason, Suzuki, Chaplin, & Matsushima, 2001; Ming, Chew, & Gallo, 2013) (Cammer & Zhang, 1999)
Olig1 Olig2 Nkx2.2 Ascl1/Mash1	Specification	(Q. Richard Lu et al., 2002; Parras et al., 2004, 2007; Soula et al., 2001)
Netrin-1	Optic nerve OPC migration	(Nathalie Spassky et al., 2002)
MMP inhibitors (ex. TIMP1)	Oligodendrogenesis and myelin compaction	(Nygårdas & Hinkkanen, 2002)

1.2. Spatial and temporal patterning in developmental neurogenesis and gliogenesis

Embryonic neural stem cells give rise to embryonic radial glia, which can self-renew or produce neurons, astrocytes and oligodendrocytes. Radial glia-derived neurogenesis occurs before gliogenesis in the developing spinal cord (reviewed by F. D. Miller & Gauthier, 2007). The neural tube, which lies above the notochord, produces cells of a neural fate in response to sonic hedgehog (SHH) released from the notochord. Different subtypes of neurons are produced along the dorsal/ventral axis of the neural tube, depending on the concentration of the morphogen gradient (Paridaen & Huttner, 2014). The transcription factors Sox9 and NFIA help orchestrate the shift from production of neurons to production of glia in development, and are in turn regulated by the developmental proteins SHH and Notch (Deneen et al., 2006; Kang et al., 2012; Stolt et al., 2003). GFAP also helps regulate the switch from neurogenesis to gliogenesis (Fan et al., 2005; Namihira et al., 2009).

At embryonic day 14-16 in the mouse, the neural tube has developed into the central nervous system (CNS) structures, the brain and spinal cord (N. Spassky, 2005). The neurogenic and gliogenic radial glia have become the ciliated ependymal cells lining the lumen of what was the neural tube, and is now the ventricles in the brain and the central canal in the spinal cord (Fu et al., 2003; Masahira et al., 2006; N. Spassky, 2005). This step produces the majority of the ependymal cells (N. Spassky, 2005), but there appears to be a second wave of radial glia-derived ependymal cell production at postnatal day 8-15 in mice that is associated with radial glia processes extending dorsally and ventrally from the central canal (Ševc, Daxnerová, Haňová, & Koval', 2011). As proposed by Ševc et al., (2011), these two separate waves of ependymal cell production could provide the foundation of the spatial heterogeneity of the central canal reported previously (Hamilton, Truong, Bednarczyk, Aumont, & Fernandes, 2009; Meletis et al., 2008; Petit et al.,

2011). Long processed-radial ependymal cells persist in the dorsal and ventral poles, whereas cuboidal ciliated ependymal cells reside in the lateral aspects of the central canal in the adult (Meletis et al., 2008).

CNS stem cells are polarized. The apical pole of the ependymal cells contacts the ventricle (which, in the case of the spinal cord, is the central canal), and the basal pole of the ependymal cells contacts the pia of the spinal cord. The apical and basal poles have different functions, and have different morphology (reviewed by Paridaen & Huttner, 2014). Apical regions contact the cerebrospinal fluid (CSF) and are ciliated; the CSF circulates through the ventricles in the brain and the central canal. Basal regions are thought to orchestrate proliferation of neural precursors; during asymmetric cell division of a radial glia cell, only one daughter cell will inherit the basal process and remains a neural stem cell, whereas the other daughter cell undergoes differentiation (Alexandre, Reugels, Barker, Blanc, & Clarke, 2010; Konno et al., 2008; Shitamukai, Konno, & Matsuzaki, 2011).

1.3. Central canal ependymal cells and subventricular zone ependymal cells

Ependymal cells line the lumen of the ventricle in the mammalian brain (a region known as the subventricular zone or SVZ), just as ependymal cells line the central canal in the spinal cord. Interestingly, ependymal cells of the SVZ of the brain do not appear to function as primary multipotent stem/progenitor cells as they do in the spinal cord (reviewed by Morrens, Van Den Broeck, & Kempermann, 2012). Instead, the main proliferative cells in the SVZ are found in the subependymal layer, and have a distinct astrocytic phenotype similar to radial glia (Kriegstein, Alvarez-buylla, & Manuscript, 2009). Another major difference between the SVZ and the central

canal stem cell niches is that while the adult SVZ is capable of generating neurons throughout adulthood (Kempermann, 2011), the central canal does not appear to. SVZ ependymal cell function seems to be mainly limited to regulating the stem cell niche, although there is evidence that SVZ ependymal cells can function as neural progenitor cells under pathological conditions (Carlén et al., 2009). At present, central canal ependymal cells have not been reported to give rise to neurons in the adult spinal cord.

1.4. Adult spinal cord ependymal cells

Adult central canal ependymal cells are mitotically active, multipotent, self-renewing stem cells (Johansson et al., 1999; Meletis et al., 2008; Shihabuddin, Horner, Ray, & Gage, 2000; Weiss et al., 1996; Xu, Kitada, Yamaguchi, Dezawa, & Ide, 2006). Self-renewal generally occurs in cells with close proximity to blood vessels (Hamilton et al., 2009). Proliferation at steady-state is typically limited to self-renewal, and located predominantly in the dorsal pole of the central canal (Hamilton et al., 2009; Horner et al., 2000). Neurospheres generated from a single ependymal cell can give rise to neurons, astrocytes and oligodendrocytes *in vitro* (Hamilton et al., 2009; Weiss et al., 1996), and have the ability to give rise to neurons when transplanted into neurogenic zones, such as the subgranular zone in the brain *in vivo* (Shihabuddin et al., 2000). Ependymal cells isolated from human spinal cords have the same multipotent and self-renewal capabilities as rodent ependymal cells (Dromard et al., 2008). Spinal cord ependymal cells are more likely to give rise to cells of the astrocyte lineage than cells of the oligodendrocyte lineage *in vivo* both at steady state (Mothe & Tator, 2005) and following injury (Meletis et al., 2008).

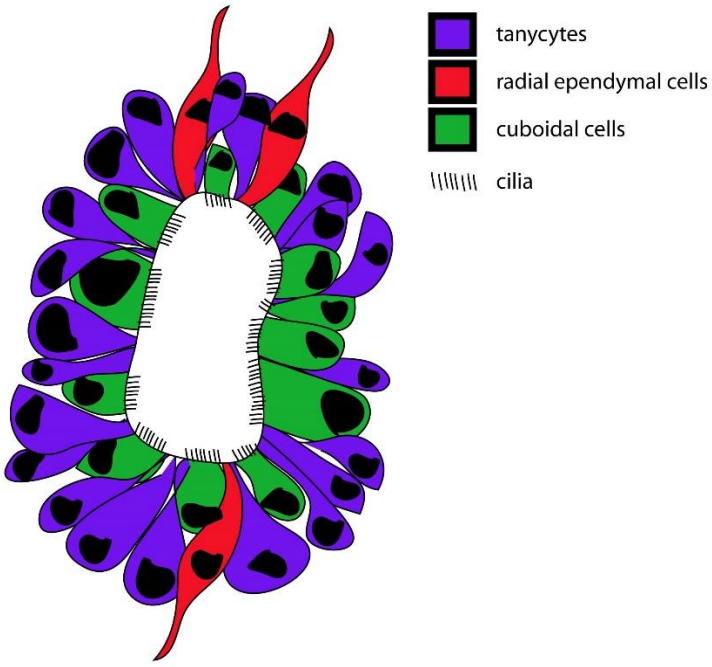

FIGURE 1.1. Three cell types make up the central canal. Radial ependymal cells (red), cuboidal cells (green), and tanycytes (purple). Figure adapted from Meletis et al. (2008)

There are three morphologically distinct ependymal cells that line the central canal in adults: radial ependymal cells, cuboidal ependymal cells, and tanycytes (Fig 1.4.1) (Meletis et al., 2008). Generally, radial ependymal cells have a similar phenotype as embryonic radial glia cells (Meletis et al., 2008; Petit et al., 2011), and are restricted to the dorsal and ventral poles (see Fig 1.2A for a schematic) of the central canal, extending long Nestin+ processes to the dorsal and ventral parts of the white matter, whereas cuboidal ependymal cells are located in the lateral aspects of the central canal (see Fig 1.2B).

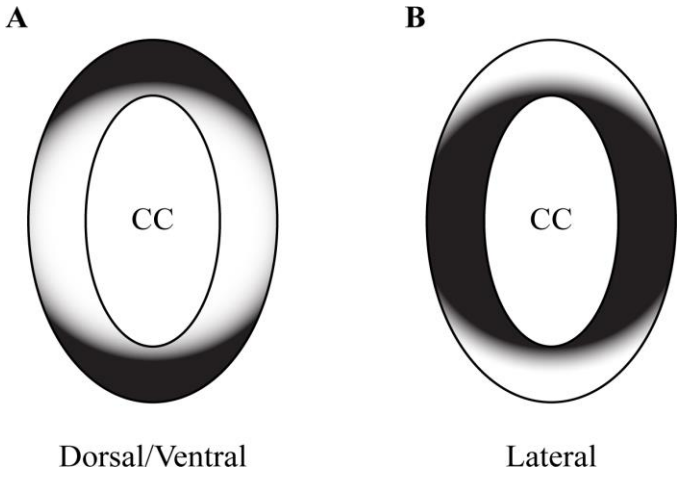

FIGURE 1.2. Dorsal ventral and lateral expression pattern schematic

Several proteins associated with rodent neural stem/progenitor cell function are expressed in the ependymal cells of the spinal cord, often in heterogeneous spatial patterns around the central canal. GFAP, an intermediate filament, is found in type-B astrocytes in the SVZ of the brain (Doetsch, Caillé, Lim, García-Verdugo, & Alvarez-Buylla, 1999), radial glia, and astrocytic neural stem cells surrounding the central canal (Hamilton et al., 2009). GFAP is mainly expressed in processes extending out of the dorsal and ventral poles of the central canal, as well as in cells immediately surrounding the ependymal cell layer, referred to here as the "subependymal area" (Hamilton et al., 2009). Nestin, another intermediate filament expressed by neural stem cells, is also enriched in the processes extending dorsally and ventrally from the central canal (Frisén, Johansson, Török, Risling, & Lendahl, 1995; Hamilton et al., 2009; Meletis et al., 2008). These Nestin+ processes stretch to the edges of the spinal cord along the midline; it is possible that direct damage to these processes enables the ependymal cells to respond following spinal cord injury (SCI), although the central canal cells also respond to injury that does not involve the dorsal and ventral poles of the spinal cord (Meletis et al., 2008). Ki67, a marker of proliferation, is generally

expressed in cells dorsal to the central canal, in the subependymal area, at steady state (Hamilton et al., 2009), but can also be expressed in the ependymal cells themselves following injury (Lacroix et al., 2014). NG2 and Olig2 are expressed in transit-amplifying C-type cells of the oligodendrocyte lineage, and are found in the subependymal area, but neither are found to be expressed in the ependymal cells themselves (Hamilton et al., 2009). Sox2, a transcription factor expressed in neural stem/progenitor cells, is expressed in all ependymal cells and some cells in the subependymal area (Hamilton et al., 2009). The neural progenitor proteins Musashi1 and CD133/prominin, and the ependymal cell proteins Vimentin and S100β are also expressed all around the central canal (Barnabé-Heider et al., 2010; Hamilton et al., 2009).

It is known that neurogenic niches express ECM molecules such as tenascin-C, netrins, laminins, and proteoglycans (reviewed by Kazanis & Ffrench-Constant, 2011). However, the extracellular matrix (ECM) is largely understudied in terms of neural stem cell niche maintenance, although it is known that a stem cell's niche is important for regulating proliferation, differentiation and maintaining stem-ness reviewed by Gattazzo, Urciuolo, & Bonaldo (2014).

Although the individual expression of typical stem/progenitor genes and protein expression patterns in the central canal ependymal cells has been reported, understanding how large-scale gene expression changes spatially and temporally, and how these differences may correspond to the production of new cells from distinct precursor pools has not been fully examined.

1.5. Regeneration in the adult CNS at steady-state

Ependymal cells of the spinal cord form a functional, multipotent stem cell population in both the adult rodent and human (Dromard et al., 2008). The cells present in this niche are capable

of producing all three main cell types (oligodendrocytes, astrocytes and neurons) of the CNS when in the proper environmental conditions (Barnabé-Heider et al., 2010; Dromard et al., 2008; Meletis et al., 2008; Qin, Zhang, & Yang, 2015; Weiss et al., 1996).

Consistent with other tissue types, the innate ability for the spinal cord to recover after injury decreases with age, due to changes in stem/progenitor cell function (reviewed by Yun, 2015). The CNS maintains the ability to regenerate new glial cell types throughout adulthood, but only the SVZ and the subgranular zone of the hippocampus maintain the ability to generate neurons into adulthood at steady state (Altman & Das, 1965; Eriksson et al., 1998; Reynolds & Weiss, 2016). Proliferation in the adult steady-state central canal ependymal cells is mainly limited to self-renewal (Meletis et al., 2008).

The rodent spinal cord maintains a distinct structure throughout life. Conversely, only around 30% of adult humans maintain a detectable central canal, and the remaining 70% of adult central canals collapse into a potentially functional structure called an ependymoma (Garcia-Ovejero et al., 2015). Human central canal ependymal cells, like those in the rodent, are capable of forming neurogenic and gliogenic neurospheres (Dromard et al., 2008). Regardless of whether the central canal is detectable or whether it has collapsed into an ependymoma, human ependymal cells express genes related to stem/progenitor function, such as Sox2, Vimentin, Nestin, and GFAP (Dromard et al., 2008; Garcia-Ovejero et al., 2015).

1.6. Glial regeneration after injury or disease in the adult mammalian CNS

Although rodent adult spinal cord ependymal cells have not been shown to produce neurons *in vivo*, they can produce robust amounts of glia after injury (Barnabé-Heider et al., 2010; Meletis

et al., 2008). Proliferation in the central canal increases after SCI (Frisén et al., 1995; Johansson et al., 1999; Lacroix et al., 2014), but not after demyelinating injury (Lacroix et al., 2014). Proliferation appears to increase only rostral to the injury following contusion SCI, and does not increase caudally (Lacroix et al., 2014). Of the cells produced by the ependymal cell layer following injury, 58% of cells are astrocytes, many of which surround the perimeter of the lesion, 25% of cells are new ependymal cells, and 17% are OPCs (Barnabé-Heider et al., 2010). Although new cells are formed after SCI by OPCs and astrocytes, only ependymal cells are multipotent (Barnabé-Heider et al., 2010). Studies *in vitro* suggest that human ependymal cells have similar multipotent features to rodent ependymal cells (Dromard et al., 2008).

Astrocytes derived from the central canal after traumatic injury contribute to the glial scar (Meletis et al., 2008). The glial scar is important to limit secondary injury and the invasion of reactive inflammatory cells (Faulkner et al., 2004; Okada et al., 2006), however, it inhibits axonal regeneration due to the production of chondroitin sulfate proteoglycans (Busch & Silver, 2007; Silver & Miller, 2004). Aside from ependymal cell-derived astrocytes, new astrocytes are also formed after injury by astrocyte mitosis (Barnabé-Heider et al., 2010) and radial glia proliferation (Petit et al., 2011).

Myelin is an essential component of the nervous system produced by Schwann cells in the peripheral nervous system (PNS) and oligodendrocytes in the CNS. Myelin is important for axon maintenance and survival, as well as for saltatory conduction of nerve impulses (Nave, 2010). Loss of myelin after SCI or in demyelinating diseases such as Multiple Sclerosis (MS) results in dysfunction of nerve impulse propagation and progressive axonal damage and cell death.

Traumatic injury to the spinal cord also results in a widespread loss of myelination (Blight, 1983; Bresnahan, King, Martin, & Yashon, 1976; Totoiu & Keirstead, 2005). The spinal cord is

capable of remyelinating the injured area to an extent, but the efficiency and functionality of the new myelin is not well understood. It appears that transplantation of myelinating cells after injury is beneficial to recovery (Cao et al., 2005; Lee, Yoon, Park, & Lee, 2005; Mitsui, 2005). There is also evidence in rodents that suggests stem cells transplanted into the injury are capable of differentiation into both myelinating cells and neurons, a process that is also associated with functional recovery (Barnabé-Heider et al., 2010; Cummings et al., 2005; Hofstetter et al., 2005). Remyelinating cells in the CNS likely come from the OPC pool, but the central canal ependymal cells also participate in the formation of new myelinating cells (Hofstetter et al., 2005). Remyelination failure during injury or disease is likely attributed to depletion of the OPC pool, loss of axon signals due to axon damage, or inhibition of OPC migration by lingering myelin debris, astrocytes, or microglia (R. J. M. Franklin, 2002).

Research into the spatial heterogeneity of proliferation following injury is just beginning – Lacroix et al., (2014) has shown differences in proliferation along the rostral-caudal axis of the spinal cord – but very little is known about the spatial differences in proliferation following injury within a localized cross-sectional area of the central canal.

1.7. Remyelination in Multiple Sclerosis

MS is a chronic inflammatory demyelinating disease caused by a combination of insufficiently understood genetic and environmental factors (reviewed recently by (Ransohoff, Hafler, & Lucchinetti, 2015). In response to demyelination in MS, attempts at spontaneous endogenous remyelination take place, predominately mediated by OPC-derived oligodendrocytes that infiltrate demyelinated lesions and form new myelin sheaths around denuded axons (Bradl & Lassmann, 2010). However, this newly formed myelin is thinner and internodes are shorter than

normal myelin, and the effectiveness of the new myelin is not well understood (reviewed by R. J. M. Franklin, 2002). Peripheral-type myelinating cells (generally considered to be Schwann cells) have also been found in rare MS spinal cord lesions, rodent models of demyelination, and after human and rodent SCI (Bruce et al., 2000; Ghatak, Hirano, Doron, & Zimmerman, 1973; Guest, Hiester, & Bunge, 2005; Harrison & Pollard, 1984; Jasmin, Janni, Moallem, Lappi, & Ohara, 2000; Nagoshi et al., 2011). Recent transgenic mouse studies have shown that both endogenous and transplanted OPCs can give rise to P_0+ Schwann-like cells after a demyelinating injury (Talbott et al., 2005; Zawadzka et al., 2010). However, as mentioned previously, the endogenous remyelination attempts are usually inadequate and neurodegeneration persists in MS patients (R. J. M. Franklin, 2002). Furthermore, the prevalence, location, and impact of Schwann cell remyelination in the MS spinal cord is poorly understood.

1.8. BLBP, an immature glial protein

Brain lipid binding protein (BLBP), also known as fatty acid binding protein 7 (Fabp7) or B-FABP, is a nervous system-specific fatty acid binding protein. BLBP appears to be involved in the transport of hydrophobic ligands with potential morphogenic activity during CNS development (Feng, Hatten, & Heintz, 1994). BLBP has been shown to have a role in the Notch pathway, and is involved in differentiation of neural and glial cells (Anthony, Mason, Gridley, Fishell, & Heintz, 2005; Feng et al., 1994). BLBP is also expressed in radial glia of the SVZ and spinal cord (Cheng, Pastrana, Tavazoie, & Doetsch, 2009; Petit et al., 2011), and can be found in Schwann cell precursors and immature Schwann cells (reviewed by Jessen & Mirsky, 2005).

Although it comprises a large area of research, MS is still a poorly understood disease. Little is known about the origin of endogenous remyelinating cells in MS, nor why endogenous remyelination attempts are unsuccessful.

1.9. Scope of thesis

We aim to explore the differences in gene expression between a population of ependymal cells with a high level of multipotency and proliferation and a population that is not as active, and apply this to how the central canal may respond following mechanical or demyelinating injury in an attempt to better understand the mechanisms behind endogenous repair.

We also aim to further understand how central canal ependymal cell proliferation changes spatially, both around and along the central canal, and with age and after injury. This will increase understanding of the differences in regenerative capacity of spatially arranged subpopulations of ependymal cells.

Finally, we aim to better understand how progenitor cells participate in the remyelination programme in MS, and why the endogenous remyelination attempts fail.

2. MATERIALS AND METHODS

2.1. Allen Institute for Brain Science images. All *in situ hybridization (ISH)* images (Figures 3.2, 3.3 and 3.6) were taken from the Allen Brain Institute's online P4 and P56 Spinal Cord Atlas (ASCA, brain-map.org), and cropped to size without any further image processing. *ISH*, Nissl and expression mask images are from one mouse per age group.

2.2. Master central canal gene expression analysis. *The work outlined in the following paragraph was performed by Mr Dongho Lee, a Roskams Lab undergraduate student.* Gene names were included in the list if they were categorized as being expressed in the central canal of the ASCA. This resulted in a list of 297 central canal-enriched genes. Genes from this list were input as group queries into GeneMANIA (http://www.genemania.org/ University of Toronto, 2014) based on their temporal or spatial classification. This outputted functionally-related genes including protein and genetic interactions, co-expression, co-localization, pathways and protein domain similarity. Settings were set to default with the following exceptions in the "Number of gene results" section: "50 related genes" and "50 related attributes" per query for P4 only, P4/P56 shared, and P4 lateral genes; and "100 related genes" and "50 related attributes" for genes expressed at P56 only. These genes were then cross-referenced with the ASCA to confirm expression within the central canal. This step was necessary, as some genes were incorrectly mis-categorized as being not expressed in the central canal on the ASCA. This increased the size of the list of genes enriched in the central canal to 363 genes. This master gene list was then separated into age of expression in the ASCA: P4 only (88 genes), P56 only (59 genes), and both (216 genes), representing genes turned off after

development, genes only turned on after development, and genes ubiquitously expressed across the mouse life span.

2.3. Gene Ontology (GO). The entire master gene list was entered as a group query into ToppGene (toppgene.cchmc.org). GO terms were returned, in order from most significant to least significant P-value. The 20 most relevant GO terms were graphed using Microsoft Excel to depict the number of genes from each age group (P4, P56, and both) present in each GO term, and the P-value of each GO term was superimposed on top of the graph.

2.4. Animals. All animal work was performed in accordance with the Canadian Animal Care Committee standards. Animals were split into two cohorts: one group of mice were used for antibody verification and one group were used for ependymal cell proliferation quantification. Antibodies were verified in either P56 or P5 Fabp7::EGFP mice, outbred with Swiss Webster (Charles River), or P90 CD-1 mice (Charles River). For PCNA quantification, animals were either 6 month old FABP7::EGFP mice outbred with Swiss Webster (Charles River) (lysolecithin-demyelination cohort), or 6 month old C57Bl/6 mice (Charles River) (SCI cohort).

2.5. Lysolecithin-induced demyelination. *This procedure was carried out by Dr Jie Liu with the assistance of Mr Greg Duncan and Mr Raymundo Aguas*. Eight 6-month old mice, 4 males and 4 females, received buprenorphine as an analgesic (30 ug/kg body weight), and isofluorane as anesthetic. The cervical spinal column was surgically exposed, and a dorsal C4 laminectomy was performed to expose the underlying cord. 0.5uL of lysolecithin (i.e. LPC, L-α-lysophosphatidylcholine 1%, Sigma) was injected using a stereotaxic pump into the dorsal column at C4 at approximately a 45° angle over a 15 minute span. Tissue was sutured closed and animals were allowed to recover. Four animals (2 males and 2 females)

were sacrificed after 7 days, and four animals (2 males and 2 females) were sacrificed 3 weeks post lesion (WPL).

2.6. Thoracic crush SCI (described in Plemel et al., 2008). *This procedure was carried out by Drs Tao Meng and Audrey Petit, assisted by Mr Brett Hilton. Behavioural tests were performed by Mr Greg Duncan and Dr Tao Meng.* Three male 3.5 month old C57Bl/6 mice, had a severe (0.2mm) forceps crush injury at the T7 level of the spinal cord. Animals were sacrificed at 10.5 weeks post-injury. Prior to injury, all three animals reached level 9 on the BMS scale and were catwalk-trained before surgery. All animals experienced hindlimb paralysis, but most regained bladder function before the experiment endpoint.

2.7. Tissue processing, mouse. *The Fabp7 mice used in the lysolecithin portion of the proliferation quantification were processed for immunofluorescence by Mr Raymundo Aguas, and the C57Bl/6 mice used in the SCI portion of the proliferation quantification were processed for immunofluorescence by Drs Tao Meng, Audrey Petit and Ms Kathryn Westerndorf. All other animals were processed by the candidate, Kathryn Douglas.* In accordance with the Canadian Animal Care Committee standards, adult and neonatal mice were anesthetized with 25 mg/ml xylaket: [120 mg/kg ketamine HCL (MTC Pharmaceuticals, Cambridge, ON) and 12 mg/kg xylazine (Bayer, Tarrytown, NY), 15% ethanol, 0.55% NaCl], perfused transcardially with 0.1 M phosphate buffered saline (PBS) and/or 4% paraformaldehyde (PFA) in PBS. Whole vertebral columns were extracted, and then the spinal cord was dissected or removed from the column using hydrostatic pressure, and then post-fixed overnight in 4% PFA at 4°C. The spinal cords were then cryoprotected in a sucrose gradient (10% and 30%) before being embedded in OCT Tissue-Tek medium (Sakura Finetek, Torrance, CA) and frozen using an isopentane/dry ice bath. Cryosections

were prepared (12 μM) and stored at −20°C. Cords were then transversely sectioned at 14um on an HM-500 cryostat (Micron) and mounted onto positively charged Superfrost glass slides (Fisher). Slides were stored at -20°C until used.

2.8. Tissue Processing, human. Human tissue was collected by Dr Moore's laboratory in accordance with the Clinical Research Ethics Board of the University of British Columbia. All cases had formal autopsy consent. Human spinal cords were obtained from 6 patients (4 MS cases: 1 primary progressive MS and 3 unknown MS, mean age 57.5 years [range 41-68 years], 2 females and 2 males; two non-MS cases, mean age 78 years [range 77-79 years], 1 female and 1 male). Post-mortem tissue was resected and fixed in 10% formalin, embedded in paraffin blocks, and sectioned at 5μm thickness. The postmortem interval (PMI), or time from when the patient expired until embedding into paraffin, where available is given in table 2.1.

Table 2.1 **- Patient information**

Patient ID	paper ID	age (years)	sex	duration (years)	diagnosis	PMI (days)
3	1	61	f	NA	MS	NA
228	2	68	m	16	PPMS	3
276	3	60	m	15	MS	4
277	4	41	f	>17	MS	6
1	5	79	m	NA	control	NA
110	6	77	f	62	SCI	1

2.9. Immunofluorescence detection. As the human tissue sections were embedded in paraffin, a deparaffinization procedure was applied before the immunostaining: three 3-minute immersions in each of xylene (Life Technologies), 100%, 95%, and 75% ethanol; followed by two washes in phosphate-buffered saline (PBS). Following deparaffinization,

the remainder of the immunofluorescence procedure was the same as in the mouse tissue. Sections were permeabilized by boiling in citric acid (0.1M pH 6.0, Sigma) for 10 mins and then being allowed to cool at room temperature for 10 minutes, followed by 30 mins in 0.1% triton X-100 (Sigma). Non-specific binding sites were blocked with 10% normal donkey or goat serum (Millipore)/2% bovine serum albumin (BSA; Life Technologies) (5% normal serum/1% BSA for mouse sections) at room temperature for 30 minutes. Immunodetection was performed by incubating slides overnight (16-20 hours) in primary antibody (see Table 2.2) diluted in 5% normal serum + 1% BSA (2.5%/0.5% respectively, for mouse tissue) in PBS at 4°C. Next, slides were incubated with secondary antibodies conjugated to Alexa fluorescent labels (either Alexa-488, -594 or -647; Jackson Labs Technologies, Inc. and Invitrogen). Sections were counterstained with 0.5mg/mL diaminopyridine imidazole (DAPI) for 5 minutes at room temperature, and then coverslips were mounted using FluoroShield mounting media (Abcam) or ProLong Gold Antifade (Life Technologies)

***Table 2.2* - Antibody information**

Antigen	Description	Host	Manufacturer	Dilution
ADAMTS20	Disintegrin and metalloproteinase	Goat	Santa Cruz	1:50
BLBP	Brain lipid binding protein	Rabbit	Millipore	1:500
BLBP	Brain lipid binding protein	Mouse	MyBiosource	1:1000
GFAP	Glial fibrillary acidic protein	Chicken	Aves	1:1000
GFP	Green fluorescent protein	Chicken	Aves Lab	1:500
MBP	Myelin basic protein	Rat	Millipore	1:500
Nestin	Type VI intermediate filament	Rabbit	Abcam	1:100
Nestin	Type VI intermediate filament	Rabbit	Covance	1:500
P_0	Myelin protein zero	Chicken	Aves	1:100
PCNA	Proliferating cell nuclear antigen	Mouse	Sigma	1:5000
phallotoxin - actin phalloidin	Actin filaments	N/A	Invitrogen	1:100
PLP	Proteolipid protein	Chicken	Aves	1:2000
Rb1	Retinoblastoma-1 cell cycle regulator	Mouse	BD Pharmingen	1:25
SMI-312	Pan-neurofilament	Mouse	Covance	1:2000
Sox2	Transcription factor to maintain pluripotency	Rabbit	Abcam	1:500
TrkB	Neurotrophic tyrosine kinase type 2	Goat	Santa Cruz	1:100
Vimentin	Type III intermediate filament	Mouse	Accurate	1:500

2.10. Image Acquisition. Images shown in Fig. 3.5, 3.7 and 3.8 were captured using a Fluoview FV1000 laser scanning confocal microscope (Olympus) using a 60x or 100x oil immersion objective (NA 1.35) at 1μm slices on the z-plane. Images shown in Fig. 3.9-11 were captured using an Axioplan II fluorescence microscope (Zeiss) with a Retiga 1350EX camera (Quantitative Imaging Corporation) with Northern Eclipse software (Empiz Imaging, Inc.) and AxioVision software (Zeiss). All images were minimally altered for clarity using Adobe Photoshop CS3, Adobe Illustrator CS2, and ImageJ (NIH, USA).

2.11. Cell Proliferation Quantification. A minimum of 7 mouse spinal cord sections were selected, at least 40um apart, along the length of the spinal cord (or spinal cord region, i.e. the rostral half of the thoracic spinal cord; T12, etc., as indicated below), and immunostained with Nestin, PCNA and DAPI (see antibody table, table 2.2) Images were captured on a laser scanning microscope throughout the z-axis to sample the entire thickness of the tissue and then minimally adjusted using Adobe Photoshop CS3, to enhance clarity of PCNA-immunoreactive nuclei. The experimenter was then blinded to animal identity and condition. The images were oriented using Nestin-immunoreactive cell processes to define the dorsal and ventral poles of the central canal, and then straight lines were superimposed on the images at right angles to the dorsal/ventral axis, perpendicular to the dorsal- or ventral-most aspect of the central canal lumen (Fig. 2.1). This segmented the ependymal cells into dorsal, ventral and lateral groups, with a greater surface area of ependymal cells represented by the lateral aspects than the dorsal/ventral poles. PCNA+ nuclei were manually counted in the ependymal cell layer only in the dorsal and ventral portions (these counts were pooled, and considered “dorsal/ventral”), and lateral portions. Total cell numbers were also counted, and compared to the sum of the

dorsal/ventral and lateral cell counts to ensure a match. Total PCNA+ cell counts were graphed using GraphPad Prism 4 (GraphPad Software, Inc), and a one-way ANOVA with a Bonferroni post-hoc test was applied to determine the difference between each experimental group (1WPL and 3WPL LPC; SCI) and the control group (naïve). Then, PCNA+ cell counts were split into dorsal/ventral and lateral groups, and graphed using GraphPad Prism 4. For the SCI analysis, PCNA+ cell counts were also split into either rostral (T1-2) or caudal (T12) to the injury. The controls for the SCI quantification were split into either less than 4.2mm into the thoracic spinal cord or greater than 4.2mm into the thoracic spinal cord. Then, for both the LPC and the SCI analyses, each transverse spinal cord section was split into the dorsal/ventral and lateral sub-regions as described above. For the statistical analyses, a two-way ANOVA was performed, followed by a Bonferroni post-hoc test, to compare each region (lateral, dorsal/ventral) to the other region at the experimental time point, and to the naïve group in the same region. The Bonferroni test was chosen over the Tukey post-hoc test, as the number of animals in each experimental group was relatively small.

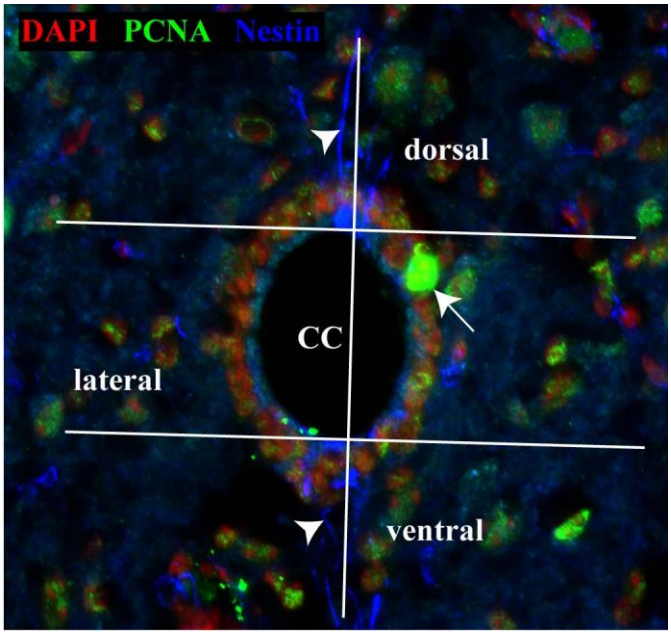

FIGURE 2.1. Procedure for determining dorsal, ventral, and lateral sub-regions of the central canal. Nestin (blue; arrowheads) was used to orient the dorsal/ventral axis, and then two lines at 90° to this line were superimposed on to the image, aligned with the boundaries of the central canal lumen. PCNA (green; arrow) cells were then counted in each sub-region.

2.12. MS within-patient radiculopathy analysis. Images were split into single channels, and three equal-sized regions (5000um^2) were delineated for quantification. The multi-point tool was used on ImageJ to count loose P_0+ myelin rings, total P_0+ myelin rings, thinly/unmyelinated SMI312+ axons and total SMI312+ axons within each unit area. The number of P_0+ myelin rings devoid of axons was difficult to manually count, so their number was determined using the formula #total P_0+ rings – (#total SMI312+ axons + #thinly myelinated axons).

3. RESULTS

3.1 Spatiotemporal gene discovery and categorization workflow

The ependymal cell layer surrounding the central canal of the spinal cord contains the primary stem/progenitor pool in the adult rodent spinal cord (Barnabé-Heider et al., 2010). These ependymal cells are thought to be remnants of the embryonic radial glia, which gave rise to glia and neurons during spinal cord development (Fu et al., 2003; Masahira et al., 2006; N. Spassky, 2005). Although the adult spinal cord lacks the endogenous ability to regenerate neurons, as neurogenesis is still progressing in the neonatal rodent spinal cord, there is a greater capacity to recover functionality following injury. In an attempt to understand if there are molecular differences in the ependymal cells between the neonate and the adult, and to help further understand the functionality of the neural stem cell niche before and after injury, we used a combination of data mining, gene ontology, and immunofluorescence techniques to determine how the ependymal cell niche may diverge both temporally and spatially.

The ASCA is an open resource with *ISH* data for ~20,000 genes sampled across the length of the mouse spinal cord at P4 (Postnatal day 4; neonate) and P56 (Postnatal day 56; adult); these ages correspond to neurogenic (P4) and non-neurogenic (P56) life stages. We[1] mined the ASCA for gene expression patterns in the central canal across age and location within the spinal cord transverse sections. Of the genes available on the ASCA, 297 were initially identified as being expressed in/around the central canal (Fig. 3.1). Eighty-two of these genes were expressed only in the neonatal spinal cord, 197 genes were expressed at both ages, and 18 genes were expressed

[1] Data mining was performed by Mr Dongho Lee.

solely in the adult. To test for additional, related genes, and to ensure no genes expressed in the central canal were missed by the ASCA, we[2] entered each of the 297 genes into GeneMANIA, an online software tool that returns other gene names associated with the query gene. This increased our gene list to 495 genes total. As GeneMANIA analysis does not include information on the spatial expression of the genes, we then verified the expression of the additional 198 genes in the central canal by closely analyzing the *ISH* images on the ASCA. This search excluded 132 genes not in the central canal, leaving us with a total list of 363 genes expressed in all or part of the central canal at either P4 or P56. This list was split into three temporal groups: 88 genes expressed at P4 only, 216 at both P4 and P56, and 59 genes expressed at P56 only. The ASCA information allowed us[3] to also group our genes into spatial patterns, relative to the central canal: genes enriched all around the central canal, and those enriched in the dorsal and ventral poles, or the lateral aspects of the canal (see introduction figure 1.2 for diagram). The temporal and spatial information was combined to allow visualization of how gene expression in the central canal changes both spatially and temporally (Fig 3.1C, Fig. 3.2A,B). The majority of genes in our list are expressed at both P4 and P56, but there are 88 genes that are expressed only in the neonatal mouse spinal cord central canal, and 59 genes that are only expressed in the adult central canal. These temporally distinct genes are of particular interest, as they may be responsible for the differences in neurogenesis and gliogenesis between the two developmental ages. For a complete list of genes, and their corresponding temporal expression patterns, see appendix A.

We found that the neonate has considerably more genes expressed in distinct spatial patterns than the adult (Fig 3.2A,B): of all 304 genes expressed at P4, 14.5% are enriched in spatial

[2] GeneMANIA analysis was performed by Mr Dongho Lee
[3] ASCA spatial patterning information compiled by Mr Dongho Lee

patterns in either the dorsal and ventral poles (16 genes) or the lateral aspects (28 genes). This heterogeneity is greatly decreased in the adult, as only 1.8% of all 275 genes expressed in the adult are enriched in a spatial pattern (3 genes enriched in the dorsa/ventral poles, 2 genes enriched in the lateral aspects. The distinct spatial subpopulations at P4 which are not maintained at P56 are worthy of further investigation, as cells could be the most actively involved in neurogenesis and gliogenesis. For a list of all gene names and their spatial expression information, see appendix A. The spatial and temporal patterning outlined in Fig 3.1 help us to appreciate the mechanisms behind how the central canal ependymal cells may be regulated differently in the neonate compared to the adult.

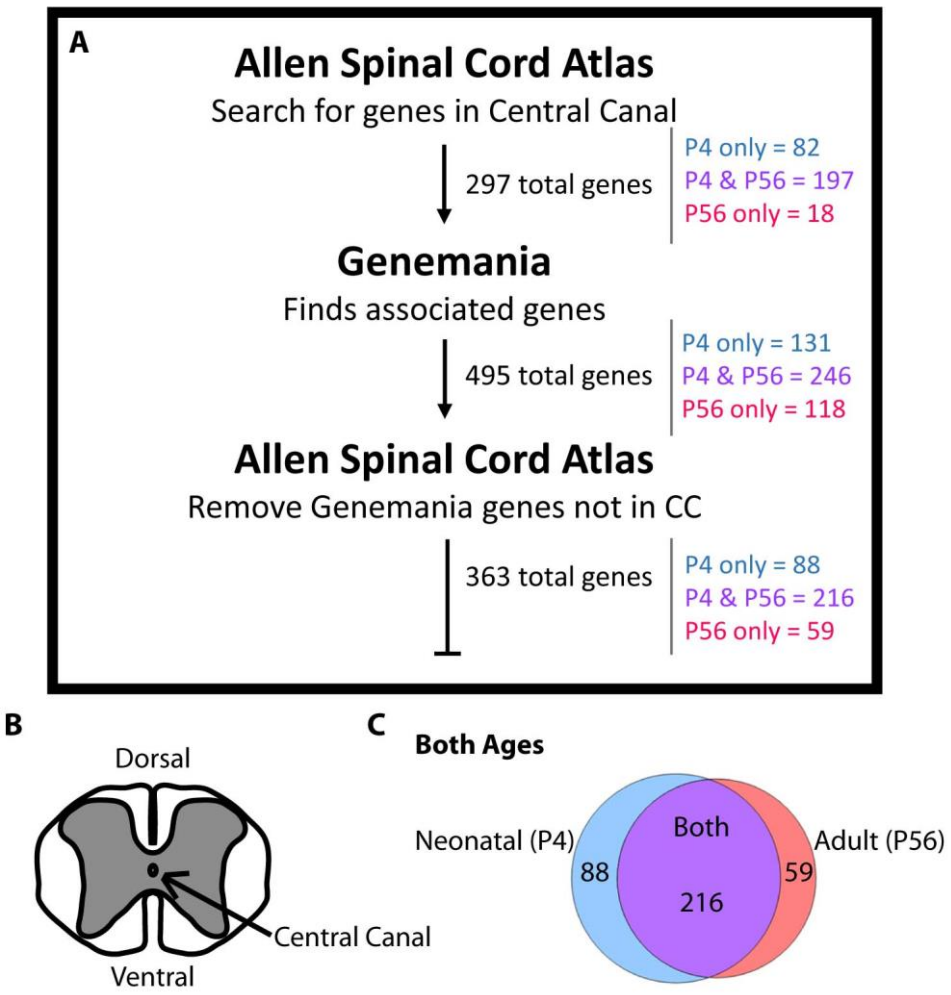
A
Allen Spinal Cord Atlas
Search for genes in Central Canal
297 total genes
P4 only = 82
P4 & P56 = 197
P56 only = 18
Genemania
Finds associated genes
495 total genes
P4 only = 131
P4 & P56 = 246
P56 only = 118
Allen Spinal Cord Atlas
Remove Genemania genes not in CC
363 total genes
P4 only = 88
P4 & P56 = 216
P56 only = 59
B
Dorsal
Central Canal
Ventral
C
Both Ages
Neonatal (P4)
Both
Adult (P56)
88
216
59

Figure 3.1

FIGURE 3.1. Workflow and gene ontology analysis overview. The ASCA has *ISH* data for ~20,000 genes expressed in the mouse spinal cord. (A) Of these, 297 genes are classified as being expressed in/around the central canal: 82 genes only expressed in the neonatal (P4) central canal, 197 genes expressed at both P4 and P56, and 18 genes expressed only in the adult (P56) central canal. We used GeneMANIA, an online software tool that returns lists of genes associated with a query gene, to increase the pool of genes analyzed to 495 and ensure no genes were missed in our analyses. Because GeneMANIA does not include spatial expression information, we then returned to the ASCA to remove genes from the lists that could not be confirmed to be expressed in the central canal, giving us a list of 363 total genes. (B) Shows a schematic of the mouse spinal cord, with the central canal in the middle of the grey matter (arrow). (C) A Venn diagram enables visualization of the shift in gene expression with time. C) 216 genes are expressed at both time points (purple), 88 genes are expressed only in the neonate (blue), and 59 genes are only expressed in the adult (red). Venn diagram is to scale.

3.2 Spatial patterning in the central canal

Heterogeneity in both the morphology and expression pattern of ependymal cells in the central canal, in both the neonatal and adult spinal cord has been outlined previously (Hamilton et al., 2009). Meletis et al. (2008) showed that ependymal cells can be split into three morphologically distinct groups: radial, cuboidal and tanycyte. Radial ependymal cells are almost always exclusive to the dorsal and ventral poles of the central canal, whereas tanycytes and cuboidal ependymal cells are found throughout the central canal (introduction fig. 1.4.1). Intermediate phenotypes (i.e. cells with overlapping characteristics) are also present (Meletis et al., 2008). Further, it has been shown that several proteins involved in neural stem/progenitor function are differentially expressed or enriched in subpopulations of cells surrounding the central canal (Hamilton et al., 2009; Petit et al., 2011).

In order to further characterize this heterogeneity, we split the ASCA central canal *ISH* data into three spatial groups (dorsal/ventral, lateral, and all around: see introduction figure 1.2). The neonatal central canal has more spatially-arranged genes than the adult central canal (Fig. 3.2A,B). Of all the genes expressed in the central canal at P4, 5.2% were enriched in the dorsal/ventral poles, compared to only 1% of genes at P56. Similarly, 9.2% of all genes expressed at P4 were enriched in the lateral aspects, compared to 0.7% at P56. Four examples of genes displaying typical "dorsal/ventral" expression patterns are shown[4] in Fig 3.2 C-F, and four examples of genes displaying "lateral" expression patterns are shown in Fig 3.2G-J; all images in Fig 3.2 are from the neonatal spinal cord data of the ASCA. The spatial patterns account for a range of expression levels within the categorization – mRNA may be expressed at a low level in

[4] All *ISH* images are from the ASCA

the rest of the central canal, provided it is highly enriched in the cells of the pattern category it has been assigned to (for example, see Fig 3.2D). This spatial expression data enables us to appreciate how subpopulations of cells surrounding the central canal may have the potential to behave and perform in very different ways, even though a quick glance may mislead one to assume all of the ependymal cells function similarly.

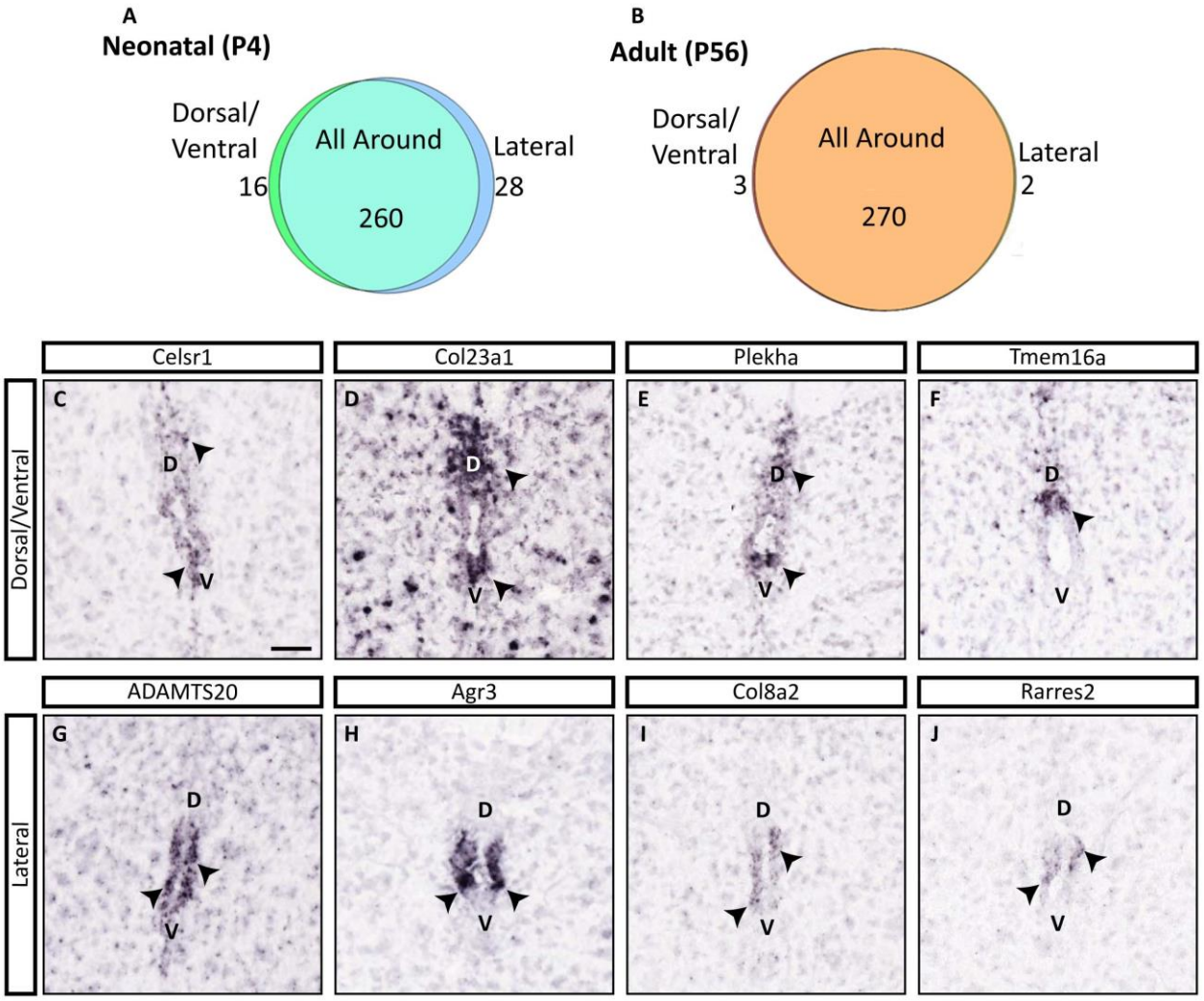
A
Neonatal (P4)
Dorsal/
Ventral
16
All Around
260
Lateral
28
B
Adult (P56)
Dorsal/
Ventral
3
All Around
270
Lateral
2
Celsr1
Col23a1
Plekha
Tmem16a
Dorsal/Ventral
C
D
E
F
D
V
ADAMTS20
Agr3
Col8a2
Rarres2
Lateral
G
H
I
J

Fig. 3.2

FIGURE 3.2. Genes in the central canal are expressed in different spatial patterns. Venn diagrams enable visualization of the spatial distribution of genes in the neonate versus the adult; the neonate (A) has 16 genes enriched in the dorsal and ventral poles (green) and 28 genes enriched in the lateral aspects (blue) of the central canal, whereas the adult (B) only has 3 genes enriched in the dorsal/ventral poles (yellow) and 2 enriched in the lateral aspects (red). Four examples of ASCA *ISH* data from the P4 mouse illustrates variability within spatial categorizations: all around (not shown), dorsal/ventral-enriched (C-F) and lateral-enriched (G-J). Some dorsal/ventral-grouped genes are expressed at similar levels in the dorsal and ventral poles (C; arrows), but some are more highly expressed in the dorsal pole (D, F; arrows) or the ventral pole (E). In the lateral group, some gene expression is excluded in only a few dorsal/ventral cells (G), or may be excluded from all cells in the dorsal and ventral poles (H-J). Sometimes, genes are not enriched in all lateral cells, but are still excluded from the dorsal and ventral poles (J). Scale bar 100μm. Venn diagrams are to scale.

3.3 Temporal patterning in the central canal

Like many other parts of the body, the CNS of neonatal mammals has a greater capacity to regenerate tissue following injury than the adult rodent spinal cord (Yun, 2015). As outlined in Fig 3.1, there is a difference in gene expression between the neonatal and adult spinal cord: some genes that are expressed in the neonate are not expressed in the adult, and vice versa. However, after further analysis of the genes that are expressed at both ages, we report that the spatial expression of many genes shifts between the two ages (Fig 3.3). Some genes shift from dorsal/ventral (Fig. 3.3A) to dorsal only (Fig. 3.3E), dorsal/ventral to all around (Fig. 3.3B vs Fig. 3.3F), or lateral to all around (Fig. 3.3 C vs G). Further, the general pattern can remain between age groups, but the expression levels can change (Fig. 3.3D vs H). The master list of all genes and their temporal expression information is found in Appendix A.

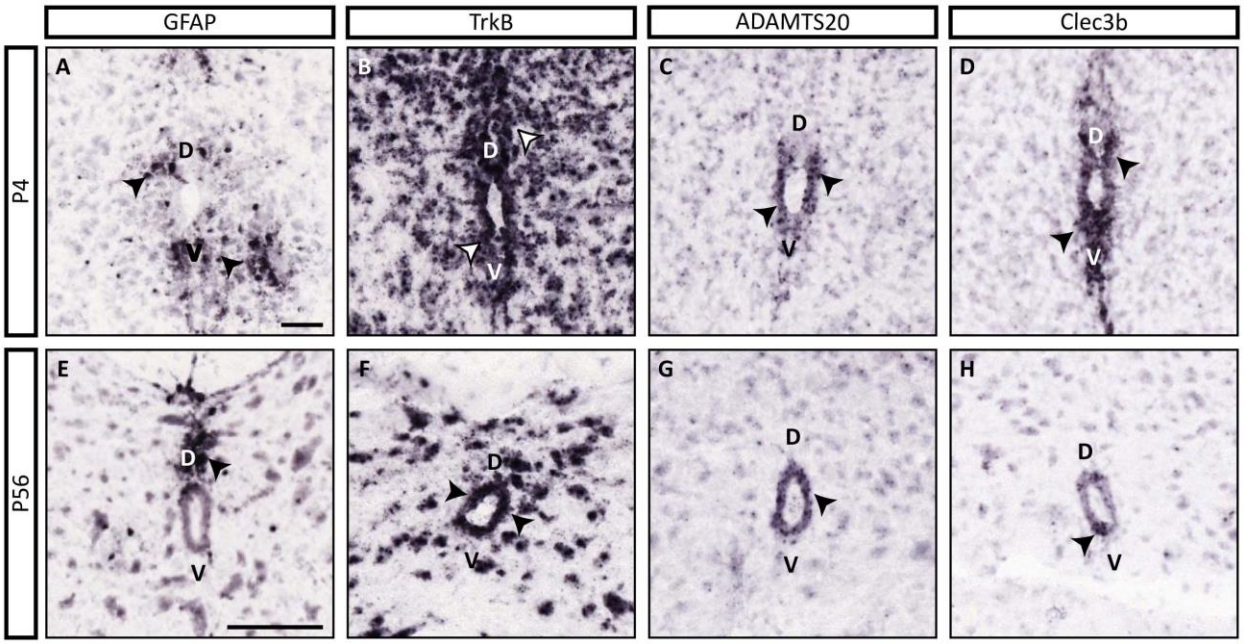

FIGURE 3.3. A subset of genes in the central canal are expressed in different distributions temporally. Four examples from the ASCA of neonatal (P4; A-D) versus adult (P56; E-H) *ISH* data illustrate variability in gene expression around the central canal in a variety of genes relevant to neurogenesis or stem/progenitor activity. "D"/"V" orients the dorsal and ventral poles of the central canal. Common temporal pattern shifts include dorsal/ventral to dorsal only (A vs E; arrowheads), dorsal/ventral to all around (B vs F; arrowheads), lateral to all around (C vs G; arrowheads), and dorsal/ventral to dorsal/ventral with decreased expression (D vs H; arrowheads). Scale bars 100μm.

3.4 Gene ontology analysis highlights genes involved in neural stem/progenitor function

Having discovered spatially and temporally patterned novel subgroups of genes expressed in the central canal, we aimed to learn more about their putative function. We hypothesized that different pathways would be utilized in the neonate compared to the adult, as there is a large difference in neurogenesis and gliogenesis between these two ages. Using ToppGene (toppgene.cchmc.org) to determine the pathways our gene lists were involved in, we found the 20 most relevant pathways to both age groups, and confirmed that while there are some pathways in common between P4 and P56, different pathways are also present (Fig. 3.4; list of 20 most relevant pathways in Appendix B). The p-value, or how relevant a pathway is to the list of genes, is plotted on the right y-axis and the top 20 most relevant pathways are ordered from most to least relevant (Fig. 3.4A). For clarity, the data in Fig. 3.4A is also summarized in Fig. 3.4B, highlighting global temporal patterns. For example, we show that, out of genes involved in cell and cytoskeletal motility, a high proportion are expressed in both ages, yet there are still a large number of genes that are specific to the P4 or the P56 central canal (Fig. 3.4B). The same is true of genes involved in cell projections and processes (Fig. 3.4B). In contrast, and perhaps unsurprisingly, a higher percentage of genes involved in development are unique to the neonatal central canal. In addition, the adult mouse central canal expresses a different subset of unique genes associated with development (Fig. 3.4B). Finally, a larger percentage of specialized genes involved in the ECM are unique to the adult central canal compared to the neonate (Fig. 3.4B). These data have allowed us to further appreciate the mechanisms behind the differences in stem/progenitor function in the neonatal and adult spinal cord central canal.

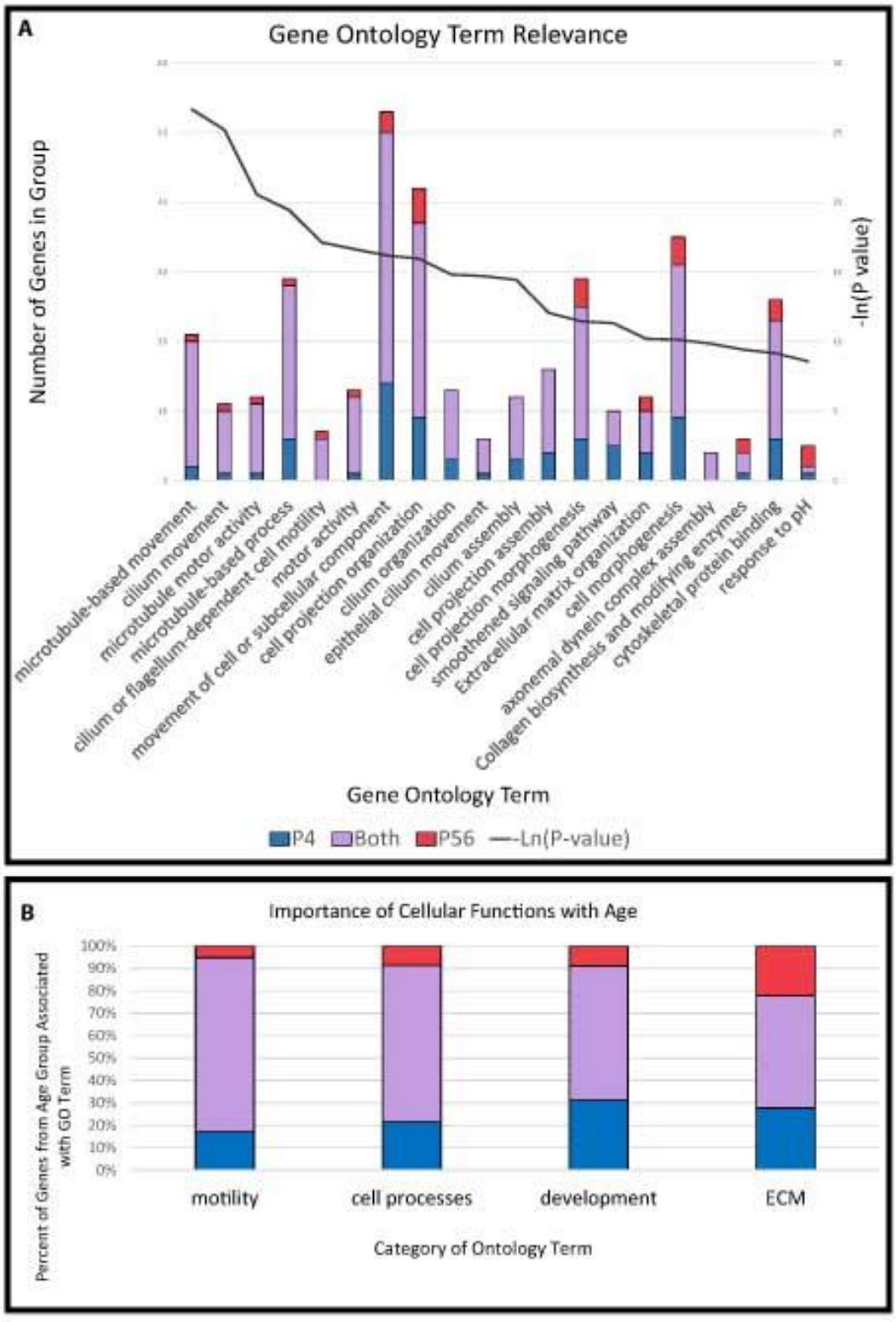
A
Gene Ontology Term Relevance
Number of Genes in Group
-ln(P value)
microtubule-based movement
cilium movement
microtubule motor activity
microtubule-based process
cilium or flagellum-dependent cell motility
motor activity
movement of cell or subcellular component
cell projection organization
cilium organization
epithelial cilium movement
cilium assembly
cell projection assembly
cell projection morphogenesis
smoothened signaling pathway
Extracellular matrix organization
cell morphogenesis
axonemal dynein complex assembly
Collagen biosynthesis and modifying enzymes
cytoskeletal protein binding
response to pH
Gene Ontology Term
P4
Both
P56
Ln(P-value)
B
Importance of Cellular Functions with Age
Percent of Genes from Age Group Associated with GO Term
100%
90%
80%
70%
60%
50%
40%
30%
20%
10%
0%
motility
cell processes
development
ECM
Category of Ontology Term

Figure 3.4

FIGURE 3.4. Genes in the central canal have different functions, and different functions are utilized at different ages. (A) Genes that are enriched in the central canal ependymal cells were grouped by age and putative function, and the percentage of genes in each group was plotted on the left y-axis. (A,B) Genes are either expressed at P4 (blue bars), both P4 and P56 (lilac bars) or P56 (red bars). (A) The inverse ln of the P-value (black line) for the gene ontology groups was plotted along the right y-axis, demonstrating the importance of each ontology term to the function of the cells at that age. (B) To summarize which age groups a given subgroup of ontology terms is most relevant to, the numbers of genes expressed at each age category were also plotted as a percent of the total number of genes in that particular subgroup of genes.

3.5 Establishing the similarity of protein expression patterns to gene expression patterns

Having furthered our understanding of how pathways are utilized differently between the neonatal and adult mouse spinal cord central canal, we next aimed to test if key genes were enriched in cells with a known phenotype. There are several proteins frequently used to identify neural stem/progenitor cells: some of these proteins are only expressed in stem/progenitor cells, such as Sox2 and Nestin, whereas some genes are enriched in progenitor cells but also expressed in differentiated cells (for example, the intermediate filaments GFAP and Vimentin). The expression patterns of these genes around the central canal has helped us understand the diversity of cells surrounding the central canal. We have combined our ASCA spatial/temporal gene expression and ToppGene GO analyses to choose three candidate genes implicated in different niche maintenance function to further characterize subpopulations of ependymal cells: ADAMTS20, Rb1, and TrkB (Fig 3.3).

ADAMTS20 is a matrix metalloproteinase (MMP) that, according to the ASCA *ISH* data, is expressed in the neonate and the adult (Fig 3.3 C,G), in a lateral-only (P5) or all-around (P56) pattern. ADAMTS20 is putatively implicated in neuroepithelial cell differentiation (see appendix A). As it is an MMP, we can infer that ADAMTS20 may perform its role in cell differentiation by helping orchestrate the adherence of ependymal stem cells to their niche. When the central canal of the neonate and the adult is tested for colocalization of ADAMTS20 with actin filaments, it is expressed adjacent to the lumen of the lateral ependymal cells only, in the apical cell border (Fig. 3.5A,B, arrows). This observation is consistent with the spatiotemporal patterning predicted from the ASCA data and a putative function in regulation of adherence to the central canal. ADAMTS20 expression did not overlap with GFAP+ or Nestin+ ependymal cell processes in the neonate or the adult central canal (arrows, Fig. 3.5A), but was coexpressed with actin (Fig. 3.5B) in the apical

cell region of the lateral ependymal cells only, confirming that ADAMTS20 is expressed intracellularly, and localized in lateral subsets of central canal ependymal cells (arrows, Fig. 3.5B).

Rb1 is a cell cycle regulation protein in stem cells that, according to the ASCA data, is only expressed in the neonate ependymal cells, and is not predicted to be expressed in the adult. It is a known oncogene and binds several transcription factors (reviewed by Korenjak & Brehm, 2005), thus we expect the protein to be localized in the nucleus. In accordance with the ASCA and the GO analyses, we did not find Rb1 in the adult central canal, but rare Rb1+ ependymal cells surrounding the central canal were found in the neonate (arrow, Fig 3.5 C). These Rb1+ cells were found predominantly in the lateral aspects of the central canal, and always coexpressed Sox2.

TrkB is a neurotrophic receptor protein critical for neurogenesis, neuron survival and oligodendrocyte differentiation (Barnabe-Heider & Miller, 2003; McTigue, Horner, Stokes, & Gage, 1998). According to the ASCA data, TrkB is expressed in most of the cells surrounding the central canal at both P4 and P56, and a few cells near the central canal, especially radiating from the dorsal and ventral poles (Fig. 3.3B,F). However, TrkB protein was not detected around the central canal at P4/5 (data not shown) and was not detected in the ependymal cells immediately surrounding the central canal at P56 (Fig 3.5D and data not shown). TrkB was, however, expressed in rare cells immediately surrounding the ependymal cell layer in the "sub-ependymal" region (arrows, Fig. 3.5D). These cells were not found at the dorsal and ventral poles of the central canal.

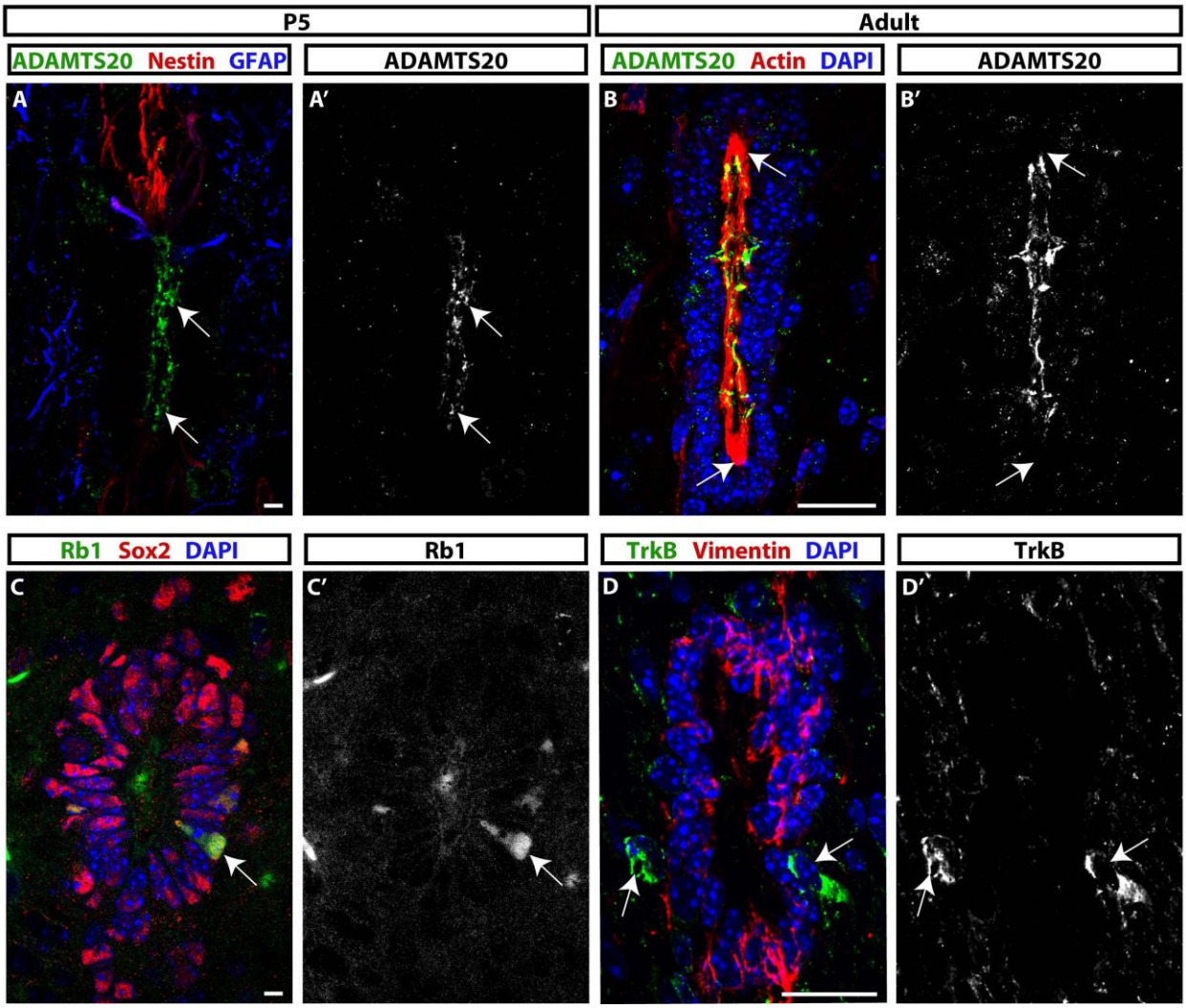
P5
Adult
ADAMTS20 Nestin GFAP
ADAMTS20
ADAMTS20 Actin DAPI
ADAMTS20
A
A′
B
B′
Rb1 Sox2 DAPI
Rb1
TrkB Vimentin DAPI
TrkB
C
C′
D
D′

Figure 3.5

FIGURE 3.5. Proteins putatively involved in neurogenesis are expressed in the central canal at P5 and in the adult, in spatially- and temporally-defined patterns. ADAMTS20, a matrix metalloproteinase putatively involved in maintaining cell-basal lamina adhesion in the central canal ependymal cells is expressed at both P5 (A,A') and adult (B,B'). (A) ADAMTS20 (green) expression is concentrated immediately surrounding the lumen of the P5 central canal (arrows), and is not in GFAP+ (blue) or Nestin+ (red) processes. ADAMTS20 alone is shown in A'. (B) In the adult central canal, ADAMTS20 (green) is also enriched immediately surrounding the central canal, and mostly overlaps with the actin (red) found in the ependymal cell apical border. ADAMTS20 is only found in the apical cell boarder of the lateral aspects of the central canal (arrows), not in the dorsal and ventral poles of the central canal. B' shows the ADAMTS20 single channel from B. (C) The cell cycle regulator protein, Rb1 (green) is found in rare Sox2+ (red) cells in the ependymal cell layer in P5 mice (arrow); usually these cells are not found in the dorsal/ventral poles of the central canal. The single channel of Rb1 is shown in C'. (D) TrkB+ cells (green) are not found in the ependymal cell layer, but rare TrkB+ cells are found near the ependymal cells, usually laterally to the central canal (arrows). TrkB alone is in panel D'. Scale bars 10μm.

3.6 Proliferation in the central canal is not uniform across space and time

Having established novel gene and protein expression changes with space and time in the mouse spinal cord central canal, we next turned our attention to exploring how the production of new cells by the central canal changes with the spatiotemporal patterns previously described. As the amount of new cells being produced in the neonatal mouse spinal cord is higher than the amount of cells produced in the uninjured adult central canal, we expect there to be more cells expressing proliferating cell markers at P4 than at P56. However, little is currently known about the spatial locations of proliferating cells in the central canal at either age, and whether they relate to distinct cell phenotypes. It is though that, during development, there are two waves of ependymal cell production (Ševc et al., 2011). It is possible that the radial ependymal cells are produced first and reside in the dorsal and ventral poles (Meletis et al., 2008; Ševc et al., 2011). A second wave of ependymal cells are produced in the neonatal rodent (approx. P8-15), which give rise to the cuboidal ciliated cells in the lateral aspects of the central canal (Ševc et al., 2011). Therefore, we expect there to be different levels of proliferation at the two ages between these spatial populations. Although for any given gene, the ASCA only has *ISH* data from one animal per developmental age, there is still robust data to be gleaned from the ASCA, particularly regarding the populations of cells within each age. We used the ASCA to determine how location and age affects the amount of proliferating cells. The ASCA has the option of viewing the images as "ISH image", "Nissl stain" or "Expression mask"; we used the "Expression mask" option to generate a heat map of PCNA expression, and superimposed these images onto the "Nissl stain" image to enable us to verify if the expression was in the ependymal cell nuclei (Fig. 3.6D-E). We took all of the transverse spinal cord images (12 images from P56 and 10 images from P4) in the ASCA for the proliferating cell protein, PCNA,

and showed that, as expected, there is less global central canal proliferation in the adult spinal cord than in the neonate (Fig 3.6). However, the proliferation occurring at each of these ages appears to be carried out by different populations of cells, residing in different spatial locations of the central canal. In the neonate, there are more proliferating cells in the dorsal/ventral poles than in the lateral aspects (Fig. 3.6A), and there is slightly higher (but more or less even) levels of proliferation in the caudal half of the spinal cord than in the rostral half of the spinal cord (Fig. 3.6B). Interestingly, proliferation in the lateral aspects only occurs in the caudal half of the P4 mouse (Fig. 3.6C). Conversely, the adult central canal has an even amount of proliferation all around the central canal when averaging across the entire length of the spinal cord (Fig. 3.6A), but proliferation is nearly entirely restricted to the caudal half of the spinal cord (Fig. 3.6B). PCNA dorsal/ventral versus lateral gene expression patterns are maintained from mRNA to protein at P56 (Fig. 3.6A). In the caudal half of the spinal cord alone, there is no proliferation in the lateral aspects of the central canal (Fig. 3.6C). In the rostral half, nearly equal levels of proliferation occur in the dorsal/ventral and lateral parts of the central canal (Fig. 3.6C). This illustrates how different subpopulations of ependymal cells behave in the central canal, and how this behaviour changes with age and the needs of the spinal cord at that time. It also tells us that there is a difference in the spinal cord along its length at steady-state, and that care must be taken to compare proliferation at the same location along the rostral-caudal axis to ensure sampling of the same population of cells.

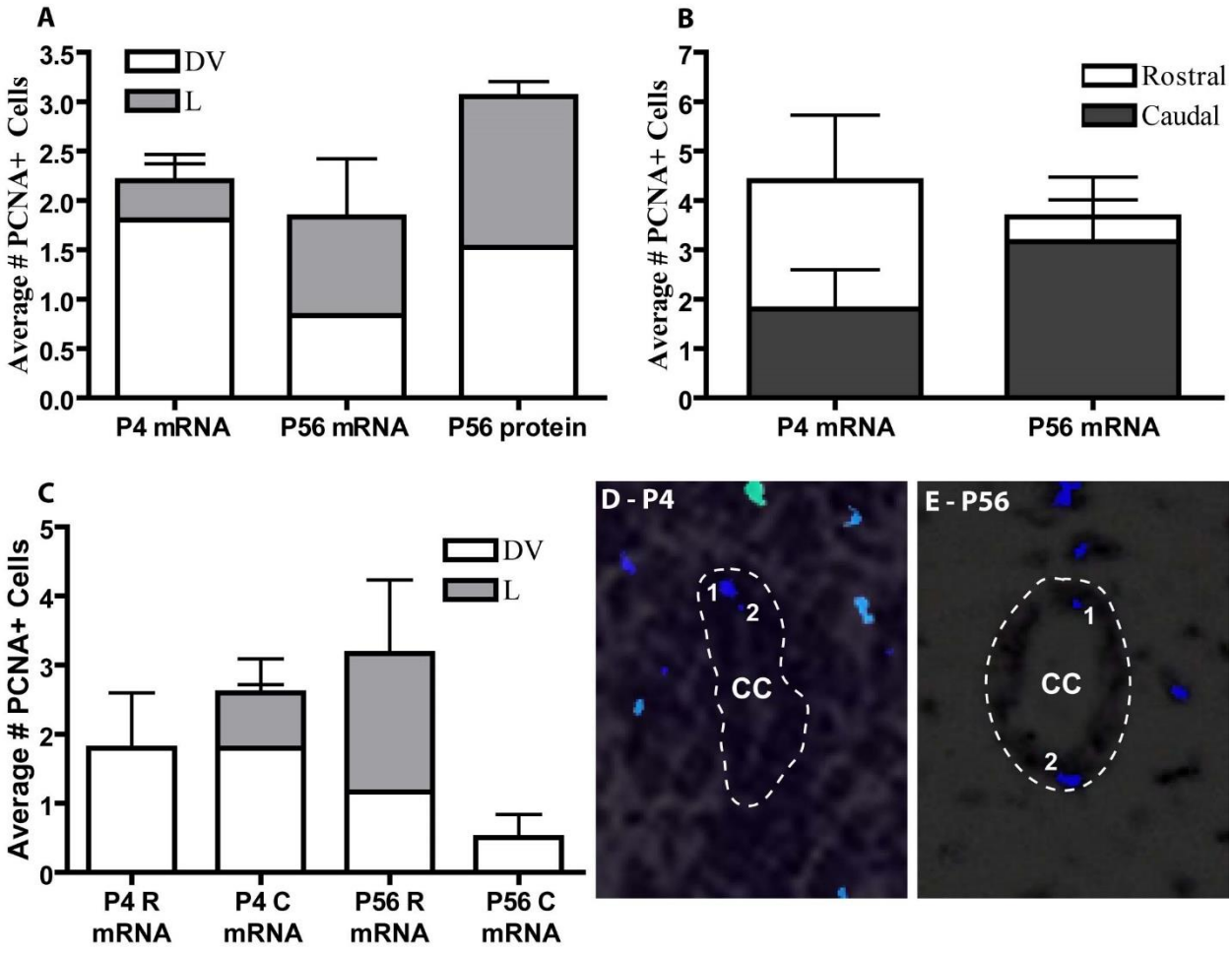
A
Average # PCNA+ Cells
DV
L
P4 mRNA
P56 mRNA
P56 protein
B
Average # PCNA+ Cells
Rostral
Caudal
P4 mRNA
P56 mRNA
C
Average # PCNA+ Cells
DV
L
P4 R mRNA
P4 C mRNA
P56 R mRNA
P56 C mRNA
D - P4
E - P56
CC
1
2

Figure 3.6

FIGURE 3.6. Proliferation data from the ASCA shows spatial differences between the neonate and the adult. Counts were taken from the ASCA's *ISH* images (12 images at P56 and 10 at P4) taken in transverse section along the length of the spinal cord. A) If the central canal transverse sections are subdivided into the spatial regions dorsal/ventral and lateral, there are more PCNA+ cells in the lateral aspects at P56 than P4; the opposite is true regarding the dorsal/ventral poles. The majority of dividing cells at P4 are located in the dorsal and ventral poles, whereas at P56, there is a near-even split between dorsal/ventral and lateral. The pattern of PCNA mRNA expression is maintained by the protein expression at P56; approximately equal amounts of proliferation occur in the dorsal/ventral and lateral aspects. B) There are many more PCNA+ cells in the caudal half of the spinal cord (i.e. first 6 transverse sections at P56 and first 5 transverse sections at P4) at P56 than at P4, whereas the opposite is true in the rostral half of the sections. The majority of the dividing cells in the adult are situated in the caudal half of the spinal cord, whereas the number of dividing cells is approximately equal along the length of the neonatal spinal cord. C) Combining the information in graphs (A) and (B) allows us to appreciate how subpopulations of dividing cells are segregated spatially and temporally. In the rostral half of the P4 spinal cord, proliferation only occurs in the dorsal and ventral poles, whereas about 1/3 of the proliferation in the caudal spinal cord occurs in the lateral aspects of the central canal. In the adult, the converse is true: caudally, no proliferation is seen in the lateral aspects, and rostrally, approximately 1/3 of the proliferation is found in the dorsal/ventral poles of the central canal. D) An example image of a P4 ASCA *ISH* transverse section, with the expression level (blue shades) superimposed on the Nissl stain to outline ependymal cell nuclei (dark grey), which allows us to define the ependymal cell layer (outlined in dotted white). This section has a total of 2 PCNA+ cells, both located in the dorsal pole. E) An example P56 transverse PCNA *ISH* image, with the

expression levels (blue shades) superimposed on the Nissl stain (dark grey) shows two PCNA+ cells, one in the dorsal pole and one in the ventral pole; the ependymal cell layer is delineated by a dotted white line. *Error bars = S.E.M.*

3.7 Production of new cells after injury

Having established that there are trends towards spatial and temporal patterns between P4 and P56 proliferating cells, we wanted to test how these patterns change after injury. Other groups have suggested that global proliferation will increase after SCI but not after demyelination injury, with spatial patterns of proliferation after injury including an increase rostral to the injury, but not caudal to the injury (Lacroix et al., 2014). Although it is established that the central canal is comprised of subpopulations of cells arranged around the central canal (Meletis et al., 2008; Petit et al., 2011), proliferation in dorsal/ventral vs lateral regions of the central canal has not been explored. Here, we use a model of demyelination (LPC) and a model of SCI (T7 severe crush injury) in 6 month old mice. Proliferation level was examined using proliferating cell nuclear antigen (PCNA)-specific antibodies to label transverse spinal cord sections to determine how dorsal/ventral and lateral populations of cells behave following injury. We used PCNA expression, segregated into dorsal/ventral vs lateral, or rostral vs caudal spatial groups, to examine how proliferation changes after demyelinating injury and SCI. Seven (+/-2) transverse sections from the cervical spinal cord of LPC mice (n=4) at each 1WPL and 3WPL; injection at a 45° angle into the cervical spine) and age- and strain-matched uninjured control mice (n=3), and 8 (+/-2) transverse sections from the thoracic spinal cord rostral to (T1-2) and caudal to (T12) the lesion (epicenter at T7) (n=3) and age- and strain-matched uninjured control mice (n=3). Representative images are found in Fig. 3.7A-C. We found that proliferation does not change significantly after LPC injection (Fig. 3.7D,E), yet we report a trend towards increasing proliferation as post-lesion interval time increases. Proliferation does not significantly change spatially after LPC, but there is a slight shift in trend after LPC injection from greater dorsal/ventral proliferation (in control mice) to greater lateral proliferation. Proliferation only increases rostral to the injury after SCI, but not

caudally (Fig. 3.7F). After SCI, the rostral spinal cord maintains the same relative proportion of dorsal/ventral to lateral proliferating cells (Fig. 3.7G); both spatial subgroups experience a similar increase in proliferation. However, prior to injury, the more caudal thoracic spinal cord has nearly equivalent levels of proliferation all around the central canal, whereas after injury proliferation in the lateral aspects appears to be somewhat diminished, although this finding is not significant. As we have found that proliferation after injury occurs to a larger extent in the rostral spinal cord, and that proliferation increases in both the dorsal/ventral and lateral aspects of the rostral but not caudal spinal cord after injury, these data support the hypothesis that spatially-arranged subpopulations contribute differently to the production of new cells.

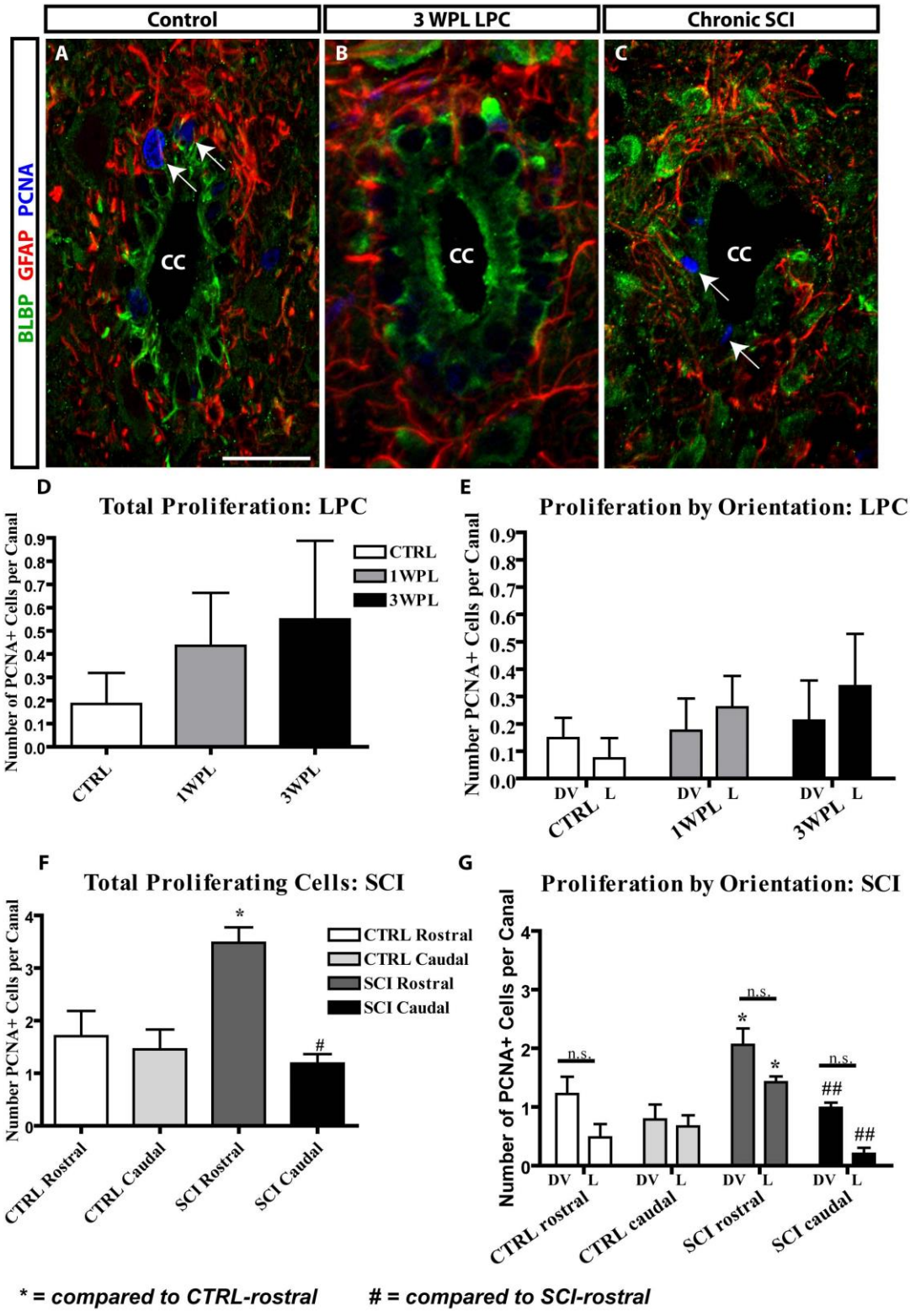
Control
3 WPL LPC
Chronic SCI
A
B
C
BLBP GFAP PCNA
CC
CC
CC
D
Total Proliferation: LPC
Number of PCNA+ Cells per Canal
CTRL
1WPL
3WPL
E
Proliferation by Orientation: LPC
Number PCNA+ Cells per Canal
DV L
CTRL
1WPL
3WPL
F
Total Proliferating Cells: SCI
Number PCNA+ Cells per Canal
CTRL Rostral
CTRL Caudal
SCI Rostral
SCI Caudal
G
Proliferation by Orientation: SCI
Number of PCNA+ Cells per Canal
n.s.
##
CTRL rostral
CTRL caudal
SCI rostral
SCI caudal
* = compared to CTRL-rostral
# = compared to SCI-rostral

Figure 3.7

FIGURE 3.7. Proliferation does not change after demyelination, but increases in certain orientations after injury. (A-C) Representative images of cervical spinal cord transverse sections from Fabp7-eGFP control (A) and 3WPL LPC lesion (B), as well as a thoracic spinal cord section of a C57Bl/6 12 weeks post-SCI (C) show varying levels of PCNA+ proliferating cells across the treatment groups. (D) Proliferation does not change appreciably 1 week following LPC injury, nor after 3 weeks: there is no difference in proliferation between the dorsal/ventral poles and lateral aspects of the central canal after demyelinating injury (E). Conversely, SCI causes an increase in proliferation rostral to the lesion only (F). (G) Proliferation is somewhat decreased in the lateral aspects of the spinal cord caudal to an injury, compared to the caudal end of the uninjured thoracic spinal cord, although these changes are not significant. (G) Proliferation is significantly increased in both the dorsal/ventral poles and the lateral aspects of the central canal rostral to the injury compared to the rostral end of the uninjured thoracic spinal cord (* = $P<0.05$). (G) Proliferation is significantly higher in both the dorsal/ventral and lateral central canal rostral to the injury compared to caudal to the injury (## = $P<0.01$) Scale bars 10μm. *2-Way-ANOVA, Bonferroni post-hoc tests. Error bars = S.E.M*

3.8 Human ependymal cells share similar characteristics to mouse ependymal cells

We have learned more about the rodent central canal ependymal cell layer in terms of spatial and temporal gene expression patterns, protein expression patterns for a subset of genes relevant to neurogenesis, and proliferation patterns. However, in order for our findings to be translational to human disease, we must determine if humans maintain a functional spinal cord ependymal cell population. Recent MRI studies have shown that approximately 30% of healthy adult humans have a detectable central canal at some point along their spinal cord (Garcia-Ovejero et al., 2015). If a detectable canal is not present, there are still morphologically distinct populations of cells maintained in the same central area, arranged similarly to a benign spinal cord tumor called an ependymoma (Garcia-Ovejero et al., 2015), that may maintain some ependymal cell functionality. Human spinal cord ependymal cells have been proposed to express Nestin, Sox2, and GFAP and, like rodent ependymal cells, can give rise to neurons, astrocytes and oligodendrocytes *in vitro* (Dromard et al., 2008). However, very little is currently known of the status of the central canal after injury or demyelination. Here, we show an example of a human patient's central canal in the lumbar spine of a 71-year old male with a spinal cord disease of unknown etiology, Pt 5. The ependymal cell nuclei (blue) look morphologically similar to those in the mouse spinal cord, although the lumen they surround is, unsurprisingly, much larger (Fig. 3.8A). There is a cluster of nuclei dorsal to the central canal, some of which are associated with BLBP (green), as is seen in the mouse (empty arrowheads). In the human central canal, the GFAP+ processes (red) are found in close proximity to the central canal (arrows). The same antibody used to detect radial ependymal cells in the mouse (Fig. 3.7A-C) was used in this human tissue. Although true central canal lumens are difficult to find in our human cohort, all patients maintained a nuclei-dense area in the centre of the gray matter in the spinal cord, similar to ependymoma (data

not shown). Here we show that the human central canal, when present, is similar to the rodent central canal both in morphology and gene expression. This allows us to make inferences on the functionality of the human central canal ependymal cells, and the spinal cord in general after injury or disease.

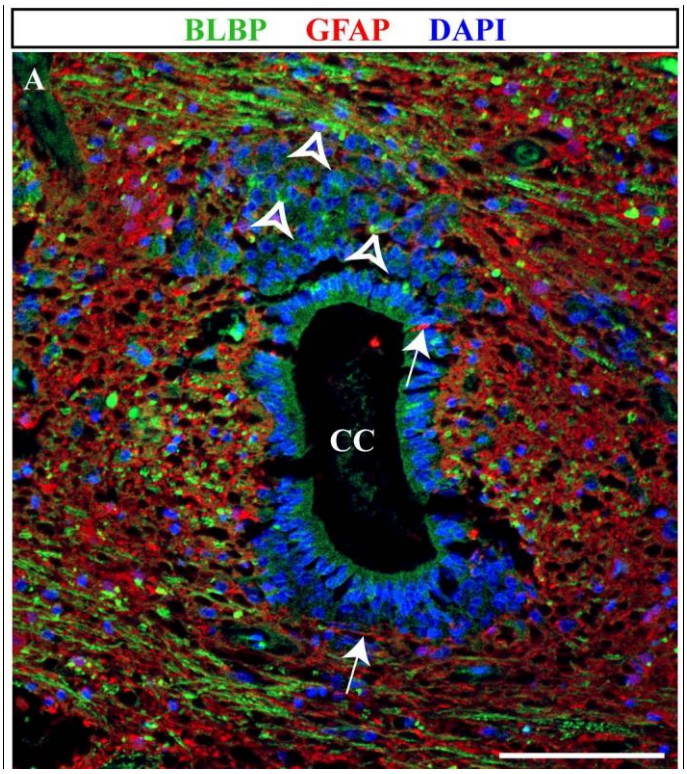

FIGURE 3.8 – The human central canal expresses similar proteins to the rodent central canal. This central canal is from the spinal cord of Pt 5, a 71 year old male with an unknown spinal cord disease. The ependymal cells outline the lumen of the central canal much like in the mouse. Like in the mouse, there is a cluster of cells dorsal to the central canal, some of which are BLBP+ (green). Some astrocyte processes (red) are present around the central canal, although no ependymal cells are positive for GFAP (red). Scale bar = 50μm.

3.9 Remyelination programmes are not shared between human and mice after demyelinating injury

Adult rodent central canal cells largely contribute to glial populations after lesion. To test how these ependymal cells may undergo gliogenesis in humans after injury, we next turned our attention to gliogenesis in human MS patients. As many adult humans do not maintain a discernable central canal, but do potentially have functional ependymal cells present, we turned our attention to the regenerative glial responses in an attempt to understand human spinal cord repair mechanisms. There are differences in demyelination and remyelination following injury between rodents and humans; any assumptions made based on the LPC mouse model regarding regeneration may be difficult to translate to human mechanisms; the LPC model of demyelination is a relatively simply model of acute demyelination and remyelination.

Here, we detected BLBP (red), which normally is expressed in some central canal ependymal cells, glial precursors, or in astrocytes responding to injury, in P_0+ myelin rings (green) within the CNS and PNS of human MS patients (Fig. 3.9C,D) and not in the LPC mouse model (Fig. 3.9B). Interestingly, we also found BLBP+/ P_0+ myelin rings in the dorsal root entry zone (DREZ) and spinal cord of these MS patients (Fig. 3.9D, arrows). There are also P_0+ myelin rings in the spinal cord of these patients that do not express BLBP (Fig. 3.9D, empty arrowhead). These BLBP+/ P_0+ myelin rings (yellow, arrows) do not express PLP, a CNS myelin marker in MS patients (Fig. 3.9E), but in one SCI patient (Pt. 6), we detected rare PLP+/BLBP+/ P_0+ myelin rings (teal/white, arrows) (Fig. 3.9F,F').

Here we show that patterns of regeneration after demyelination injury in mice do not adequately describe the mechanisms occurring in attempts at remyelination in human MS. Applying our understanding of how gene expression changes correlate to a decreased

regenerative capacity as rodents age, we can infer that the pathogenic environment found in the MS spinal cord alters the remyelination programme such that inappropriate expression of developmental markers in mature cells is present.

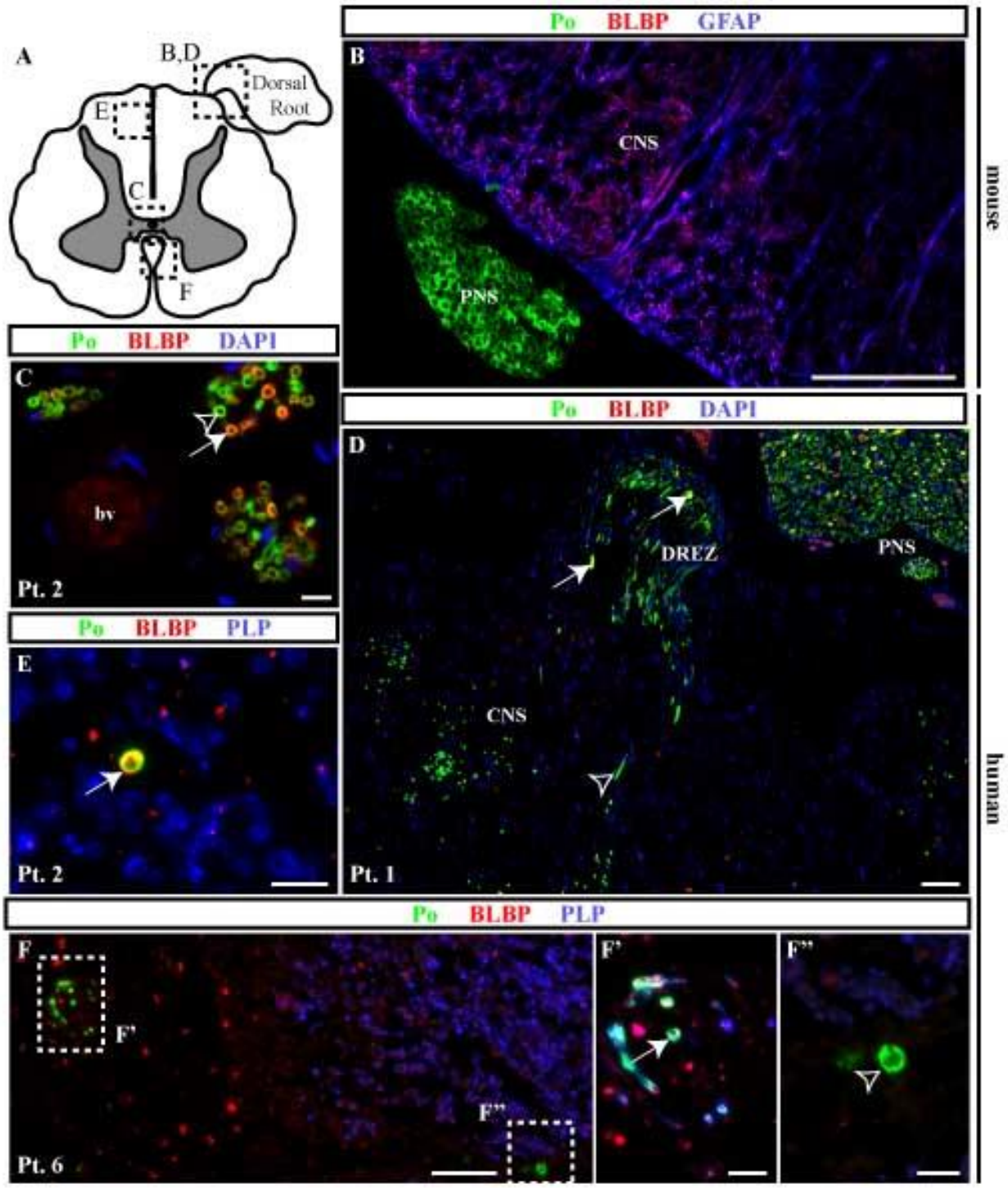
A
B,D
Dorsal Root
E
C
F
Po BLBP GFAP
B
CNS
PNS
mouse
Po BLBP DAPI
C
bv
Pt. 2
Po BLBP DAPI
D
DREZ
PNS
CNS
Pt. 1
Po BLBP PLP
E
Pt. 2
Po BLBP PLP
F
F'
F''
Pt. 6
F'
F''
human

Figure 3.9

FIGURE 3.9. Human Schwann cells express BLBP in the PNS and spinal cord. A) Cartoon of human spinal cord cross-section illustrating the location of photomicrographs. Mouse spinal cord root Schwann cells (B) express P_0 (green; empty arrowheads), but not BLBP (red); BLBP is expressed in nearby GFAP+ spinal cord radial glia (arrows, C-F''). BLBP (red) is often co-expressed with the PNS myelin protein, P_0 (green) in the spinal cord of MS Patients (arrows, C,D) and SCI patients (arrows, F'). Some cells express P_0 (green) but not BLBP (red) (empty arrowheads) in MS and SCI (C,D,F''). In MS (E), these BLBP+/P_0+ cells (yellow, arrow) do not co-express the CNS myelin protein PLP (blue); however, some BLBP+ rings express PLP (blue) and P_0 (green) (arrows) in SCI (F'). Scale bars 100μm (B,D,F), 10μm (C,E,F',F'') bv = blood vessel

3.10 Human MS patients exhibit varying degrees of central and peripheral neuropathy

As we have confirmed that the presence of P_0+ cells in the CNS, often to a large extent, in MS, and that these cells aberrantly express the developmental protein BLBP, we aimed to further understand the extent of pathology in these human patients in an attempt to discover the source of these P_0+ cells. These P_0+ cells potentially enter from the peripheral nerve roots, which are populated by Schwann cells and connect to the CNS via the DREZ and blood vessels of the nervous system; these areas may be pathologically involved in the MS disease process and thus behaving abnormally. Previous reports (Gartzen, Katzarava, Diener, & Putzki, 2011; Krökki, Bloigu, Ansakorpi, Reunanen, & Remes, 2014; Misawa et al., 2008; Ng, Howells, Pollard, & Burke, 2008; Schoene, Carpenter, Behan, & Geschwind, 1977) have outlined circumstantial evidence of peripheral neuropathy co-morbid with MS in human patients, but the presence of peripheral pathology in MS patients has not been examined in fine detail, at the level of cellular pathology. MS patients exhibit several pathological characteristics, and there is some heterogeneity in the relative amounts of pathology between patients. There are areas of peripheral nerve (Fig. 3.10 cross sections in B,C; longitudinal section in G) and DREZ (Fig. 3.10H,I) within these patients that look healthy: uniform brightness of MBP+ myelin (green) and spacing between myelin rings, compactly-wrapped myelin, and brightly-staining SMI-312+ axons (red). However, we do see areas of pathology in these patients. Frequently-detected pathological features include peripheral-type myelin within the CNS either in perivascular spaces (Fig. 3.10D, arrow) or near the DREZ (Fig 3.10F, arrow) – a feature also seen in parenchymal white matter distant from these areas (unpublished) – loose myelin rings (Fig. 3.10E, arrow), and areas with little or no myelin (green) or axons (red) in the PNS (Fig. 3.10J,L, arrowheads) and typical CNS demyelinated plaques (Fig. 3.10K, arrowhead). Here

we gain further appreciation for the extent of pathological features in the peripheral nerve roots surrounding the spinal cord in MS patients, further expanding the understanding of the pathogenic environment in MS.

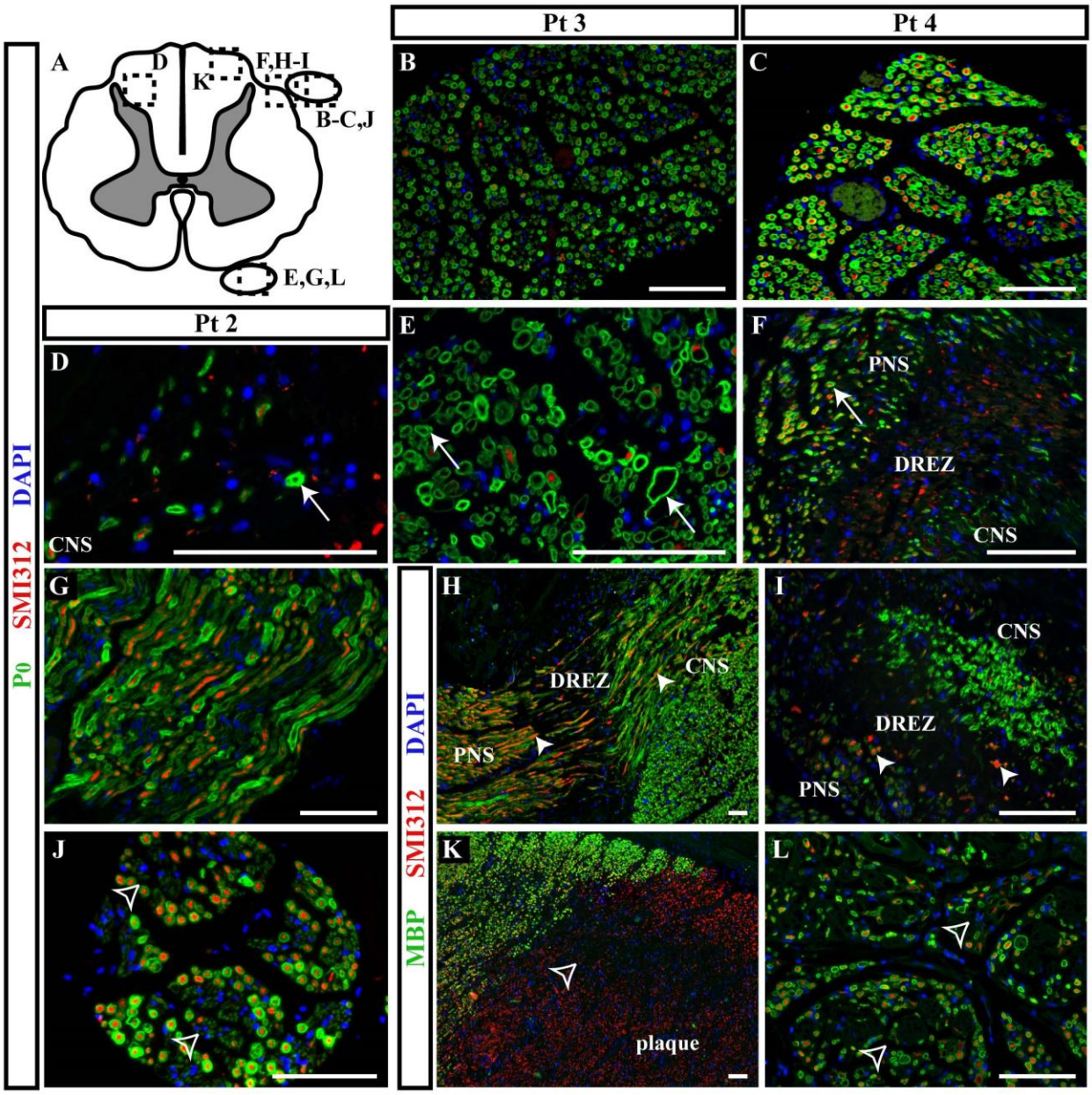
Pt 3
Pt 4
Pt 2
A
D
K
F,H-I
B-C,J
E,G,L
B
C
D
E
F
PNS
DREZ
CNS
G
H
I
J
K
L
P0 SMI312 DAPI
MBP SMI312 DAPI
DREZ
CNS
PNS
plaque

Figure 3.10

FIGURE 3.10. Human MS patients exhibit varying degrees of pathology in the spinal cord and surrounding roots. A) Cartoon of where images B-L are located. Normal areas of peripheral nerve (cross-sections: B,C, longitudinal section: G) exhibit uniformly-distributed, brightly-staining axons (red) and myelin (green), and compact myelin rings. Peripheral-type myelin can be found in the CNS in perivascular spaces (D) and near the DREZ (F) (arrows), even though the DREZ in these patients looks relatively normal (H,I), with intact and brightly-staining axons (red) and myelin rings (green) (solid arrowheads). The peripheral-type myelin (green) is often pathologically loosely wrapped around the axon (D,E, arrows). Some areas of peripheral nerve have areas pathologically lacking axons (red) and myelin (green) (J,L, empty arrowheads). There is a large demyelinated plaque in the spinal cord of Pt 3 (K) that has regions of sparse axons (red, empty arrowhead). Scale bars 100μm.

3.11 Peripheral pathology varies within MS patients

We observed varying levels of pathology in the MS patients studied, including Schwann cells in the CNS, loosely-wrapped myelin rings, and areas with sparse axons/myelin rings. We wanted to learn more about how peripheral pathology varies within a single patient, to further understand the varying degrees of pathology in the PNS of MS patients. To illustrate this within-patient variation, we quantified the myelin rings in three 5000μm^2 squares in 3 different adjacent rootlets from MS Pt 2. A cervical spinal cord section from this patient had surrounding rootlets (Fig 3.11 A-ii,A-iii) from near the level of section (i.e. they were very close to the cord, and were large in diameter), and also appeared to have a rootlet from an adjacent part of the spinal cord (Fig. 3.11 A-i), just above the level of section. This allowed us to simultaneously test the extent of pathological features from the same level of the spinal cord (i.e. cervical), potentially with different microenvironments. Here we confirmed with axonal and myelin immunodetection that some areas of Pt 2 had many axons that appeared either thinly myelinated or did not appear to be myelinated at all (Fig. 3.11Aii,Aiii, empty arrowheads), whereas adjacent areas had very few thinly-myelinated axons (Fig. 3.11Ai, empty arrowhead). Although this relationship is not statistically significant, there was a clear trend towards higher pathology in rootlets ii and iii, and lower pathology in rootlet I (Fig. 3.11B). Rootlet iii had significantly ($P<0.01$) more myelin rings that loosely wrap their axons in distinct concentric rings (Fig. 3.11Aiii, arrows; Fig 3.11B), compared to the other two rootlets analyzed, and rootlet ii in turn had significantly more loose rings (Fig. 3.11Aii, Fig 3.11B) than rootlet i (Fig. 3.11Ai). This pattern was also seen in the third pathological hallmark; there were very significantly more myelin rings lacking a detectable corresponding axon in rootlet iii than in either other rootlet, and there are significantly more ($P<0.05$) empty myelin rings in rootlet ii than rootlet i (Fig. 3.11Ai-iii; Fig 3.11B). These data suggest that the PNS in MS

may be much more affected by the disease than previously thought, and suggests that the PNS may have a direct or indirect involvement in MS pathogenesis.

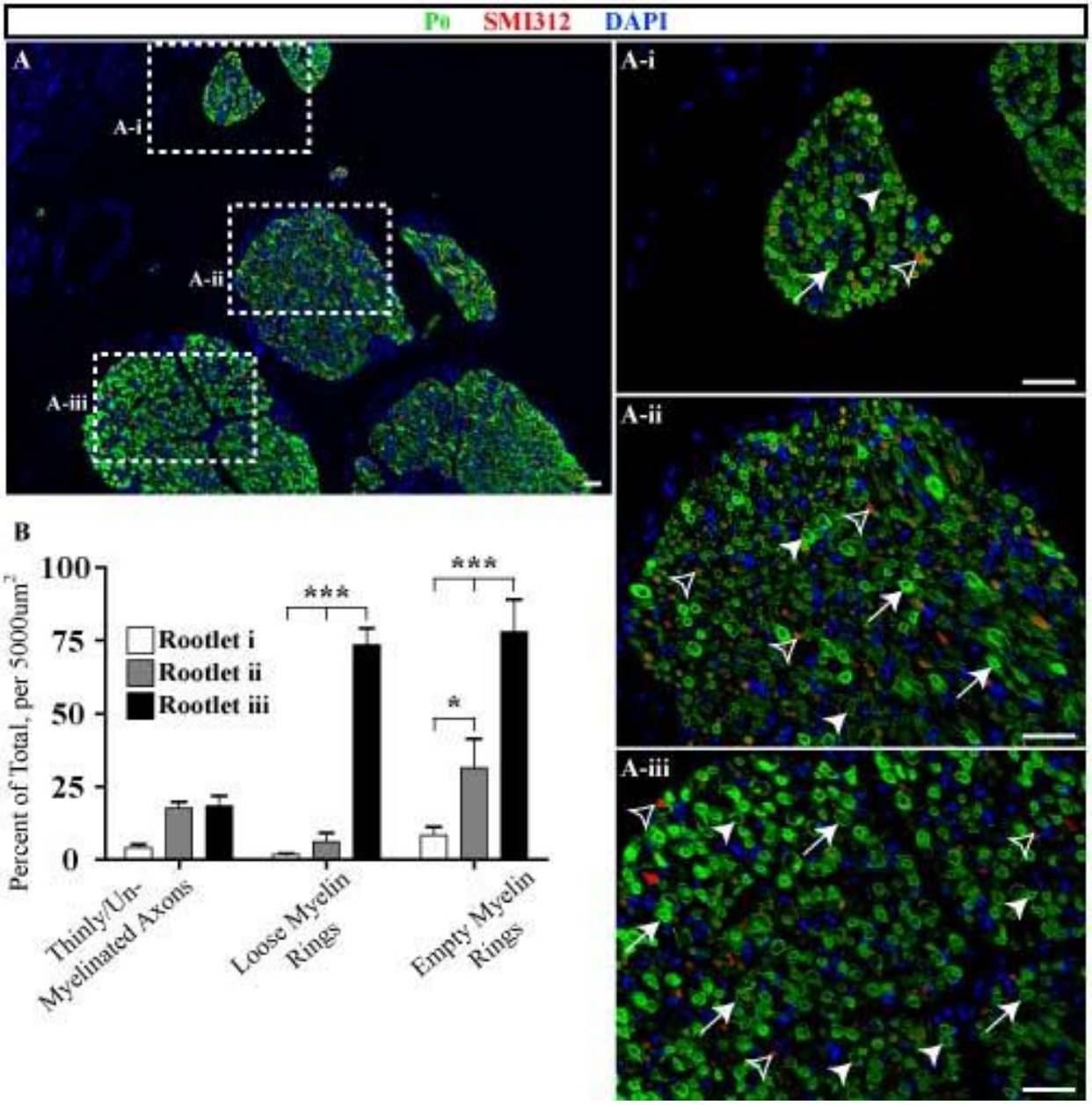
P0 SMI312 DAPI
A
A-i
A-ii
A-iii
B
Percent of Total, per 5000um²
100
75
50
25
0
Rootlet i
Rootlet ii
Rootlet iii
***
***
*
Thinly/Un-Myelinated Axons
Loose Myelin Rings
Empty Myelin Rings

Figure 3.11

FIGURE 3.11 MS Patients exhibit varying degrees of radiculopathy. MS Pt 2 has varying degrees of thinly-myelinated axons (red), loose myelin rings (green) and empty myelin rings (A), quantified in (B). Rootlet i (A-i) has significantly fewer loose myelin rings (arrows) and empty myelin rings (arrowheads) than the other two areas quantified (A-ii and A-iii; 5000μm^2 areas within the visual field). There was no statistical difference between the three areas sampled for thin/un-myelinated axons (empty arrowheads). *Two-way ANOVA, error bars S.E.M. * = P<0.05, ***=P<0.001*. Scale bars = 50μm.

4. DISCUSSION

4.1. *Subpopulations of spinal cord ependymal cells are spatially and temporally heterogeneous*

The adult mammalian spinal cord has decreased regenerative capacity relative to the neonatal mammalian spinal cord, which has profound effects on the ability for recovery from disease or injury (Gilson & Blakemore, 1993). We aimed to identify glial precursors persisting in the adult mouse and human spinal cord. We used a combination of data mining and gene ontology analyses, using online software and tools, to understand the global spatial and temporal shifts in genes important to central canal ependymal cell function and stem/progenitor potential on a large scale, and then applied these findings on a much finer scale to further compare and contrast subgroups of ependymal cells, both before and after injury and disease.

To better understand the function of ependymal cells, and how the function may change across developmental stages in ways that correlate with decreased regenerative capacity, we aimed to develop a global gene expression profile of all the genes expressed by mouse ependymal cells at P4 and P56. The ASCA contains approximately 15 *in situ* hybridization (*ISH)* images in transverse section, taken along the length of a neonatal mouse spinal cord at P4 and an adult mouse spinal cord at P56, for each of the >20,000 genes the ASCA tested. The early postnatal CNS has a very robust regenerative capacity compared to the adult CNS, early postnatal mice have much more regenerative capacity in their CNS than adult mice (Conboy et al., 2005; Gilson & Blakemore, 1993; Yun, 2015), making these time points useful to explore the differences in gene expression in a mouse with a higher capacity for regeneration compared to a mouse with a lower capacity for regeneration. The ASCA also includes general data on where in the spinal cord the genes are expressed: expression categories include the ventral-dorsal midline in grey matter, the

white matter and, most pertinent to our study, the central canal, forming a starting point for our analyses (see Fig 3.1 for data mining overview). We were able to increase the number of genes included in our analyses by entering each gene listed as expressed in the central canal according to the ASCA into GeneMANIA, which returns the names of genes involved in the same pathway as the query gene, and then cross-referencing the new genes against the ASCA with an in-depth look at the *ISH* data that may have been missed by the ASCA. The genes that are likely to be responsible for the central canal's regenerative capability are genes that are turned off in the adult (i.e. the genes expressed only in the neonate), or genes that have expression turned on in the adult. We examined the genes that changed over time to establish temporal heterogeneity in the central canal ependymal cells.

Furthermore, we could look at each individual gene expression pattern in the ASCA *ISH* images and classify them by their expression pattern around the central canal: genes were generally expressed either all around the central canal, only in the dorsal and/or ventral poles, or only in the left/right lateral aspects of the central canal. Expression of several stem/progenitor cell proteins including Olig2, Nestin and GFAP is limited to distinct spatial sub-regions of the central canal (Hamilton et al., 2009). For a protein such as Olig2, which is involved in the differentiation and development of oligodendrocyte precursors into oligodendrocytes (reviewed by Goldman & Kuypers, 2015), the fact that it is generally enriched in cells in and near the dorsal pole of the central canal is intriguing. Perhaps oligodendrocyte precursors are only made from the ependymal cells asymmetrically dividing in the dorsal poles, meaning the production of remyelinating cells after injury could be enhanced by specifically targeting the dorsal cells to proliferate and differentiate. Furthermore, Ševc et al. (2011) has shown that ependymal cells may be made in two groups during development. It appears that the ciliated cuboidal cells are made first before birth,

and then the radial ependymal cells are made second and reside in the dorsal and ventral poles (Ševc et al., 2011). As we have shown that proliferation in the dorsal/ventral poles is high at P4 (Fig 3.6A), perhaps these dorsal and ventral cells are the best targets to encourage regeneration following injury. While there are fewer genes expressed only in the adult than only in the neonate (Fig. 3.1), there are also fewer genes restricted to one subgroup of spatially arranged cells in the adult than in the neonate (Fig 3.2). This supports the hypothesis that ependymal cells in the neonatal spinal cord are more diverse, specialized, and active than in the adult, and therefore more capable of giving rise to a larger number of differentiated cells.

The spatial gene patterns, dorsal/ventral and lateral, have some diversity within them as well (Fig 3.2). Genes were considered to be "dorsal/ventral" if their expression was enriched in and/or near the dorsal-most and ventral-most parts of the central canal. Genes that are only expressed in the dorsal or, rarely, in the ventral part of the central canal were also included in the group. Laterally-expressed genes were categorized as such if they are not enriched in the dorsal and ventral parts of the central canal. The expression of the genes in either subgroup did not necessarily have to be limited to the central canal proper – often genes are expressed in the central canal, the surrounding subependymal area, or elsewhere in the spinal cord

Of note, many genes that are expressed in both the neonatal and adult central canal are expressed differently at P4 than at P56 (Fig 3.3). Even some genes that are expressed in the same general spatial subcategory, (for example the dorsal/ventral category) at both ages often have strikingly different spatial expression patterns, intensities, and abundance. The intermediate filament protein, GFAP, expressed in astrocytes and neural progenitors, is a marked example of this – the cells expressing GFAP at P4 are more or less limited to the dorsal and ventral poles of the central canal, but GFAP is much more restricted to the dorsal pole in the adult (Fig. 3.3A,E).

We next wanted to learn more about the genes expressed in the central canal, by analyzing their putative function. To learn more about the genes expressed in the central canal, we entered our gene list into ToppGene, an online tool that groups genes into biological and molecular pathways, leading us to further understand their role in stem/progenitor cells, and give us the potential to infer which type of cells could be produced from the subgroups of progenitors in the central canal (Fig 3.4). We selected the top 20 most relevant pathways (determined using the p-value calculated by ToppGene), and broke down how many genes are expressed in each of the three temporal subgroups (P4, P56 and both). This gives us an idea of how important a given pathway is to the central canal in the neonate versus the adult, assuming that the number of genes involved in each pathway correlates with the importance of that pathway to the central canal. Unsurprisingly, pathways such as the smoothened signaling pathway contain a higher number of relevant genes in P4 than in the adult, whereas pathways involved in building and maintaining the ECM have more genes specific to the adult than the neonate. This reflects how the gene expression shifts from producing an environment conducive to development and plasticity in the neonate to promoting quiescence by maintaining the stem cell niche via the ECM in the adult. However, it is intriguing that the adult has a substantial number of age-specific genes involved in development that are not utilized in neonatal development. Genes involved in cellular and cytoskeletal motility, and cell projection/processes are often maintained from the neonate to the adult, but both ages also have age-specific subsets of genes. Using the data gathered from the ASCA and ToppGene, we were able to select three genes which are involved in neurogenesis-related pathways and are expressed in interesting spatial and temporal patterns to further explore the effect these variables have on the function of the central canal.

We next wanted to further investigate how a select group of genes behaves *in vivo*, by determining the spatial protein expression in the ependymal cell niche. We selected ADAMTS20 (A Disintegrin And Metalloproteinase with Thrombospondin motifs 20), a matrix metalloproteinase (MMP), due to its ASCA expression in the lateral aspects of both the neonate and in the adult, and its putative function in positively regulating neuroepithelial differentiation and ECM organization as determined by ToppGene. Like all MMPs, ADAMTS20 is a secreted protein that can influence how the ECM is organized (Llamazares, Cal, Quesada, & López-Otín, 2003). Based on the ToppGene analysis, ADAMTS20 likely decreases the ependymal cell's adhesion to the basal lamina, thus enabling the cell to leave the niche and proliferate along an epithelial cell lineage. ADAMTS20 is not produced by cells in the dorsal and ventral poles of the central canal according to our ASCA analysis. As an MMP, ADAMTS20 likely does not directly influence the fate of the cell, so it is possible that it is only produced by cells that have a greater propensity to differentiate into epithelial cells. We confirm that ADAMTS20 protein is expressed in the apical region of the ependymal cells in both the neonatal and adult central canal, and is excluded from the dorsal and ventral poles, where cells express progenitor proteins such as Nestin and GFAP (Fig 3.5A,B). To properly visualize this, and ensure that the signal we detected was not attributed to ADAMTS20 secreted into the lumen of the central canal, potentially from cells outside of the field of view, we used an actin phalloidin stain to confirm that the ADAMTS20 is expressed in the apical region of the ependymal cells (Fig 3.5B). Actin is expressed in all of the cells of the ependymal cell layer, thus enabling us to clearly see that ADAMTS20 is not expressed in the dorsal and ventral poles. ADAMTS20 serves as an example of a protein whose spatial and temporal patterning was accurately predicted by the ASCA's gene expression information.

Additionally, we selected Rb1 (Retinoblastoma 1), a cell cycle checkpoint regulator that is involved in neurogenesis, the smoothened signaling pathway, cell morphogenesis, the Id signaling pathway (which regulates growth and differentiation: reviewed by Sikder, Devlin, Dunlap, Ryu, & Alani, 2003), and several other pathways. Rb1 has opposing functions in the cell, either promoting entry into the cell cycle when phosphorylated or inhibiting proliferation when de-phosphorylated (Riley, Lee, & Lee, 1994). Rb1 is an oncogene involved in retinoblastoma, a common tumor of the eye, and also regulates the cell cycle in stem cells and is implicated in neural development (reviewed by Korenjak & Brehm, 2005). The antibody we utilized to localize Rb1 is able to detect both forms (BD Pharmingen; see table 2.2 for more information). The ASCA predicts Rb1 will only be expressed in the neonatal central canal, without any marked spatial patterning. We confirm that Rb1 protein is not found in the adult central canal but, unlike the ASCA data, we showed that Rb1 is generally not found in the dorsal or ventral poles (Fig 3.5C). Rb1+ cells are rare in the neonatal central canal, and are found nearly entirely in the lateral aspects of the central canal. It is possible that Rb1 is utilized as a cell cycle checkpoint regulator in a subset of cells found only in the lateral aspects of the central canal. Rb1 is one example of how protein distribution may differ from RNA distribution.

Finally, we explored the protein expression patterning of TrkB. TrkB, (or Ntrk2, Neurotrophic Receptor Tyrosine Kinase 2) is a transmembrane neurotrophic receptor protein that, when bound by its ligand neurotrophin, activates the MAPK signaling pathway, leading to cell differentiation. TrkB is critical for regulating both neurogenesis and gliogenesis (Barnabe-Heider & Miller, 2003). TrkB regulates many components of the CNS, including differentiation and proliferation of progenitors into neurons, as well as neurogenesis, plasticity and synapse formation (Bergami et al., 2008; Li et al., 2008). TrkB is involved in, among many other pathways, cell

morphogenesis, neurogenesis, and astrocytoma, according to our ToppGene analysis. The ASCA *ISH* data show TrkB mRNA is transcribed all around the central canal in both the neonate and adult. However, we did not detect TrkB protein in or around the neonatal central canal, nor do we find it in the ependymal cell layer of the adult central canal (Fig 3.5D). We did detect TrkB in cells immediately surrounding the ependymal cell layer in the subependymal area. TrkB is not found in cells near the dorsal and ventral poles, but rare cells are found lateral to the central canal. This observation builds further evidence for the idea that different sub-regions of the central canal have different capacities to produce subsets of cells; TrkB may be expressed in an intermediate transit amplifying cell that is produced by the lateral ependymal cells.

Taken together, the data described above outline how the central canal may be split into zones that have differing abilities to produce different cell types. We next aimed to learn more about how these subpopulations of ependymal cells change in their ability to produce new cells both between the neonate and the adult. We used the ASCA to explore the gene expression of a proliferating cell marker, PCNA, to determine how proliferation changes spatially and with developmental age in the mouse spinal cord (Fig 3.6). The expression mask for each section was overlaid on the nearest Nissl stain provided by the ASCA, to ensure cells included in counts were part of the ependymal cell layer (Fig 3.6D,E). All available *ISH* images from both P4 and P56 were analyzed (Fig 3.6A-C), showing that for these representative animals, there is a nearly equivalent amount of proliferation along the rostral/caudal axis in the neonatal mouse, but that proliferation is greatly suppressed in the posterior half of the spinal cord of the adult mouse. As gene expression is not always the same as protein expression, we verified that PCNA protein expression patterns along the dorsal/ventral and lateral axes is consistent with the ASCA gene expression data (Fig 3.6A). We showed that, as expected, total proliferation has decreased slightly

in the adult compared to the neonate, yet we still do see a high amount of proliferation in the adult (approx. 3 PCNA+ cells in each anterior transverse section and 0.5 PCNA+ cells in each caudal section). Additionally, if the central canal is split into the dorsal/ventral and lateral regions as described previously, we see a shift from predominantly dorsal/ventral proliferation at P4 to a nearly equal dorsal/ventral and lateral balance at P56 (Fig 3.6A). Interestingly, the number of proliferating cells along the length of the spinal cord was relatively even in the neonate, but very different in the adult; proliferation in the adult spinal cord is nearly entirely restricted to the caudal half of the cord (Fig. 3.6B). To further explore how spatial orientation around and across the length of the central canal influences proliferation, we split the ASCA images into rostral and caudal domains, and then into dorsal/ventral and lateral domains (Fig. 3.6C). We discovered that proliferation in the rostral half of the neonatal spinal cord was restricted to the dorsal and ventral poles, whereas proliferation in the rostral adult spinal cord was fairly uniform around the central canal. Proliferation patterns in the caudal half of the spinal cord were very different; the caudal neonatal spinal cord has uniform proliferation around the central canal, whereas the caudal adult spinal cord has proliferation only in the dorsal and ventral poles. Generally, proliferation was more abundant in the dorsal/ventral poles than in the lateral aspects, regardless of age or longitudinal position along the length of the spinal cord. These differences in spatially arranged proliferation could be attributed to the fact that different cell types are being made in the neonate than in the adult, and gives more insight into which regions may contribute to which cell types. Taken together, these data show that there is a shift in how the central canal ependymal cells function to produce new cells across space and time, allowing us to gain insight on potential spatially-arranged subpopulations of cells for regenerative therapeutics.

4.2. ***Proliferation in the adult mammalian spinal cord ependymal cells changes with space and time, and also after injury.***

To further our understanding of how these different spatial subpopulations of neural stem/progenitor cells in the central canal behave after injury, we explored how cell proliferation proceeds following different injuries. We utilized a rodent model of chemical demyelination, LPC, which displays demyelination throughout the lesion by 1WPL, and has completed remyelination at 3WPL (Jeffery & Blakemore, 1995), and a rodent chronic SCI model 10.5 weeks post injury. Remyelination in the LPC model is predominantly carried out by resident OPCs that differentiate and produce remyelinating oligodendrocytes, but as the central canal is capable of producing a small number of OPCs (Barnabé-Heider et al., 2010), we were interested to determine if the central canal cells undergo proliferation after LPC in an attempt to replenish OPC pools. Neurons are not generated by the central canal following injury but large amounts of astrocytes are produced by the central canal after injury (Barnabé-Heider et al., 2010; Meletis et al., 2008). The ependymal cells undergo symmetrical self-replication at steady-state (Hamilton et al., 2009), and after injury (Barnabé-Heider et al., 2010; Meletis et al., 2008). Therefore, observing which spatial regions of the central canal undergo proliferation following different types of injury that cause production of different types of cells could provide insight into whether progenitors are spatially organized in the central canal.

Previous groups have shown that proliferation does not appreciably increase after demyelination injury, and that proliferation only increases rostral to the injury site after SCI (Lacroix et al., 2014). Here, we confirm these findings (Fig 3.7D-F). We induced LPC lesions in 6 month old Fabp7-eGFP mice on a Swiss Webster background, and control mice were strain- and age-matched, but uninjured. Based on work done in uninjured mice spinal cord ependymal cells

by (Alfaro-Cervello, Soriano-Navarro, Mirzadeh, Alvarez-Buylla, & Garcia-Verdugo, 2012), we expect proliferation around the central canal to dramatically decrease after 1 month of age, and continue to decrease as the mouse ages. When we compared the proliferation analysis on strain-matched 2-month old mice, we saw a considerable increase in proliferation relative to the 6-month old mouse. Average total proliferation at 2 months was 3.05 PCNA+ cells per transverse section (+0.31, -0.16), whereas average proliferation in the uninjured 6 month animals was 0.19 PCNA+ cells per transverse section (+0.26, -0.19) – a 16-fold difference. This shows that ependymal cell proliferation dramatically decreases between two and six months of age, and emphasizes the importance of proper age-matched controls in proliferation assays in the central canal. Furthermore, as the SCI was performed in C57Bl/6 non-transgenic mice, the age-matched controls were also from a C57Bl/6 background. Comparing the Swiss Webster (0.19 PCNA+ cells per transverse section) and the C5Bl/6 (1.5 PCNA+ cells per transverse section) strains allows us to appreciate the fact that proliferation can vary across age-matched mouse strains by nearly 800%. This further re-iterates the necessity for properly controls during central canal proliferation experiments.

Although proliferation does not appreciably change during recovery after LPC-induced demyelination, there is a mild shift in where the proliferation occurs spatially around the central canal (Fig 3.7E). At steady-state, the dorsal/ventral poles have a nonsignificant trend towards greater levels of proliferation than the lateral aspects, even though the dorsal and ventral poles contain fewer cells than the lateral aspects of the central canal. However, at 1WPL and 3WPL following LPC injury, that trend shifts to favour proliferation in the lateral aspects. It is possible that the depletion of the OPC pool after remyelination does not trigger a swift increase in proliferation in the central canal, and proliferation peaks more than 3 weeks after the lesion, as

there appears to be a trend towards increasing proliferation, especially in the lateral regions of the central canal at 1WPL and again at 3WPL relative to controls (Fig. 3.7E). However, others have previously looked as late as 5WPL and seen no increase in proliferation following LPC (Lacroix et al., 2014).

Proliferation has been shown to increase following SCI, and recently it has been shown that the increase is restricted to areas rostral to the lesion (Lacroix et al., 2014), a finding also supported by our data (Fig 3.6F). We aimed to determine if proliferation is altered spatially, perpendicular to the rostral/caudal axis. Although we see that proliferation increases to a similar extent in the rostral injury in both the dorsal/ventral and lateral central canal (Fig 3.6G), we report a trend towards a suppression of proliferation in the lateral aspects of the thoracic spinal cord caudal to the injury. Both of these findings – the increased proliferation rostral to the injury and the suppression caudal to the injury – have persisted chronically (10.5 weeks) after the injury. These findings conflict with those recently found by Lacroix et al. (2014), but as we have shown that age can vastly influence the proliferative capacity of the central canal, we can reconcile these differences as we have used 6 month old mice, but the specific ages of the mice used by (Lacroix et al., 2014) were not reported. Here we have shown that different injury modalities can result in different ependymal cell activation in the spinal cord. Taken with what we have shown about the identities of the spatially and temporally arranged subpopulations of ependymal cells, we can further appreciate how the ependymal cells may be a robust therapeutic target.

4.3. *Remyelination after demyelinating lesion in the mouse does not appear to be the same as remyelination in human MS*

In accordance with previous reports (Dromard et al., 2008; Garcia-Ovejero et al., 2015), we show here that a subpopulation of humans have a detectable central canal, surrounded by ependymal cells (Fig 3.8). These cells are similar in morphology and organization to their rodent counterparts, and express similar proteins such as BLBP. There exists a population of cells dorsal to the central canal which expresses BLBP, a phenomenon also observed in the mouse (data not shown).

Having established that human MS and SCI patients sometimes have a detectable central canal, and with the assumption that even if no distinct central canal is present that there may be ependymal cells that maintain stem/progenitor functionality present along the spinal cord, we next applied our understanding of the behaviour of the central canal after injury in an attempt to better understand the mechanisms behind endogenous remyelination programmes in human MS. Human spinal cords with MS exhibit areas of demyelination, some of which have sparse areas that appear to be remyelinated (Fig 3.9C-E). Interestingly, not all of these myelin wrappings within the lesions express typical CNS myelin proteins – in fact, many express the peripheral myelin protein P_0 (Fig 3.9). Intriguingly, these P_0+ myelin rings were also infrequently PLP+ in spinal cord injured patients, but never in MS patients (Fig 3.9F), suggesting that the endogenous remyelination programmes differ between MS and SCI. The presence of P_0+ myelin rings in the CNS has been confirmed in up to 80% of the MS patients sampled (unpublished). Although sparse sub-populations of axons with P_0+ myelin have been previously reported in the spinal cord of occasional MS cases (Ghatak et al., 1973; Itoyama, Webster, Richardson, & Trapp, 1983; Yamamoto, Kawamura, Hashimoto, & Nakamura, 1991), there is little information on the extent

to which these myelin rings can contribute to endogenous remyelination in MS. Moreover, the origin of these myelin rings is unknown: fate-mapping studies in the mouse suggest OPC-derived myelinating cells can express peripheral markers (Zawadzka et al., 2010). Alternatively, Schwann cells may be able to infiltrate the spinal cord from the periphery, especially in areas proximal to blood vessels and the dorsal/ventral root entry zones (Duncan & Hoffman, 1997; R. J. Franklin & Blakemore, 1993).

Surprisingly, many of the P_0+ rings in the MS patients express the developmental glial protein BLBP (Fig 3.9). BLBP is expressed in immature stages of Schwann cell differentiation (reviewed by Jessen & Mirsky, 2005), but has never before been reported within myelinating cells of any kind. BLBP is never found in myelin rings in the LPC rodent model of demyelination (Fig 3.9 B), suggesting that the mechanisms behind remyelination in MS are different than those in the LPC mouse model. Therefore, we can conclude that the abnormal, pathogenic environment in MS causes progenitor cells to give rise to remyelinating cells that are not currently well understood.

The progenitor source of the remyelinating cells is also not known. It has been proposed by other groups that Schwann cells can enter the CNS via the peripheral nerve roots or blood vessels, and can infiltrate into areas depleted of astrocytes due to injury or disease (Bruce et al., 2000), and it is known that the blood-CNS barrier is compromised in MS (Minagar & Alexander, 2003). Other bodies of work suggest that spinal cord OPCs can differentiate into myelinating Schwann cells *in vivo* (Zawadzka et al., 2010). The BLBP+/P_0+ cells we have described are located both near peripheral sources, such as dorsal and ventral root entry zones and blood vessels, and also deep within the spinal cord parenchyma (Fig. 3.9). Such cells were not found in the brains of these patients (unpublished).

In addition to the possibility that the PNS has a role in providing remyelinating cells to the CNS in MS, the PNS may be directly impacted by the disease itself. MS patients display distinct peripheral root pathology, although the prevalence of reported PNS pathology varies with the mechanism of testing (Gartzen, Katzarava, Diener, & Putzki, 2011; Krökki, Bloigu, Ansakorpi, Reunanen, & Remes, 2014; Misawa et al., 2008; Ng, Howells, Pollard, & Burke, 2008; Schoene, Carpenter, Behan, & Geschwind, 1977). Interestingly, the Schwann cells residing in the PNS also often express BLBP in these patients (Fig. 3.9). Many of the PNS Schwann cells are also pathologically loosely wrapped around their axons (Fig. 3.10 and 3.11). The percentage of Schwann cells expressing BLBP in the peripheral roots varies between patients, ranging between 21-75% of all Schwann cell rings (unpublished). Between 5% and 30% of all Schwann cells in the roots of these patients were pathologically loose (unpublished). Interestingly, in MS but not in SCI, BLBP expression and loose rings are inversely correlated, that is, MS patients either have many loose rings and few BLBP+ rings or few loose rings and many BLBP+ rings (unpublished). However, at the level of an individual Schwann cell, BLBP expression and pathologically loose wrapping are positively correlated; a BLBP+ ring is more likely to be loosely wrapped than compact (unpublished).

In addition to pathologically loose wrapping and BLBP expression, we see other hallmarks of peripheral pathology, including areas with sparse myelinated axons, thinly or unmyelinated axons, and myelin rings lacking a detectable axon, along with more typical MS pathology such as large demyelinated CNS plaques (Fig. 3.10 and 3.11). The level of pathology across patients is highly variable: patients with CNS P_0+ cells and peripheral pathology often have normal-appearing adjacent areas of peripheral nerve, DREZ and spinal cord parenchyma (Fig. 3.10). These data suggest that MS may have a more widespread impact on the PNS than previously reported (Gartzen

et al., 2011; Krökki et al., 2014; Misawa et al., 2008; Ng et al., 2008; Schoene et al., 1977), and does little to describe the source of the P_0+ cells within the CNS of these patients.

In addition to variation in pathology between patients, we see large variation of pathology within individual patients, between neighbouring peripheral rootlets (Fig 3.11). The cervical spinal cord of Pt 2 had rootlets from near the level of section (ii and iii), and rootlets likely from slightly higher in the cervical spinal cord (i). Three pathological hallmarks were chosen to examine for differences between these rootlets, (1) axons that either had a thin myelin sheath or no visible myelin sheath surrounding them; (2) loosely wrapped myelin rings, with clearly differentiable concentric myelin rings; and (3) empty myelin rings with no detectable axon. The numbers of each hallmark were counted within three 5000um^2 regions per rootlet. Rootlet iii has significantly more loose myelin rings and empty myelin rings than both rootlet ii and i, and rootlet ii has significantly more empty myelin rings than rootlet i. This within-patient heterogeneity provides evidence that the pathology seen is attributable to the disease itself, and not due to other variables such as age, post-mortem interval, or any other tissue processing; and also highlights the importance of sampling many different areas of the peripheral roots in these patients. It is unclear if the PNS damage extends past the roots, whether the damage is caused directly by similar immune-mediated mechanisms as in the CNS, or if the damage is a secondary consequence of CNS degeneration. More work is needed to understand the extent and mechanisms behind both the aberrant Schwann cell myelination and the PNS involvement seen in these patients.

Insight gained here into the adult spinal cord, particularly after injury, outlines the potential for the ependymal stem cell niche as an endogenous source of remyelinating cells with potential therapeutic applications. We have learned that there are spatially-arranged subpopulations of cells with distinct gene expression profiles, which may allow certain spinal cord ependymal cells to

have different stem/progenitor function than their neighbours. We have also learned that these subpopulations undergo changes in gene expression patterns between development and adulthood, suggesting a possible mechanism for the reduction in regeneration capability with time. Taken together, we can speculate on how the pathological environment in a disease such as MS could hinder endogenous spinal cord progenitors from adequately regenerating lost cell populations by influencing expression of certain genes, such as BLBP, which are crucial for successful proliferation, differentiation and subsequent regeneration.

5. FUTURE DIRECTIONS

The data presented here support our hypothesis that the spinal cord ependymal cell layer is made of spatially- and temporally-arranged subpopulations of cells, which appear to respond differently to injury. It would be pertinent to determine how expressions of our three proteins of interest (ADAMTS20, Rb1 and TrkB) change with injury – any shifts in their expression pattern following injury could help explain the function of the ependymal cells. Exploring expression of these three proteins in the human central canal would also help us to better understand the difference between human and mouse progenitor cell function. Similarly, if we could find enough human samples that contain a patent central canal, it would be useful to perform the spatial proliferation analyses, to determine which subpopulations of the central canal are active in humans with demyelinating disease.

To also help bridge the gap between the rodent models and the human patients, it would be valuable to further determine the origin of the P_0+ myelinating cells in the spinal cord of the human MS patients. As it is possible that these cells come from either an oligodendrocyte/central lineage, or a Schwann cell/peripheral lineage, but it is not possible to perform lineage-tracing experiments in human patients, generating a protein expression profile of these cells is a logical first step in determining if these cells are more "Schwann cell" or "oligodendrocyte". Furthermore, it would be interesting to determine the role the immature glial protein, BLBP, plays in the remyelination programme. Using electron microscopy to determine where it is found within the myelin sheath, and which other proteins it interacts with, would help us understand whether BLBP is encouraging or discouraging remyelination. From there, we could explore what features of the environment cause BLBP expression to persist in mature myelinating glial cells.

6. CONCLUDING REMARKS

This thesis has explored the adult mammalian spinal cord ependymal cell layer in the context of its function as a stem cell niche; how the functionality of the cells may vary with space and time; and the potential of the stem cell niche as a target to enhance endogenous remyelination programmes in diseases such as MS. The data outlined here support the theory that ependymal cells have unequal abilities to give rise to different cell types after injury, dependent on spatial location within the niche and age of the organism. These data also provide evidence that the developmental protein, BLBP, plays a role in the mammalian spinal cord's ability to remyelinate. Here, it is also hypothesized that the failure to successfully remyelinate in disease is due to the spinal cord ependymal cell's inability to replenish the OPC pool.

Further work is needed, possibly utilizing lineage tracing technology, to explore how the different spatiotemporal areas of the ependymal cell niche proliferate and differentiate into functional cells. From here, exploration can be done to determine which genes influence the differentiation of these cells, and therapeutics could be based on this work to encourage endogenous cells to produce the cells required to recover from injury, as an alternative to cell transplant therapy. The activation of the ependymal cell niche to produce OPCs could perhaps remedy the OPC pool depletion that potentially occurs in MS.

The role that BLBP plays in the production of myelinating cells in a pathogenic environment is also an attractive area of research. The LPC mouse model, which is capable of full remyelination and functional recovery, does not express BLBP in the myelinating cells. Perhaps this protein limits the production of myelin formation in human MS. However, work in this area will be difficult, as an appropriate mouse model, which mimics the BLBP expression patterns seen in human disease, is not currently available.

REFERENCES

Aguirre, A., & Gallo, V. (2007). Reduced EGFR signaling in adult progenitors of the subventricular zone attenuates oligodendrogenesis after demyelination. *Neuron Glia Biology*, *3*(3), 209–220. http://doi.org/10.1017/S1740925X08000082.Reduced

Alexandre, P., Reugels, A. M., Barker, D., Blanc, E., & Clarke, J. D. W. (2010). Neurons derive from the more apical daughter in asymmetric divisions in the zebrafish neural tube. *Nature Neuroscience*, *13*(6), 673–9. http://doi.org/10.1038/nn.2547

Alfaro-Cervello, C., Soriano-Navarro, M., Mirzadeh, Z., Alvarez-Buylla, A., & Garcia-Verdugo, J. M. (2012). Biciliated ependymal cell proliferation contributes to spinal cord growth. *Journal of Comparative Neurology*, *520*(15), 3528–3552. http://doi.org/10.1002/cne.23104

Altman, J., & Das, G. D. (1965). Autoradiographic and histological evidence of postnatal hippocampal neurogenesis in rats. *The Journal of Comparative Neurology*, *124*(3), 319–35. Retrieved from http://www.ncbi.nlm.nih.gov/pubmed/5861717

Anthony, T. E., Mason, H. a, Gridley, T., Fishell, G., & Heintz, N. (2005). Brain lipid-binding protein is a direct target of Notch signaling in radial glial cells service Brain lipid-binding protein is a direct target of Notch signaling in radial glial cells. *Genes & Development*, *19*, 1028–1033. http://doi.org/10.1101/gad.1302105

Barnabé-Heider, F., Göritz, C., Sabelström, H., Takebayashi, H., Pfrieger, F. W., Meletis, K., & Frisén, J. (2010). Origin of New Glial Cells in Intact and Injured Adult Spinal Cord. *Cell Stem Cell*, *7*(4), 470–482. http://doi.org/10.1016/j.stem.2010.07.014

Barnabe-Heider, F., & Miller, F. D. (2003). Endogenously Produced Neurotrophins Regulate Survival and Differentiation of Cortical Progenitors via Distinct Signaling Pathways. *J. Neurosci.*, *23*(12), 5149–5160. Retrieved from http://www.jneurosci.org/content/23/12/5149.full

Barnabé-Heider, F., Wasylnka, J. A., Fernandes, K. J. L., Porsche, C., Sendtner, M., Kaplan, D. R., & Miller, F. D. (2005). Evidence that embryonic neurons regulate the onset of cortical gliogenesis via cardiotrophin-1. *Neuron*, *48*(2), 253–265. http://doi.org/10.1016/j.neuron.2005.08.037

Barres, B. A., Lazar, M. A., & Raff, M. C. (1994). A novel role for thyroid hormone, glucocorticoids and retinoic acid in timing oligodendrocyte development. *Development (Cambridge, England)*, *120*(5), 1097–108. Retrieved from http://www.ncbi.nlm.nih.gov/pubmed/8026323

Bergami, M., Rimondini, R., Santi, S., Blum, R., Götz, M., & Canossa, M. (2008). Deletion of TrkB in adult progenitors alters newborn neuron integration into hippocampal circuits and increases anxiety-like behavior. *Proceedings of the National Academy of Sciences of the United States of America*, *105*, 15570–15575. http://doi.org/10.1073/pnas.0803702105

Blight, A. R. (1983). Cellular morphology of chronic spinal cord injury in the cat: Analysis of myelinated axons by line-sampling. *Neuroscience*, *10*(2), 521–543. http://doi.org/10.1016/0306-4522(83)90150-1

Bonaguidi, M. a, McGuire, T., Hu, M., Kan, L., Samanta, J., & Kessler, J. a. (2005). LIF and BMP signaling generate separate and discrete types of GFAP-expressing cells. *Development (Cambridge, England)*, *132*(24), 5503–14. http://doi.org/10.1242/dev.02166

Bonni, A. (1997). Regulation of Gliogenesis in the Central Nervous System by the JAK-STAT Signaling Pathway. *Science*, *278*(5337), 477–483. http://doi.org/10.1126/science.278.5337.477

Bradl, M., & Lassmann, H. (2010). Oligodendrocytes: biology and pathology. *Acta Neuropathologica*, *119*(1), 37–53. http://doi.org/10.1007/s00401-009-0601-5

Bresnahan, J. C., King, J. S., Martin, G. F., & Yashon, D. (1976). A neuroanatomical analysis of spinal cord injury in the rhesus monkey (Macaca mulatta). *Journal of the Neurological Sciences*, *28*(4), 521–542. http://doi.org/10.1016/0022-510X(76)90122-2

Bruce, J. H., Norenberg, M. D., Kraydieh, S., Puckett, W., Marcillo, A., & Dietrich, D. (2000). Proteoglycan Injury. *Journal of Neurotrauma*, *17*(9).

Busch, S. A., & Silver, J. (2007). The role of extracellular matrix in CNS regeneration. *Current Opinion in Neurobiology*, *17*(1), 120–127. http://doi.org/10.1016/j.conb.2006.09.004

Caillava, C., Vandenbosch, R., Jablonska, B., Deboux, C., Spigoni, G., Gallo, V., … Evercooren, A. B. Van. (2011). Cdk2 loss accelerates precursor differentiation and remyelination in the adult central nervous system. *Journal of Cell Biology*, *193*(2), 397–407. http://doi.org/10.1083/jcb.201004146

Calver, A. R., Hall, A. C., Yu, W. P., Walsh, F. S., Heath, J. K., Betsholtz, C., & Richardson, W. D. (1998). Oligodendrocyte population dynamics and the role of PDGF in vivo. *Neuron*, *20*(5), 869–882. http://doi.org/10.1016/S0896-6273(00)80469-9

Cammer, W., & Zhang, H. (1999). Maturation of oligodendrocytes is more sensitive to TNF alpha than is survival of precursors and immature oligodendrocytes. *Journal of Neuroimmunology*, *97*(1-2), 37–42. Retrieved from http://www.ncbi.nlm.nih.gov/pubmed/10408976

Cao, Q., Xu, X., Devries, W. H., Enzmann, G. U., Ping, P., Tsoulfas, P., … Whittemore, S. R. (2005). Functional Recovery in Traumatic Spinal Cord Injury after Transplantation of Multineurotrophin-Expressing Glial- Restricted Precursor Cells. *Construction*, *25*(30), 6947– 6957. http://doi.org/10.1523/JNEUROSCI.1065-05.2005

Carlén, M., Meletis, K., Göritz, C., Darsalia, V., Evergren, E., Tanigaki, K., … Frisén, J. (2009). Forebrain ependymal cells are Notch-dependent and generate neuroblasts and astrocytes after stroke. *Nature Neuroscience*, *12*(3), 259–267. http://doi.org/10.1038/nn.2268

Cheng, L.-C., Pastrana, E., Tavazoie, M., & Doetsch, F. (2009). miR-124 regulates adult neurogenesis in the subventricular zone stem cell niche. *Nature Neuroscience*, *12*(4), 399–408. http://doi.org/10.1038/nn.2294

Chew, L.-J., Shen, W., Ming, X., Senatorov, V. V., Chen, H.-L., Cheng, Y., … Gallo, V. (2011). SRY-Box Containing Gene 17 Regulates the Wnt/ -Catenin Signaling Pathway in Oligodendrocyte Progenitor Cells. *Journal of Neuroscience*, *31*(39), 13921–13935. http://doi.org/10.1523/JNEUROSCI.3343-11.2011

Cohen, R. I., Marmur, R., Norton, W. T., Mehler, M. F., & Kessler, J. A. (1996). Nerve growth factor and neurotrophin-3 differentially regulate the proliferation and survival of developing rat brain oligodendrocytes. *The Journal of Neuroscience : The Official Journal of the Society for Neuroscience*, *16*(20), 6433–42. Retrieved from http://www.ncbi.nlm.nih.gov/pubmed/8815922

Conboy, I. M., Conboy, M. J., Wagers, A. J., Girma, E. R., Weissman, I. L., & Rando, T. A. (2005). Rejuvenation of aged progenitor cells by exposure to a young systemic environment. *Nature*, *433*(7027), 760–4. http://doi.org/10.1038/nature03260

Crockett, D. P., Burshteyn, M., Garcia, C., Muggironi, M., & Casaccia-Bonnefil, P. (2005). Number of oligodendrocyte progenitors recruited to the lesioned spinal cord is modulated by the levels of the cell cycle regulatory protein p27Kip-1. *Glia*, *49*(2), 301–308. http://doi.org/10.1002/glia.20111

Cummings, B. J., Uchida, N., Tamaki, S. J., Salazar, D. L., Hooshmand, M., Summers, R., … Anderson, A. J. (2005). Human neural stem cells differentiate and promote locomotor recovery in spinal cord-injured mice. *Proceedings of the National Academy of Sciences of the United States of America*, *102*(39), 14069–14074. http://doi.org/10.1073/pnas.0507063102

Deneen, B., Ho, R., Lukaszewicz, A., Hochstim, C. J., Gronostajski, R. M., & Anderson, D. J. (2006). The Transcription Factor NFIA Controls the Onset of Gliogenesis in the Developing Spinal Cord. *Neuron*, *52*(6), 953–968. http://doi.org/10.1016/j.neuron.2006.11.019

Doetsch, F., Caillé, I., Lim, D. A., García-Verdugo, J. M., & Alvarez-Buylla, A. (1999). Subventricular Zone Astrocytes Are Neural Stem Cells in the Adult Mammalian Brain. *Cell*, *97*(6), 703–716. http://doi.org/10.1016/S0092-8674(00)80783-7

Dromard, C., Guillon, H., Rigau, V., Ripoll, C., Sabourin, J. C., Perrin, F. E., … Bauchet, L. (2008). Adult human spinal cord harbors neural precursor cells that generate neurons and glial cells in vitro. *Journal of Neuroscience Research*, *86*, 1916–1926. http://doi.org/10.1002/jnr.21646

Duncan, I. D., & Hoffman, R. L. (1997). Schwann cell invasion of the central nervous system of the myelin mutants. *Journal of Anatomy, 190 (Pt 1*(September 1995), 35–49. http://doi.org/10.1046/j.1469-7580.1997.19010035.x

Emsley, J. G., & Macklis, J. D. (2006). Astroglial heterogeneity closely reflects the neuronal-defined anatomy of the adult murine CNS. *Neuron Glia Biology*, *2*(3), 175–86. http://doi.org/10.1017/S1740925X06000202

Eriksson, P. S., Perfilieva, E., Björk-Eriksson, T., Alborn, A. M., Nordborg, C., Peterson, D. A., & Gage, F. H. (1998). Neurogenesis in the adult human hippocampus. *Nature Medicine*, *4*(11), 1313–7. http://doi.org/10.1038/3305

Fan, G., Martinowich, K., Chin, M. H., He, F., Fouse, S. D., Hutnick, L., … Sun, Y. E. (2005). DNA methylation controls the timing of astrogliogenesis through regulation of JAK-STAT signaling. *Development (Cambridge, England)*, *132*, 3345–3356. http://doi.org/10.1242/dev.01912

Faulkner, J. R., Herrmann, J. E., Woo, M. J., Tansey, K. E., Doan, N. B., & Sofroniew, M. V. (2004). Reactive astrocytes protect tissue and preserve function after spinal cord injury. *The Journal of Neuroscience : The Official Journal of the Society for Neuroscience*, *24*(9), 2143–55. http://doi.org/10.1523/JNEUROSCI.3547-03.2004

Feng, L., Hatten, M. E., & Heintz, N. (1994). Brain lipid-binding protein (BLBP): A novel signaling system in the developing mammalian CNS. *Neuron*, *12*(4), 895–908. http://doi.org/10.1016/0896-6273(94)90341-7

Fortin, D. (2005). Distinct Fibroblast Growth Factor (FGF)/FGF Receptor Signaling Pairs Initiate Diverse Cellular Responses in the Oligodendrocyte Lineage. *Journal of Neuroscience*, *25*(32), 7470–7479. http://doi.org/10.1523/JNEUROSCI.2120-05.2005

Franklin, R. J., & Blakemore, W. F. (1993). Requirements for Schwann cell migration within CNS environments: a viewpoint. *International Journal of Developmental Neuroscience : The Official Journal of the International Society for Developmental Neuroscience*, *11*(5), 641–9. Retrieved from http://www.ncbi.nlm.nih.gov/pubmed/8116476

Franklin, R. J. M. (2002). Why does remyelination fail in multiple sclerosis? *Nature Reviews Neuroscience*, *3*(9), 705–714. http://doi.org/10.1038/nrn917

Frisén, J., Johansson, C. B., Török, C., Risling, M., & Lendahl, U. (1995). Rapid, widespread, and longlasting induction of nestin contributes to the generation of glial scar tissue after CNS injury. *The Journal of Cell Biology*, *131*(2), 453–64. http://doi.org/10.1083/jcb.131.2.453

Fu, H., Qi, Y., Tan, M., Cai, J., Hu, X., Liu, Z., … Qiu, M. (2003). Molecular mapping of the origin of postnatal spinal cord ependymal cells: evidence that adult ependymal cells are derived from Nkx6.1+ ventral neural progenitor cells. *The Journal of Comparative Neurology*, *456*(3), 237–244. http://doi.org/10.1002/cne.10481

Garcia-Ovejero, D., Arevalo-Martin, A., Paniagua-Torija, B., Florensa-Vila, J., Ferrer, I., Grassner, L., & Molina-Holgado, E. (2015). The ependymal region of the adult human spinal cord differs from other species and shows ependymoma-like features. *Brain*, 1–15. http://doi.org/10.1093/brain/awv089

Gartzen, K., Katzarava, Z., Diener, H.-C., & Putzki, N. (2011). Peripheral nervous system involvement in multiple sclerosis. *European Journal of Neurology : The Official Journal of the European Federation of Neurological Societies*, *18*(5), 789–91. http://doi.org/10.1111/j.1468-1331.2010.03149.x

Gattazzo, F., Urciuolo, A., & Bonaldo, P. (2014). Extracellular matrix: a dynamic microenvironment for stem cell niche. *Biochimica et Biophysica Acta*, *1840*(8), 2506–19. http://doi.org/10.1016/j.bbagen.2014.01.010

Gensert, J. M., & Goldman, J. E. (1997). Endogenous progenitors remyelinate demyelinated axons in the adult CNS. *Neuron*, *19*(1), 197–203. http://doi.org/10.1016/S0896-6273(00)80359-1

Ghatak, N. R., Hirano, A., Doron, Y., & Zimmerman, H. M. (1973). Remyelination in multiple sclerosis with peripheral type myelin. *Arch Neurol*, *29*(262), 262–267.

http://doi.org/10.1001/archneur.1973.00490280074011

Gilson, J., & Blakemore, W. F. (1993). Failure of remyelination in areas of demyelination produced in the spinal cord of old rats. *Neuropathology and Applied Neurobiology*, *19*(2), 173–181. http://doi.org/10.1111/j.1365-2990.1993.tb00424.x

Goldman, S. A., & Kuypers, N. J. (2015). How to make an oligodendrocyte. *Development*, *142*(23), 3983–3995. http://doi.org/10.1242/dev.126409

Grinspan, J., Edell, E., Carpio, D. F., Beesley, J. S., Lavy, L., Pleasure, D., & Golden, J. A. (2000). Stage-specific effects of bone morphogenetic proteins on the oligodendrocyte lineage. *Journal of Neurobiology*, *43*(1), 1–17. http://doi.org/10.1002/(SICI)1097-4695(200004)43:1<1::AID-NEU1>3.0.CO;2-0

Guest, J. D., Hiester, E. D., & Bunge, R. P. (2005). Demyelination and Schwann cell responses adjacent to injury epicenter cavities following chronic human spinal cord injury. *Experimental Neurology*, *192*, 384–393. http://doi.org/10.1016/j.expneurol.2004.11.033

Hamilton, L. K., Truong, M. K. V, Bednarczyk, M. R., Aumont, a., & Fernandes, K. J. L. (2009). Cellular organization of the central canal ependymal zone, a niche of latent neural stem cells in the adult mammalian spinal cord. *Neuroscience*, *164*(3), 1044–1056. http://doi.org/10.1016/j.neuroscience.2009.09.006

Harrison, B. M., & Pollard, J. D. (1984). to identify some of the factors that might influence the dispersal of Schwann cells in central lesions . A dorsal laminectomy was performed over two vertebral segments in the lower thoracic region of 5 anesthetized adult DA strain rats . Two microliters o. *Neuroscience Letters*, *52*, 275–280.

Hochstim, C., Deneen, B., Lukaszewicz, A., Zhou, Q., & Anderson, D. J. (2008). Identification of positionally distinct astrocyte subtypes whose identities are specified by a homeodomain code. *Cell*, *133*(3), 510–22. http://doi.org/10.1016/j.cell.2008.02.046

Hofstetter, C. P., Holmström, N. a V, Lilja, J. a, Schweinhardt, P., Hao, J., Spenger, C., … Olson, L. (2005). Allodynia limits the usefulness of intraspinal neural stem cell grafts; directed differentiation improves outcome. *Nature Neuroscience*, *8*(3), 346–53. http://doi.org/10.1038/nn1405

Horner, P. J., Power, a E., Kempermann, G., Kuhn, H. G., Palmer, T. D., Winkler, J., … Gage, F. H. (2000). Proliferation and differentiation of progenitor cells throughout the intact adult rat spinal cord. *The Journal of Neuroscience : The Official Journal of the Society for Neuroscience*, *20*(6), 2218–2228.

Huang, J. K., Jarjour, A. A., Nait Oumesmar, B., Kerninon, C., Williams, A., Krezel, W., … Franklin, R. J. M. (2011). Retinoid X receptor gamma signaling accelerates CNS remyelination. *Nature Neuroscience*, *14*(1), 45–53. http://doi.org/10.1038/nn.2702

Itoyama, Y., Webster, H. D., Richardson, E. P., & Trapp, B. D. (1983). Schwann cell remyelination of demyelinated axons in spinal cord multiple sclerosis lesions. *Annals of Neurology*, *14*(3), 339–46. http://doi.org/10.1002/ana.410140313

Jasmin, L., Janni, G., Moallem, T. M., Lappi, D. A., & Ohara, P. T. (2000). Schwann cells are removed from the spinal cord after effecting recovery from paraplegia. *The Journal of*

Neuroscience : The Official Journal of the Society for Neuroscience, *20*(24), 9215–9223. Retrieved from http://www.ncbi.nlm.nih.gov/entrez/query.fcgi?db=pubmed&cmd=Retrieve&dopt=AbstractPlus&list_uids=11124999\npapers3://publication/uuid/45FBF62B-6D97-4BD6-B348-190972FEA980

Jeffery, N. D., & Blakemore, W. F. (1995). Remyelination of mouse spinal cord axons demyelinated by local injection of lysolecithin. *Journal of Neurocytology*, *24*(10), 775–81. Retrieved from http://www.ncbi.nlm.nih.gov/pubmed/8586997

Jessen, K. R., & Mirsky, R. (2005). The origin and development of glial cells in peripheral nerves. *Nature Reviews*, *6*(9), 671–682. http://doi.org/10.1038/nrn1746

Johansson, C. B., Momma, S., Clarke, D. L., Risling, M., Lendahl, U., & Frisén, J. (1999). Identification of a neural stem cell in the adult mammalian central nervous system. *Cell*, *96*(1), 25–34. http://doi.org/10.1016/S0092-8674(00)80956-3

Kang, P., Lee, H. K., Glasgow, S. M., Finley, M., Donti, T., Gaber, Z. B., … Deneen, B. (2012). Sox9 and NFIA Coordinate a Transcriptional Regulatory Cascade during the Initiation of Gliogenesis. *Neuron*, *74*(1), 79–94. http://doi.org/10.1016/j.neuron.2012.01.024

Kazanis, I., & Ffrench-Constant, C. (2011). Extracellular matrix and the neural stem cell niche. *Developmental Neurobiology*, *71*(11), 1006–1017. http://doi.org/10.1002/dneu.20970

Kempermann, G. (2011). Seven principles in the regulation of adult neurogenesis. *The European Journal of Neuroscience*, *33*(6), 1018–24. http://doi.org/10.1111/j.1460-9568.2011.07599.x

Kessaris, N., Fogarty, M., Iannarelli, P., Grist, M., Wegner, M., & Richardson, W. D. (2006). Competing waves of oligodendrocytes in the forebrain and postnatal elimination of an embryonic lineage. *Nature Neuroscience*, *9*(2), 173–179. http://doi.org/10.1038/nn1620

Konno, D., Shioi, G., Shitamukai, A., Mori, A., Kiyonari, H., Miyata, T., & Matsuzaki, F. (2008). Neuroepithelial progenitors undergo LGN-dependent planar divisions to maintain self-renewability during mammalian neurogenesis. *Nature Cell Biology*, *10*(1), 93–U78. http://doi.org/Doi 10.1038/Ncb1673

Korenjak, M., & Brehm, A. (2005). E2F-Rb complexes regulating transcription of genes important for differentiation and development. *Current Opinion in Genetics & Development*, *15*(5), 520–7. http://doi.org/10.1016/j.gde.2005.07.001

Kriegstein, A., Alvarez-buylla, A., & Manuscript, A. (2009). NIH Public Access, *25*(3), 184–195. http://doi.org/10.1002/cne.22282.Regional

Krökki, O., Bloigu, R., Ansakorpi, H., Reunanen, M., & Remes, A. M. (2014). Neurological comorbidity and survival in multiple sclerosis. *Multiple Sclerosis and Related Disorders*, *3*(1), 72–77. http://doi.org/10.1016/j.msard.2013.06.006

Lacroix, S., Hamilton, L. K., Vaugeois, A., Beaudoin, S., Breault-Dugas, C., Pineau, I., … Fernandes, K. J. L. (2014). Central Canal Ependymal Cells Proliferate Extensively in Response to Traumatic Spinal Cord Injury but Not Demyelinating Lesions. *PLoS ONE*, *9*(1), e85916. http://doi.org/10.1371/journal.pone.0085916

Lee, K. H., Yoon, D. H., Park, Y. G., & Lee, B. H. (2005). Effects of glial transplantation on functional recovery following acute spinal cord injury. *Journal of Neurotrauma*, *22*(5), 575–89. http://doi.org/10.1089/neu.2005.22.575

Li, Y., Luikart, B. W., Birnbaum, S., Chen, J., Kwon, C. H., Kernie, S. G., … Parada, L. F. (2008). TrkB Regulates Hippocampal Neurogenesis and Governs Sensitivity to Antidepressive Treatment. *Neuron*, *59*(3), 399–412. http://doi.org/10.1016/j.neuron.2008.06.023

Llamazares, M., Cal, S., Quesada, V., & López-Otín, C. (2003). Identification and characterization of ADAMTS-20 defines a novel subfamily of metalloproteinases-disintegrins with multiple thrombospondin-1 repeats and a unique GON domain. *Journal of Biological Chemistry*, *278*(15), 13382–13389. http://doi.org/10.1074/jbc.M211900200

Lu, Q. R., Sun, T., Zhu, Z., Ma, N., Garcia, M., Stiles, C. D., & Rowitch, D. H. (2002). Common developmental requirement for Olig function indicates a motor neuron/oligodendrocyte connection. *Cell*, *109*(1), 75–86. http://doi.org/10.1016/S0092-8674(02)00678-5

Lu, Q. R., Yuk, D., Alberta, J. a, Zhu, Z., Pawlitzky, I., Chan, J., … Rowitch, D. H. (2000). Sonic hedgehog--regulated oligodendrocyte lineage genes encoding bHLH proteins in the mammalian central nervous system. *Neuron*, *25*(2), 317–329. http://doi.org/10.1016/S0896-6273(00)80897-1

Masahira, N., Takebayashi, H., Ono, K., Watanabe, K., Ding, L., Furusho, M., … Ikenaka, K. (2006). Olig2-positive progenitors in the embryonic spinal cord give rise not only to motoneurons and oligodendrocytes, but also to a subset of astrocytes and ependymal cells. *Developmental Biology*, *293*(2), 358–369. http://doi.org/10.1016/j.ydbio.2006.02.029

Mason, J. L., Suzuki, K., Chaplin, D. D., & Matsushima, G. K. (2001). Interleukin-1beta promotes repair of the CNS. *Journal of Neuroscience*, *21*(18), 7046–7052. http://doi.org/21/18/7046 [pii]

McKinnon, R. D., Matsui, T., Dubois-Dalcq, M., & Aaronsont, S. A. (1990). FGF modulates the PDGF-driven pathway of oligodendrocyte development. *Neuron*, *5*(5), 603–614. http://doi.org/10.1016/0896-6273(90)90215-2

McTigue, D. M., Horner, P. J., Stokes, B. T., & Gage, F. H. (1998). Neurotrophin-3 and Brain-Derived Neurotrophic Factor Induce Oligodendrocyte Proliferation and Myelination of Regenerating Axons in the Contused Adult Rat Spinal Cord. *J. Neurosci.*, *18*(14), 5354–5365. Retrieved from http://www.jneurosci.org/content/18/14/5354.full

Mekki-Dauriac, S., Agius, E., Kan, P., & Cochard, P. (2002). Bone morphogenetic proteins negatively control oligodendrocyte precursor specification in the chick spinal cord. *Development (Cambridge, England)*, *129*(22), 5117–5130.

Mela, A., & Goldman, J. E. (2013). CD82 Blocks cMet Activation and Overcomes Hepatocyte Growth Factor Effects on Oligodendrocyte Precursor Differentiation. *The Journal of Neuroscience : The Official Journal of the Society for Neuroscience*, *33*(18), 7952–60. http://doi.org/10.1523/JNEUROSCI.5836-12.2013

Meletis, K., Barnabé-Heider, F., Carlén, M., Evergren, E., Tomilin, N., Shupliakov, O., & Frisén,

J. (2008). Spinal Cord Injury Reveals Multilineage Differentiation of Ependymal Cells. *PLoS Biology*, *6*(7), e182. http://doi.org/10.1371/journal.pbio.0060182

Menn, B., Garcia-Verdugo, J. M., Yaschine, C., Gonzalez-Perez, O., Rowitch, D., & Alvarez-Buylla, A. (2006). Origin of oligodendrocytes in the subventricular zone of the adult brain. *The Journal of Neuroscience : The Official Journal of the Society for Neuroscience*, *26*(30), 7907–7918. http://doi.org/10.1523/JNEUROSCI.1299-06.2006

Miller, F. D., & Gauthier, A. S. (2007). Timing Is Everything: Making Neurons versus Glia in the Developing Cortex. *Neuron*, *54*(3), 357–369. http://doi.org/10.1016/j.neuron.2007.04.019

Miller, R. H. (2002). Regulation of oligodendrocyte development in the vertebrate CNS. *Progress in Neurobiology*, *67*(6), 451–467. http://doi.org/10.1016/S0301-0082(02)00058-8

Minagar, A., & Alexander, J. S. (2003). Blood-brain barrier disruption in multiple sclero sis. *Multiple Sclerosis Journal*, *9*, 540–549. http://doi.org/10.1191/1352458503ms965oa

Ming, X., Chew, L.-J., & Gallo, V. (2013). Transgenic overexpression of Sox17 promotes oligodendrocyte development and attenuates demyelination. *The Journal of Neuroscience : The Official Journal of the Society for Neuroscience*, *33*(30), 12528–42. http://doi.org/10.1523/JNEUROSCI.0536-13.2013

Misawa, S., Kuwabara, S., Mori, M., Hayakawa, S., Sawai, S., & Hattori, T. (2008). Peripheral nerve demyelination in multiple sclerosis. *Clinical Neurophysiology : Official Journal of the International Federation of Clinical Neurophysiology*, *119*(8), 1829–33. http://doi.org/10.1016/j.clinph.2008.04.010

Mitsui, T. (2005). Transplantation of Neuronal and Glial Restricted Precursors into Contused Spinal Cord Improves Bladder and Motor Functions, Decreases Thermal Hypersensitivity, and Modifies Intraspinal Circuitry. *Journal of Neuroscience*, *25*(42), 9624–9636. http://doi.org/10.1523/JNEUROSCI.2175-05.2005

Morrens, J., Van Den Broeck, W., & Kempermann, G. (2012). Glial cells in adult neurogenesis. *Glia*, *60*(2), 159–174. http://doi.org/10.1002/glia.21247

Mothe, a, & Tator, C. (2005). Proliferation, migration, and differentiation of endogenous ependymal region stem/progenitor cells following minimal spinal cord injury in the adult rat. *Neuroscience*, *131*, 177–187. http://doi.org/10.1016/j.neuoscience.2004.10.011

Mozell, R. L., & McMorris, F. A. (1991). Insulin-like growth factor I stimulates oligodendrocyte development and myelination in rat brain aggregate cultures. *Journal of Neuroscience Research*, *30*(2), 382–90. http://doi.org/10.1002/jnr.490300214

Murtie, J. C., Zhou, Y. X., Le, T. Q., Vana, A. C., & Armstrong, R. C. (2005). PDGF and FGF2 pathways regulate distinct oligodendrocyte lineage responses in experimental demyelination with spontaneous remyelination. *Neurobiology of Disease*, *19*(1-2), 171–182. http://doi.org/10.1016/j.nbd.2004.12.006

Nagoshi, N., Shibata, S., Hamanoue, M., Mabuchi, Y., Matsuzaki, Y., Toyama, Y., … Okano, H. (2011). Schwann cell plasticity after spinal cord injury shown by neural crest lineage tracing. *Glia*, *59*, 771–784. http://doi.org/10.1002/glia.21150

Namihira, M., Kohyama, J., Semi, K., Sanosaka, T., Deneen, B., Taga, T., & Nakashima, K. (2009). Committed Neuronal Precursors Confer Astrocytic Potential on Residual Neural Precursor Cells. *Developmental Cell*, *16*(2), 245–255. http://doi.org/10.1016/j.devcel.2008.12.014

Nave, K.-A. (2010). Myelination and the trophic support of long axons. *Nature Reviews. Neuroscience*, *11*(4), 275–83. http://doi.org/10.1038/nrn2797

Ng, K., Howells, J., Pollard, J. D., & Burke, D. (2008). Up-regulation of slow K(+) channels in peripheral motor axons: a transcriptional channelopathy in multiple sclerosis. *Brain : A Journal of Neurology*, *131*(Pt 11), 3062–71. http://doi.org/10.1093/brain/awn180

Nygårdas, P. T., & Hinkkanen, A. E. (2002). Up-regulation of MMP-8 and MMP-9 activity in the BALB/c mouse spinal cord correlates with the severity of experimental autoimmune encephalomyelitis. *Clinical and Experimental Immunology*, *128*(2), 245–254. http://doi.org/10.1046/j.1365-2249.2002.01855.x

Ohya, W., Funakoshi, H., Kurosawa, T., & Nakamura, T. (2007). Hepatocyte growth factor (HGF) promotes oligodendrocyte progenitor cell proliferation and inhibits its differentiation during postnatal development in the rat. *Brain Research*, *1147*(1), 51–65. http://doi.org/10.1016/j.brainres.2007.02.045

Okada, S., Nakamura, M., Katoh, H., Miyao, T., Shimazaki, T., Ishii, K., … Okano, H. (2006). Conditional ablation of Stat3 or Socs3 discloses a dual role for reactive astrocytes after spinal cord injury. *Nature Medicine*, *12*(7), 829–34. http://doi.org/10.1038/nm1425

Paridaen, J. T., & Huttner, W. B. (2014). Neurogenesis during development of the vertebrate central nervous system. *EMBO Reports*, *15*(4), 351–364. http://doi.org/10.1002/embr.201438447

Parras, C. M., Galli, R., Britz, O., Soares, S., Galichet, C., Battiste, J., … Guillemot, F. (2004). Mash1 specifies neurons and oligodendrocytes in the postnatal brain. *The EMBO Journal*, *23*(22), 4495–505. http://doi.org/10.1038/sj.emboj.7600447

Parras, C. M., Hunt, C., Sugimori, M., Nakafuku, M., Rowitch, D., & Guillemot, F. (2007). The proneural gene Mash1 specifies an early population of telencephalic oligodendrocytes. *The Journal of Neuroscience : The Official Journal of the Society for Neuroscience*, *27*(16), 4233–42. http://doi.org/10.1523/JNEUROSCI.0126-07.2007

Petit, A., Sanders, A. D., Kennedy, T. E., Tetzlaff, W., Glattfelder, K. J., Dalley, R. a, … Roskams, a J. (2011). Adult spinal cord radial glia display a unique progenitor phenotype. *PloS One*, *6*(9), e24538. http://doi.org/10.1371/journal.pone.0024538

Plemel, J. R., Duncan, G., Chen, K.-W. K., Shannon, C., Park, S., Sparling, J. S., & Tetzlaff, W. (2008). A graded forceps crush spinal cord injury model in mice. *Journal of Neurotrauma*, *25*(4), 350–70. http://doi.org/10.1089/neu.2007.0426

Qin, Y., Zhang, W., & Yang, P. (2015). Current states of endogenous stem cells in adult spinal cord. *Journal of Neuroscience Research*, *93*(3), 391–398. http://doi.org/10.1002/jnr.23480

Ransohoff, R. M., Hafler, D. A., & Lucchinetti, C. F. (2015). Multiple sclerosis—a quiet revolution. *Nature Reviews Neurology*, *11*(3), 134–142.

http://doi.org/10.1038/nrneurol.2015.14

Reynolds, B. A., & Weiss, S. (2016). Generation of Neurons and Astrocytes from Isolated Cells of the Adult Mammalian Central Nervous System Authors (s): Brent A . Reynolds and Samuel Weiss Published by : American Association for the Advancement of Science Stable URL : http://www.jstor.org/, *255*(5052), 1707–1710.

Riley, D. J., Lee, E. Y.-H. P., & Lee, W.-H. (1994). The retinoblastoma protein: More than a tumor suppressor. *Annual Review of Cell Biology*, *10*, 1–29.

Rowitch, D. H. (2004). Glial specification in the vertebrate neural tube. *Nature Reviews. Neuroscience*, *5*(5), 409–419. http://doi.org/10.1038/nrn1389

Schoene, W. C., Carpenter, S., Behan, P. O., & Geschwind, N. (1977). "Onion Bulb" Formations in the Central and Peripheral Nervous System in Association With Multiple Sclerosis and Hypertrophic Polyneuropathy. *Brain*, *100*(4), 755–773. http://doi.org/10.1093/brain/100.4.755

Scott, C. E., Wynn, S. L., Sesay, A., Cruz, C., Cheung, M., Gomez Gaviro, M.-V., … Briscoe, J. (2010). SOX9 induces and maintains neural stem cells. *Nature Neuroscience*, *13*(10), 1181–1189. http://doi.org/10.1038/nn.2646

Ševc, J., Daxnerová, Z., Haňová, V., & Koval', J. (2011). Novel observations on the origin of ependymal cells in the ventricular zone of the rat spinal cord. *Acta Histochemica*, *113*(2), 156–162. http://doi.org/10.1016/j.acthis.2009.09.007

Shihabuddin, L. S., Horner, P. J., Ray, J., & Gage, F. H. (2000). Adult spinal cord stem cells generate neurons after transplantation in the adult dentate gyrus. *The Journal of Neuroscience : The Official Journal of the Society for Neuroscience*, *20*(23), 8727–35. http://doi.org/20/23/8727 [pii]

Shitamukai, A., Konno, D., & Matsuzaki, F. (2011). Oblique Radial Glial Divisions in the Developing Mouse Neocortex Induce Self-Renewing Progenitors outside the Germinal Zone That Resemble Primate Outer Subventricular Zone Progenitors. *J Neurosci*, *31*(10), 3683–3695. http://doi.org/10.1523/JNEUROSCI.4773-10.2011

Sikder, H. A., Devlin, M. K., Dunlap, S., Ryu, B., & Alani, R. M. (2003). Id proteins in cell growth and tumorigenesis. *Cancer Cell*, *3*(6), 525–530. http://doi.org/10.1016/S1535-6108(03)00141-7

Silver, J., & Miller, J. H. (2004). Regeneration beyond the glial scar. *Nature Reviews Neuroscience*, *5*(2), 146–156. http://doi.org/10.1038/nrn1326

Soula, C., Danesin, C., Kan, P., Grob, M., Poncet, C., & Cochard, P. (2001). Distinct sites of origin of oligodendrocytes and somatic motoneurons in the chick spinal cord: oligodendrocytes arise from Nkx2.2-expressing progenitors by a Shh-dependent mechanism. *Development (Cambridge, England)*, *128*(8), 1369–1379.

Spassky, N. (2005). Adult Ependymal Cells Are Postmitotic and Are Derived from Radial Glial Cells during Embryogenesis. *Journal of Neuroscience*, *25*(1), 10–18. http://doi.org/10.1523/JNEUROSCI.1108-04.2005

Spassky, N., de Castro, F., Le Bras, B., Heydon, K., Quéraud-LeSaux, F., Bloch-Gallego, E., … Thomas, J.-L. (2002). Directional guidance of oligodendroglial migration by class 3 semaphorins and netrin-1. *The Journal of Neuroscience : The Official Journal of the Society for Neuroscience*, *22*(14), 5992–6004. http://doi.org/20026573

Stankoff, B., Aigrot, M.-S., Noël, F., Wattilliaux, A., Zalc, B., & Lubetzki, C. (2002). Ciliary neurotrophic factor (CNTF) enhances myelin formation: a novel role for CNTF and CNTF-related molecules. *The Journal of Neuroscience : The Official Journal of the Society for Neuroscience*, *22*(21), 9221–7. http://doi.org/22/21/9221 [pii]

Stolt, C. C., Lommes, P., Sock, E., Chaboissier, M., Schedl, A., & Wegner, M. (2003). The Sox9 transcription factor determines glial fate choice in the developing spinal cord, 1677–1689. http://doi.org/10.1101/gad.259003.)

Talbott, J. F., Loy, D. N., Liu, Y., Qiu, M. S., Bunge, M. B., Rao, M. S., & Whittemore, S. R. (2005). Endogenous Nkx2.2+/Olig2+ oligodendrocyte precursor cells fail to remyelinate the demyelinated adult rat spinal cord in the absence of astrocytes. *Experimental Neurology*, *192*(1), 11–24. http://doi.org/10.1016/j.expneurol.2004.05.038

Taylor, M. K., Yeager, K., & Morrison, S. J. (2007). Physiological Notch signaling promotes gliogenesis in the developing peripheral and central nervous systems. *Development*, *134*(13), 2435–2447. http://doi.org/10.1242/dev.005520

Tien, A.-C., Tsai, H.-H., Molofsky, A. V, McMahon, M., Foo, L. C., Kaul, A., … Rowitch, D. H. (2012). Regulated temporal-spatial astrocyte precursor cell proliferation involves BRAF signalling in mammalian spinal cord. *Development (Cambridge, England)*, *139*(14), 2477–87. http://doi.org/10.1242/dev.077214

Totoiu, M. O., & Keirstead, H. S. (2005). Spinal cord injury is accompanied by chronic progressive demyelination. *The Journal of Comparative Neurology*, *486*(4), 373–83. http://doi.org/10.1002/cne.20517

Tsai, H.-H., Li, H., Fuentealba, L. C., Molofsky, A. V, Taveira-Marques, R., Zhuang, H., … Rowitch, D. H. (2012). Regional astrocyte allocation regulates CNS synaptogenesis and repair. *Science (New York, N.Y.)*, *337*(6092), 358–62. http://doi.org/10.1126/science.1222381

Vallstedt, A., Klos, J. M., & Ericson, J. (2005). Multiple dorsoventral origins of oligodendrocyte generation in the spinal cord and hindbrain. *Neuron*, *45*(1), 55–67. http://doi.org/10.1016/j.neuron.2004.12.026

Vondran, M. W., Clinton-Luke, P., Honeywell, J. Z., & Dreyfus, C. F. (2010). BDNF +/- mice exhibit deficits in oligodendrocyte lineage cells of the basal forebrain. *Glia*, *58*(7), 848–856. http://doi.org/10.1002/glia.20969

VonDran, M. W., Singh, H., Honeywell, J. Z., & Dreyfus, C. F. (2011). Levels of BDNF impact oligodendrocyte lineage cells following a cuprizone lesion. *The Journal of Neuroscience : The Official Journal of the Society for Neuroscience*, *31*(40), 14182–90. http://doi.org/10.1523/JNEUROSCI.6595-10.2011

Weiss, S., Dunne, C., Hewson, J., Wohl, C., Wheatley, M., Peterson, a C., & Reynolds, B. a.

(1996). Multipotent CNS stem cells are present in the adult mammalian spinal cord and ventricular neuroaxis. *The Journal of Neuroscience : The Official Journal of the Society for Neuroscience*, *16*(23), 7599–7609.

Xu, Y., Kitada, M., Yamaguchi, M., Dezawa, M., & Ide, C. (2006). Increase in bFGF-responsive neural progenitor population following contusion injury of the adult rodent spinal cord. *Neuroscience Letters*, *397*(3), 174–9. http://doi.org/10.1016/j.neulet.2005.12.051

Yamamoto, T., Kawamura, J., Hashimoto, S., & Nakamura, M. (1991). Extensive proliferation of peripheral type myelin in necrotic spinal cord lesions of multiple sclerosis. *Journal of the Neurological Sciences*, *102*(2), 163–9. Retrieved from http://www.ncbi.nlm.nih.gov/pubmed/2072116

Yun, M. (2015). Changes in Regenerative Capacity through Lifespan. *International Journal of Molecular Sciences*, *16*(10), 25392–25432. http://doi.org/10.3390/ijms161025392

Zawadzka, M., Rivers, L. E., Fancy, S. P. J., Zhao, C., Tripathi, R., Jamen, F., … Franklin, R. J. M. (2010). CNS-resident glial progenitor/stem cells produce Schwann cells as well as oligodendrocytes during repair of CNS demyelination. *Cell Stem Cell*, *6*(6), 578–90. http://doi.org/10.1016/j.stem.2010.04.002

APPENDICES

APPENDIX A – Spatial and temporal information of all genes in central canal

The accompanying excel spreadsheet shows the list of all genes expressed in the central canal, with details of their spatial (i.e. dorsal/ventral, lateral, etc.) and temporal expression (i.e. P4 vs P56) patterns. “y” stands for “Yes”, i.e. the gene qualifies for the given categorization.

Age	Gene Name	in the CC?	Dorsal (D)	Ventral (V)	Lateral (L)	DV	mostly D	mostly V	All Around
P4	1110004E09Rik	y							y
P56									
P4	1110007C02Rik	y				y			
P56		y				y			
P4	1200011O22Rik	y							y
P56									
P4	1500015O10Rik	y							y
P56		y							y
P4	1700003E16Rik	y							y
P56		y							y
P4	1700009P17Rik	y							y
P56		y							y
P4	1700019L03Rik	y							y
P56		y							y
P4	1700026D08Rik	y					y		
P56		y							y
P4	1700027A23Rik	y					y		
P56		y							y
P4	1700028P14Rik	y					y		
P56		y							y
P4	1700041C02Rik	y					y		
P56		y							y
P4	2010001J22Rik	y							y
P56		y							y
P4	2010001K21Rik	y			y				
P56		y							y
P4	2210020M01Rik								
P56		y							y
P4	2300002G24Rik								
P56		y		y					
P4	2310016C16Rik	y							y
P56		y							y
P4	2410004P03Rik	y							y
P56									
P4	2610301B20Rik	y							y
P56									
P4	2810051F02Rik	y				y			
P56		y							y
P4	3100002J23Rik	y					y		
P56		y							y
P4	3230401M21Rik	y					y		
P56		y							y
P4	4432405B04Rik	y					y		
P56		y							y
P4	4921528H16Rik	y							y
P56		y							y
P4	4921531P07Rik	y							y
P56		y							y
P4	4930430E16Rik	y							y
P56									

Age	Gene Name	in the CC?	Dorsal (D)	Ventral (V)	Lateral (L)	DV	mostly D	mostly V	All Around
P4	4930438O03Rik	y							y
P56		y							y
P4	4930451C15Rik	y					y		
P56		y							y
P4	4930526H21Rik	y			y				
P56		y							y
P4	4930579J09Rik	y					y		
P56		y							y
P4	4933407L21Rik	y				y			
P56									
P4	5133400G04Rik	y							y
P56									
P4	5730403M16Rik								
P56		y							y
P4	5730593F17Rik	y							y
P56									
P4	8430416H19Rik	y			y				
P56		y							y
P4	A330021E22Rik	y							y
P56		y							y
P4	Adamts16	y							y
P56									
P4	Adamts20	y			y				
P56		y			y				
P4	Adck4	y							y
P56		y							y
P4	Aebp1	y					y		
P56		y							y
P4	Amotl2	y			y				
P56		y							y
P4	Ankfn1	y							y
P56		y							y
P4	Anxa11	y							y
P56		y							y
P4	Armc2	y					y		
P56		y							y
P4	Arvcf	y							y
P56		y							y
P4	Asahl	y							y
P56		y							y
P4	Asb14	y					y		
P56		y							y
P4	Atp8a2								
P56									
P4	Atxn1	y					y		
P56									
P4	AU021034	y							y
P56		y							y
P4	B230363K08Rik	y					y		
P56		y							y

Age	Gene Name	in the CC?	Dorsal (D)	Ventral (V)	Lateral (L)	DV	mostly D	mostly V	All Around
P4	B3gnt4	y							y
P56		y							y
P4	B430201A12Rik								
P56									
P4	Bbox1	y							y
P56		y							y
P4	BC013491	y							y
P56		y							y
P4	BC023179	y			y				
P56		y							y
P4	BC060267	y							y
P56		y							y
P4	Bmp6	y	y						
P56									
P4	Btg1	y					y		
P56									
P4	C1qtnf3	y					y		
P56		y							y
P4	C230030N03Rik	y							y
P56		y							y
P4	C330001K17Rik	y					y		
P56									
P4	Calml4	y							y
P56		y							y
P4	Capn6	y					y		
P56		y							y
P4	Capsl	y							y
P56		y							y
P4	Casc1	y							y
P56		y							y
P4	Ccdc113	y							y
P56		y							y
P4	Ccdc40	y							y
P56		y							y
P4	Ccdc60	y							y
P56		y							y
P4	Ccdc65	y							y
P56									
P4	Ccdc80	y				y			
P56									
P4	Ccdc96	y							y
P56		y							y
P4	Cd24a	y			y				
P56		y							y
P4	Cd63	y				y			
P56		y							y
P4	Cdk5rap2	y							y
P56									
P4	Cdk6	y						y	
P56									

Age	Gene Name	in the CC?	Dorsal (D)	Ventral (V)	Lateral (L)	DV	mostly D	mostly V	All Around
P4	Celsr1	y				y			
P56									
P4	Chia	y							y
P56		y							y
P4	Clec3b	y				y			
P56		y				y			
P4	Clu								
P56		y							y
P4	Cnn3	y							y
P56		y							y
P4	col23a1	y				y			
P56		y							y
P4	Col5a3								
P56		y							y
P4	Col8a2	y			y				
P56		y							y
P4	Col9a1	y							y
P56		y							y
P4	Crb2	y							y
P56		y							y
P4	Crocc	y							y
P56		y							y
P4	Ctdsp2	y					y		
P56									
P4	Ctnna1	y							y
P56									
P4	Ctsh	y					y		
P56		y							y
P4	Cyp4v3	y	y						
P56		y							y
P4	D16Ertd642e	y							y
P56		y							y
P4	D19Ertd652e	y							y
P56		y							y
P4	D430033N04Rik	y							y
P56		y							y
P4	D430042O09Rik	y							y
P56									
P4	D630039A03Rik	y							y
P56									
P4	Daf2	y					y		
P56		y							y
P4	Dbi	y							y
P56		y							y
P4	Dbp	y							y
P56									
P4	Dcbld1	y	y						
P56									
P4	Dcdc2a	y							y
P56		y							y

Age	Gene Name	in the CC?	Dorsal (D)	Ventral (V)	Lateral (L)	DV	mostly D	mostly V	All Around
P4	Dchs1	y							y
P56									
P4	Dcn	y							y
P56		y							y
P4	Ddc								
P56		y							y
P4	Ddo	y							y
P56									
P4	Ddr1	y							y
P56		y							y
P4	Dnahc11	y			y				
P56		y							y
P4	Dnahc12	y							y
P56		y							y
P4	Dnahc2	y							y
P56		y							y
P4	Dnahc5								
P56		y							y
P4	Dnahc6	y					y		
P56		y							y
P4	Dnahc9	y							y
P56		y							y
P4	Dnaja4	y			y				
P56		y							y
P4	Dnali1	y			y				
P56		y							y
P4	Dok5	y						y	
P56									
P4	Drctnnb1a	y							y
P56		y							y
P4	Dusp14	y							y
P56									
P4	Dynlrb2	y							y
P56		y							y
P4	E030025L21Rik	y			y				
P56									
P4	E030034C22Rik	y			y				
P56		y							y
P4	E130009J12Rik	y			y				
P56									
P4	E230008N13Rik	y							y
P56		y							y
P4	Ecgf1	y			y				
P56		y							y
P4	Efcab1	y							y
P56		y							y
P4	Efhb	y					y		
P56		y							y
P4	Efhc1	y							y
P56		y							y

Age	Gene Name	in the CC?	Dorsal (D)	Ventral (V)	Lateral (L)	DV	mostly D	mostly V	All Around
P4	Elof1	y							y
P56		y							y
P4	Entpd5	y	y						
P56									
P4	Epb4.1l4a	y							y
P56		y							y
P4	Eppk1	y							y
P56									
P4	F2r	y							y
P56									
P4	Fbxo36	y							y
P56									
P4	Fhad1	y							y
P56		y							y
P4	Flnc	y							y
P56									
P4	Frmpd2	y			y				
P56		y							y
P4	Fzd3	y							y
P56		y							y
P4	Gja1								
P56		y							y
P4	Gm1060	y							y
P56		y							y
P4	Gm770	y							y
P56		y							y
P4	Gm872	y							y
P56		y							y
P4	Gm967	y					y		
P56									
P4	Got1l1	y			y				
P56									
P4	Gpld1	y							y
P56									
P4	Gpr177	y							y
P56									
P4	Grap2	y			y				
P56		y							y
P4	Gsta4	y							y
P56									
P4	H19	y							y
P56									
P4	Hacl1	y							y
P56									
P4	Hipk1	y							y
P56		y							y
P4	Hspa2	y							y
P56		y							y
P4	Htr5b	y			y				
P56									

Age	Gene Name	in the CC?	Dorsal (D)	Ventral (V)	Lateral (L)	DV	mostly D	mostly V	All Around
P4	Id4	y							y
P56		y							y
P4	Ift80	y							y
P56									
P4	Ift81	y							y
P56		y							y
P4	Igsf9								
P56		y							y
P4	Iqcd	y							y
P56		y							y
P4	Iqcg	y							y
P56		y							y
P4	Irs1	y							y
P56									
P4	Itfg3	y							y
P56									
P4	Itih3	y						y	
P56									
P4	Itm2b	y							y
P56		y							y
P4	Itm2c	y							y
P56		y							y
P4	Itpkb	y							y
P56		y							y
P4	Kcnmb4	y							y
P56									
P4	Kif27	y					y		
P56									
P4	Kif6	y			y				
P56		y							y
P4	Kif9	y							y
P56		y							y
P4	Lman1	y						y	
P56									
P4	LOC380889	y							y
P56		y							y
P4	LOC432426	y							y
P56		y							y
P4	LOC432456	y							y
P56		y							y
P4	LOC434061	y							y
P56									
P4	LOC434130	y				y			
P56									
P4	Lrp10	y							y
P56									
P4	Lrp2	y					y		
P56		y							y
P4	Lrrc18	y						y	
P56		y							y

Age	Gene Name	in the CC?	Dorsal (D)	Ventral (V)	Lateral (L)	DV	mostly D	mostly V	All Around
P4	Lrrc23	y					y		
P56		y							y
P4	Lrrc43	y							y
P56		y							y
P4	Lrrc46	y							y
P56		y							y
P4	Lrrc56	y							y
P56									
P4	Lrrc6	y							y
P56		y							y
P4	Ltb4dh	y						y	
P56		y							y
P4	Lxn	y							y
P56		y							y
P4	Mamdc2	y						y	
P56		y							y
P4	Mapk15	y							y
P56		y							y
P4	mCG21281.2	y							y
P56		y							y
P4	Mdh1b								
P56		y							y
P4	Mef2b	y							y
P56		y							y
P4	Meig1	y							y
P56		y							y
P4	MGC58818	y					y		
P56		y							y
P4	Mia1	y							y
P56		y							y
P4	Mlc1	y							y
P56		y							y
P4	Mns1	y							y
P56		y							y
P4	Mpdz	y							y
P56		y							y
P4	Msi2	y							y
P56									
P4	Msn	y							y
P56		y							y
P4	Mt1	y							y
P56		y							y
P4	Mt3	y							y
P56		y							y
P4	Musk	y			y				
P56									
P4	Mxra8	y							y
P56		y							y
P4	Mycbpap	y							y
P56		y							y

Age	Gene Name	in the CC?	Dorsal (D)	Ventral (V)	Lateral (L)	DV	mostly D	mostly V	All Around
P4	Myo7a	y					y		
P56		y							y
P4	Nfix	y							y
P56		y							y
P4	Nin	y							y
P56		y							y
P4	Nnat	y							y
P56		y							y
P4	Notch2	y							y
P56									
P4	Npl	y							y
P56									
P4	Nr4a3	y			y				
P56									
P4	Ntrk2	y							y
P56		y							y
P4	Nxn	y							y
P56		y							y
P4	Osbpl3	y							y
P56		y							y
P4	Pacrg	y							y
P56		y							y
P4	Pamci	y							y
P56		y							y
P4	Pdia4	y							y
P56		y							y
P4	Pdlim4	y							y
P56		y							y
P4	Pdzk1ip1	y							y
P56		y							y
P4	Phkg1	y							y
P56		y							y
P4	Pi15	y					y		
P56		y							y
P4	Pipox	y							y
P56									
P4	Pir	y			y				
P56									
P4	Pkd1l2	y			y				
P56		y							y
P4	Pkd2l1	y			y				
P56		y			y				
P4	Pklr	y			y				
P56									
P4	Plekha2	y				y			
P56									
P4	Plekhb1								
P56		y							y
P4	Plod2								
P56		y							y

Age	Gene Name	in the CC?	Dorsal (D)	Ventral (V)	Lateral (L)	DV	mostly D	mostly V	All Around
P4	Pltp	y							y
P56		y							y
P4	Prdx6	y							y
P56		y							y
P4	Prelp	y							y
P56		y							y
P4	Prokr2	y							y
P56									
P4	Ptbp1	y							y
P56		y							y
P4	Ptpro	y							y
P56									
P4	Rarres2	y			y				
P56		y							y
P4	Rb1	y							y
P56									
P4	Rcc2	y							y
P56									
P4	Ren2								
P56									
P4	Rfx2	y							y
P56		y							y
P4	Rfx3	y							y
P56		y							y
P4	Rfx4	y							y
P56		y							y
P4	Rhpn1	y							y
P56									
P4	Rnase4	y							y
P56		y							y
P4	Rnh1	y							y
P56									
P4	Rshl3	y							y
P56		y							y
P4	Sall1	y							y
P56									
P4	Scd1								
P56		y							y
P4	Scnn1a								
P56		y							y
P4	Sdc2	y							y
P56		y							y
P4	Sdcbp	y							y
P56		y							y
P4	Sec24d	y							y
P56		y							y
P4	Serinc2	y							y
P56									
P4	Serpinh1	y							y
P56									

Age	Gene Name	in the CC?	Dorsal (D)	Ventral (V)	Lateral (L)	DV	mostly D	mostly V	All Around
P4	Slc14a1	y							y
P56		y							y
P4	Slc1a3	y							y
P56		y							y
P4	Slc25a18	y							y
P56		y							y
P4	Slc26a4								
P56									
P4	Slc26a4	y							y
P56		y							y
P4	Slc7a11	y	y						
P56									
P4	Sned1	y							y
P56									
P4	Sod3	y							y
P56		y							y
P4	Sorbs3								
P56		y							y
P4	Sox2	y							y
P56		y							y
P4	Spata18	y							y
P56		y							y
P4	Spef1	y							y
P56		y							y
P4	Srebf1	y							y
P56		y							y
P4	St5	y							y
P56		y							y
P4	St6galnac5	y							y
P56		y							y
P4	Stk33	y							y
P56		y							y
P4	Stk36	y							y
P56		y							y
P4	Syngap1								
P56		y							y
P4	Syt10	y							y
P56		y							y
P4	Tagln2								
P56		y							y
P4	Tcp11l2	y							y
P56									
P4	Tekt1	y							y
P56		y							y
P4	Tekt4	y							y
P56									
P4	Tm4sf1	y							y
P56		y							y
P4	Tmem16a	y	y						
P56									

Age	Gene Name	in the CC?	Dorsal (D)	Ventral (V)	Lateral (L)	DV	mostly D	mostly V	All Around
P4	Tmem47	y							y
P56		y							y
P4	Tnni3	y							y
P56									
P4	Traf1	y			y				
P56		y							y
P4	Tsnaxip1	y							y
P56		y							y
P4	Tsnaxip1	y							y
P56		y							y
P4	Tspan6								
P56		y							y
P4	Ttc12	y							y
P56									
P4	Ttc16	y							y
P56		y							y
P4	Ttc18	y							y
P56									
P4	Ttc21a	y							y
P56		y							y
P4	Ttc25	y							y
P56		y							y
P4	Ttc29	y							y
P56		y							y
P4	Ttc8	y							y
P56		y							y
P4	Ubxd3	y							y
P56		y							y
P4	Ulk4	y							y
P56		y							y
P4	V1rc15	y							y
P56		y							y
P4	Vil2	y							y
P56		y							y
P4	Vit	y							y
P56		y							y
P4	Wdr16	y							y
P56		y							y
P4	Wdr63	y							y
P56		y							y
P4	Wdr78	y							y
P56		y							y
P4	X99384	y							y
P56									
P4	Ysk4	y							y
P56		y							y
P4	Zbtb20	y							y
P56		y							y
P4	Zfp36l1	y							y
P56		y							y

Age	Gene Name	in the CC?	Dorsal (D)	Ventral (V)	Lateral (L)	DV	mostly D	mostly V	All Around
P4	Zfp474	y							y
P56		y							y
P4	Zmynd10	y							y
P56		y							y

APPENDIX B – Twenty most relevant pathways from ToppGene analysis

The accompanying excel spreadsheet shows the list of the 20 most relevant pathways according to our ToppGene analysis, with the associated genes from each pathway from our query list. “p-value” was determined by ToppGene, “Hit count” refers to the number of genes in this pathway, and gene names under “Hit in Query list” are all the central canal genes included in that pathway from our original query list.

Name of pathway	p-value	Hit Count in Query List	Hit in Query List					
microtubule-based movement	2.60E-12	21	STK36	LRRC6	DNALI1	KIF9	DYNLRB2	ULK4
			IFT80	DNAH5	DNAH6	DNAH9	CCDC40	KIF6
			KIF27	RSPH4A	IFT81	DNAH2	RFX3	DNAH1
			DNAH12	CASC1	DNAH11			
cilium movement	1.13E-11	11	STK36	LRRC6	DNALI1	ULK4	DNAH5	CCDC40
			KIF27	RSPH4A	RFX3	DNAH1	DNAH11	
microtubule motor activity	1.18E-09	12	DNALI1	KIF9	DYNLRB2	DNAH5	DNAH6	DNAH9
			KIF6	KIF27	DNAH2	DNAH1	DNAH12	DNAH11
microtubule-based process	3.64E-09	29	STK36	LRRC6	RCC2	DNALI1	KIF9	DYNLRB2
			TEKT1	ULK4	IFT80	DNAH5	DNAH6	DNAH9
			CCDC40	KIF6	KIF27	RSPH4A	RB1	IFT81
			CAPN6	DNAH2	RFX3	DNAH1	DNAH12	CDK5RAP2
			TEKT4	CASC1	CROCC	DNAH11	NIN	
cilium or flagellum-dependent cell motility	3.68E-08	7	DRC1	DNAH5	DNAH6	DNAH2	RFX3	DNAH1
			DNAH11					
motor activity	5.98E-08	13	MYO7A	DNALI1	KIF9	DYNLRB2	DNAH5	DNAH6
			DNAH9	KIF6	KIF27	DNAH2	DNAH1	DNAH12
			DNAH11					
movement of cell or subcellular component	9.39E-08	53	STK36	MYO7A	DRC1	IRS1	LRRC6	F2R
			SLC7A11	RCC2	DNALI1	TTC8	GJA1	KIF9
			PTPRO	BTG1	TSPO	DYNLRB2	ULK4	IFT80
			DNAH5	DNAH6	DNAH9	PLTP	SDCBP	CCDC40
			GPLD1	EZR	DDR1	COL9A1	DCDC2	KIF6
			ANG	KIF27	RARRES2	RSPH4A	FZD3	NTRK2
			IFT81	DNAH2	NR4A3	COL5A3	RFX3	DNAH1
			MSN	CELSR1	DNAH12	CD24	CD63	CTNNA1
			CASC1	TNNI3	CTSH	CDK6	DNAH11	
cell projection organization	1.18E-07	42	STK36	MNS1	MYO7A	LRRC6	SYNGAP1	TTC8
			GJA1	ZMYND10	CLU	PTPRO	FAM161A	TSPO
			ULK4	IGSF9	ITM2C	IFT80	DNAH9	SDC2
			SDCBP	EZR	COL9A1	DCDC2	KIF27	RSPH4A
			RB1	FZD3	NTRK2	IFT81	WDR60	NR4A3
			COL5A3	PIFO	RFX3	RFX4	PRDX6	MT3
			CD24	LRP4	TEKT4	CTNNA1	CROCC	TCTN2
cilium organization	3.72E-07	13	STK36	MNS1	LRRC6	TTC8	ZMYND10	FAM161A
			IFT80	KIF27	RSPH4A	IFT81	RFX3	RFX4
			TCTN2					
epithelial cilium movement	4.15E-07	6	STK36	LRRC6	ULK4	CCDC40	KIF27	RFX3

Name of pathway	p-value	Hit Count in Query List	Hit in Query List	Name of pathway	p-value	Hit Count in Query List	Hit in Query List	Name of pathway
cell projection assembly	5.83E-06	16	STK36	LRRC6	TTC8	ZMYND10	PTPRO	FAM161A
			IFT80	SDCBP	EZR	KIF27	RSPH4A	IFT81
			RFX3	RFX4	PRDX6	TCTN2		
cell projection morphogenesis	1.07E-05	29	STK36	LRRC6	SYNGAP1	TTC8	GJA1	ZMYND10
			CLU	PTPRO	FAM161A	ULK4	IFT80	SDC2
			SDCBP	EZR	COL9A1	DCDC2	KIF27	RSPH4A
			FZD3	NTRK2	IFT81	NR4A3	COL5A3	RFX3
			RFX4	MT3	CD24	LRP4	TCTN2	
smoothened signaling pathway	1.23E-05	10	STK36	HIPK1	SALL1	IFT80	KIF27	RB1
			PKD2L1	RFX4	CTNNA1	TCTN2		
Extracellular matrix organization	3.74E-05	12	DCN	ADAMTS16	PLOD2	SDC2	DDR1	COL8A2
			COL9A1	COL5A3	SERPINH1	COL23A1	LRP4	MUSK
cell morphogenesis	4.00E-05	35	STK36	MYO7A	LRRC6	RCC2	SYNGAP1	TTC8
			GJA1	SALL1	ZMYND10	CLU	PTPRO	FAM161A
			ULK4	IFT80	SDC2	SDCBP	EZR	COL9A1
			DCDC2	KIF27	RSPH4A	RB1	FZD3	NTRK2
			IFT81	NR4A3	COL5A3	RFX3	RFX4	SLC1A3
			MT3	CD24	LRP4	CRB2	TCTN2	
axonemal dynein complex assembly	5.36E-05	4	DRC1	LRRC6	ZMYND10	CCDC40		
cellular component assembly involved in morphogenesis	7.31E-05	12	STK36	LRRC6	TTC8	ZMYND10	FAM161A	IFT80
			KIF27	RSPH4A	IFT81	RFX3	RFX4	TCTN2
Collagen biosynthesis and modifying enzymes	8.24E-05	6	PLOD2	COL8A2	COL9A1	COL5A3	SERPINH1	COL23A1
cytoskeletal protein binding	1.06E-04	26	MYO7A	EPB41L4A	RCC2	GJA1	KIF9	SCNN1A
			SDC2	CNN3	SDCBP	EZR	FLNC	KIF6
			ANG	KIF27	IFT81	CAPN6	PKD2L1	PIFO
			PDLIM4	MSN	SORBS3	CDK5RAP2	CTNNA1	CASC1
			CROCC	TNNI3				
response to pH	1.91E-04	5	PKD1L2	GJA1	GPLD1	PKD2L1	ARSB	